The loading of gallium-68 into polymersomes

by

Kevin Yuk Mien Fung

Bachelor thesis performed at:

Section Applied Radiation & Isotopes
Department Radiation Science & Technology
Faculty of Applied Sciences
Delft University of Technology

to be defended publicly on Wednesday October 28, 2020 at 11:00

Graduation committee:

dr. ir. A.G. Denkova
dr. ir. R.M. de Kruijff

Supervisor: dr. ir. A.G. Denkova
Daily supervisor: dr. ir. R.M. de Kruijff

TU Delft

Page left blank intentionally

Abstract

A polymersome is a type of nanocarrier made of amphiphilic block copolymers, consisting of a hydrophobic bilayer, a hydrophilic brush-like outer shell and a hollow, aqueous core, which is formed through self-assembly. Polymersomes could be useful in the treatment of cancer as carrier to deliver and release drugs or radionuclides to tumours locally to reduce them without damaging healthy tissue. For this purpose, it could rely on the Enhanced Permeation and Retention (EPR) effect to accumulate in tumours, which requires a long blood circulation time. Reports have shown that while the circulation half-life in healthy mice is in the order of hours, it decreases to the order of minutes in diseased mice, preventing any uptake of polymersomes in tumours. So, more research needs to be done on the *in vivo* biodistribution for each type of polymersome to assess whether it is suitable for radiotherapy. Thus far, imaging for polymersome *in vivo* biodistribution mostly relies on the use of In-111 and Single Photon Emission Computed Tomography/Computed Tomography (SPECT/CT) as imaging technique. In this report it is researched whether it is possible to load gallium-68 (positron emitter, half-life 67.71 min) into poly(1,2-butadiene)-b-poly(ethylene oxide) {PBd(1800 g mol^{-1})-b-PEO(600 g mol^{-1})} polymersomes using an active loading method, which has not been done so far. This would allow short-term imaging using Positron Emission Tomography (PET) as an alternative imaging technique. PET has a much higher sensitivity than SPECT, which allows better image quality or shorter scan times. These advantages make PET better than SPECT for clinical use.

Using Ga-68 as the positron emitting source has the advantage on being able to rely on a germanium-68/gallium-68 generator to produce Ga-68 on-site and being independent of external radionuclide suppliers.

In this report the pH dependency of the formation of complex of Ga-68 with a lipophilic ligand was researched, the transfer of Ga-68 from the lipophilic ligand to a hydrophilic chelator was optimised, and loading experiments of Ga-68 into polymersomes were conducted. It was demonstrated that it is indeed possible to load Ga-68 into polymersomes, and maximum loading efficiencies of up to 36% were found. It is argued that the low loading efficiency could be caused by an unexpectedly thick hydrophobic bilayer of the prepared polymersomes, and possibly by a low amount of encapsulated hydrophilic chelator compared to the applied amount of lipophilic ligand. But more research needs to be done to confirm these observations.

Table of Contents

Abbreviations and acronyms

a	membrane thickness
$A_i(t)$	(time dependent) activity of index *i*
c	speed of light
c_i	concentration of index *i*
CryoTEM	Cryogenic Transmission Electron Microscopy
CT	Computed Tomography
C_{tot}	mass concentration of polymer
D	diameter
D	diffusion coefficient
DLS	Dynamic Light Scattering
DOTA	1,4,7,10-Tetraazacyclododecane-N,N',N'', N'''-tetraacetic acid
DTPA	diethylenetriaminepentaacetic acid
E_i	energy of index *i*
EM	electron microscope
EPR	Enhanced Permeation and Retention
eq.	equation
f	hydrophilic mass fraction
HEPES	4-(2-hydroxyethyl)piperazine-1-ethanesulfonic acid
I	intensity
k	number of half-lives
k_b	Boltzmann's constant
K_i	equilibrium constant of index *i*
L	ligand
LE_{low}	lower bound estimate of the loading efficiency
LE_{max}	maximum loading efficiency
LOR	line of response
M	metal
m_0	rest mass
M_h	hydrophobic molecular weight
MW	molecular weight of the total polymer
MW_f	molecular weight of the hydrophilic fraction
$MW_{hydrophobic}$	molecular weight of the hydrophobic part of the polymer
n	number of measurements
N_i	number of counts of index *i*
n_i	number of index *i*
NOTA	2,2′,2"-(1,4,7-triazacyclononane-1,4,7-triyl)triacetic acid
PBd	polybutadiene
PEG	poly(ethylene glycol)
PEO	poly(ethylene oxide)
PET	Positron Emission Tomography
PS	polymersome
$ratio_{trop/DTPA}$	amount of tropolone divided by amount of DTPA
RCY	radiochemical yield
r_h	hydrodynamic radius
SD	sample standard deviation

SE	standard error of the mean
SEC	size-exclusion chromatography
SEM	scanning electron microscope
SPECT	Single Photon Emission Computed Tomography
T	temperature
t	time
$T_{1/2,i}$	half-life of index i
TEM	transmission electron microscope
trop	tropolone
tropolone	2-hydroxy-2,4,6-cycloheptatrien-1-one
V_i	volume of index i
η	dynamic viscosity
θ	angle
λ_i	decay constant of index i
ρ_{bi}	density of polymersome membrane
φ	volume fraction

1. Introduction

A polymersome is a type of nanocarrier made of amphiphilic block copolymers. It consists of a hydrophobic bilayer, a hydrophilic brush-like outer shell and a hollow, aqueous core, and it is formed through self-assembly of the block copolymers. Polymersomes could be useful in the treatment of cancer by loading drugs or radionuclides in the hydrophobic bilayer or in the aqueous cavity, and act as carrier to deliver and release these drugs or radionuclides to tumours locally to reduce them without damaging healthy tissue.

In order to make this possible, polymersomes should be able to accumulate at the tumours, which requires a long blood circulation half-life. However, i*n vivo* experiments have shown that there is a significant difference of the blood circulation half-life between polymersomes in healthy mice and in tumour-bearing mice. *Wang, G. et al.* (2016) have reported a circulation half-life of 80 nm diameter PBd-PEO (1800-900 g/mol) polymersomes of >6 hours in healthy mice, whereas the circulation half-life decreased to <1.5 hours in tumour-bearing mice. Here the activity was mostly found in the spleen and the liver. [1]
De Kruijff, R.M. (2018) has reported a circulation half-life of 80 nm diameter PBd-PEO (1900-900 g/mol) polymersomes of 139 minutes in healthy mice, whereas the circulation half-life decreased to 7 minutes in tumour-bearing mice. Here, activity was mostly found in the spleen, bone marrow and liver. [2].

These results indicate that there is a lot to learn about the behaviour of polymersomes *in vivo*. When engineering new polymersomes with different compositions, *in vivo* studies need to be done to understand its biodistribution and to determine whether it is feasible for these polymersomes to be deployed in radiotherapy.

Indium-111 has been successfully loaded in the aqueous core of polymersomes using a so-called active loading method [3]. The above-mentioned results of *Wang et al.* and *de Kruijff* were determined using In-111 as radionuclide and using SPECT/CT (Single Photon Emission Computed Tomography/Computed Tomography) as nuclear imaging technique.

Gallium-68, a positron emitter (89%), can be used as imaging agent in a PET (Positron Emission Tomography)/CT scan, using the property that emitted positrons annihilate to two 511 keV γ photons that travel in opposite direction.

The use of PET imaging has several advantages over SPECT imaging. PET has a much higher sensitivity than SPECT, since SPECT scans use physical collimators that reject a high percentage of emitted photons. This means that a higher percentage of emitted events is detected in PET compared to SPECT. A higher sensitivity leads to a higher signal-to-noise ratio, which improves the image quality. A higher sensitivity in PET also allows the ability to perform shorter scans than SPECT to create images with similar signal-to-noise-ratio [4]. Therefore, PET can be better than SPECT in clinical use.

Additionally, it should be possible to inject a patient with a higher activity of Ga-68 ($T_{1/2}$ = 67.71 min) than In-111 ($T_{1/2}$ = 2.8 d), without exposing a patient to a higher total dose of radiation, due to the short half-life of Ga-68 compared to In-111. Such higher activity could increase image quality.

A huge practical benefit of Ga-68 is that it can be obtained by elution of a germanium-68/gallium-68 generator. This allows activity of Ga-68 to be obtained on-site, while being completely independent of an external supplier for the radionuclide.

But so far, no attempt has been made to load gallium-68 into the aqueous cavity of polymersomes.

This report focuses on loading gallium-68 into polymersomes with the goal of giving researchers an extra, viable tool to determine the biodistribution of polymersomes for short-term *in vivo* studies.

Inspired by the active loading method of In-111 into polymersomes, the attempt will be made to load Ga-68 into polymersomes using an active loading method. This resulted in the following research questions of this report:

- Is it possible to load gallium-68 into polymersomes using an active loading mechanism?
- And what factors affect the loading of gallium-68 into polymersomes?

Overview of the experiments

The experiments in this report can be divided into three main sections:

i. (§4.1) Ga-68 was bound to a lipophilic ligand: the radiochemical yield (*RCY*) was determined as function of pH using extraction experiments. The pH range that yielded the highest *RCY* was determined. Tropolone was chosen as lipophilic ligand.

ii. (§4.2) This chapter describes experiments in which tropolone in the Ga-tropolone complex took place in a ligand exchange reaction to form a complex of Ga-68 with a hydrophilic chelator. Three hydrophilic chelators were compared with each other.

iii. (§4.3). The best hydrophilic chelator was chosen and used in the preparation of polymersomes. Loading experiments were performed and the maximum loading efficiency was determined. The goal was to load Ga-68 into polymersomes and to compare the results of different conditions (pH, polymer concentration, loading time, loading temperature) with each other.

2. Theory

In the upcoming sections of this chapter, a short description is given about several theoretical concepts and basic principles that are related to this project, without going into too much depth.

2.1. Self-assembled structures by amphiphilic block copolymers

Amphiphilic block copolymers are polymers that consist of (at least) one hydrophilic block and (at least) one hydrophobic block, which are bonded to each other.

In a solvent, they can self-assemble into various morphologies. The mass fraction of the hydrophilic block (*f*) determines what nanostructure is more favourably formed in aqueous solution [5][6]. (See **Table 1**). The *f* value is defined as:

$$f = \frac{MW_f}{MW} \times 100\% \qquad (2.1)$$

where MW_f is the molecular weight of the hydrophilic fraction of the polymer, MW is the molecular weight of the total polymer.

Table 1. Overview of self-assembled structures of amphiphilic block copolymer in aqueous solution as function of the *f* value.

morphology	***f* value**	**reference**
polymersome	35% ± 10%	[6]
	25% - 40%	[5][6]
worm-like micelle	< 50%	[6]
	40% - 50%	[5][6]
spherical micelle	> 45%	[6]
	> 50%	[5][6]

In this report the amphiphilic diblock copolymer poly(1,2-butadiene)-b-poly(ethylene oxide) {PBd(1800 g mol^{-1})-b-PEO(600 g mol^{-1})} was used to create polymersomes. This polymer will be simply referred to as 'PBd(1800)-PEO(600)' or 'PBd_{33}-PEO_{14}' (see **Figure 1**) .

The PBd block is the hydrophobic part of the polymer, while the PEO block is the hydrophilic part. The corresponding *f* value for PBd(1800)-PEO(600) is 25%. According to **Table 1** the formation of polymersomes is most favourable for this polymer.

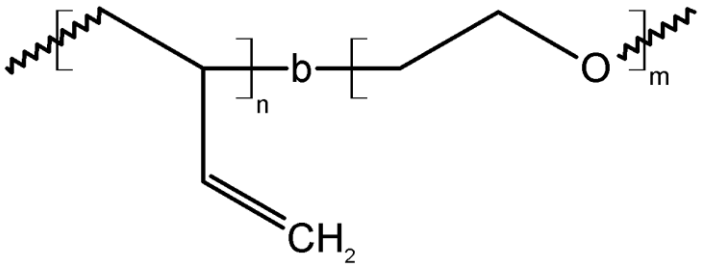

Figure 1. Structure of the amphiphilic PBd(1800)-PEO(600) polymer. n = 33, m = 14.

2.2. Active loading mechanism

A so-called active loading mechanism was applied to load Ga-68 into polymersomes. This means that Ga-68 from outside of the polymersomes is transported through the membrane (hydrophobic bilayer) into the interior, aqueous cavity of the polymersomes. The strategy to enable this loading process involves three steps, which are illustrated in **Figure 2**.

Step 1 involves the formation of the complex of Ga-68 with a lipophilic ligand. The purpose of this step is to ensure that Ga-68 gets attracted towards the hydrophobic bilayer of the polymersome. In this report, tropolone was chosen as the lipophilic ligand.

Step 2 involves the transport of Ga-68 towards and through the hydrophobic bilayer of the polymersome.

Step 3 involves the substitution of the tropolone ligand in the [^{68}Ga]Ga-tropolone complex with a hydrophilic chelator (in this case, DTPA) in the aqueous cavity of the polymersome. This is possible if the stability constant of DTPA with gallium is higher than the stability constant of tropolone with gallium (see Appendix F). The DTPA is encapsulated in the aqueous cavity during the polymersome formation.

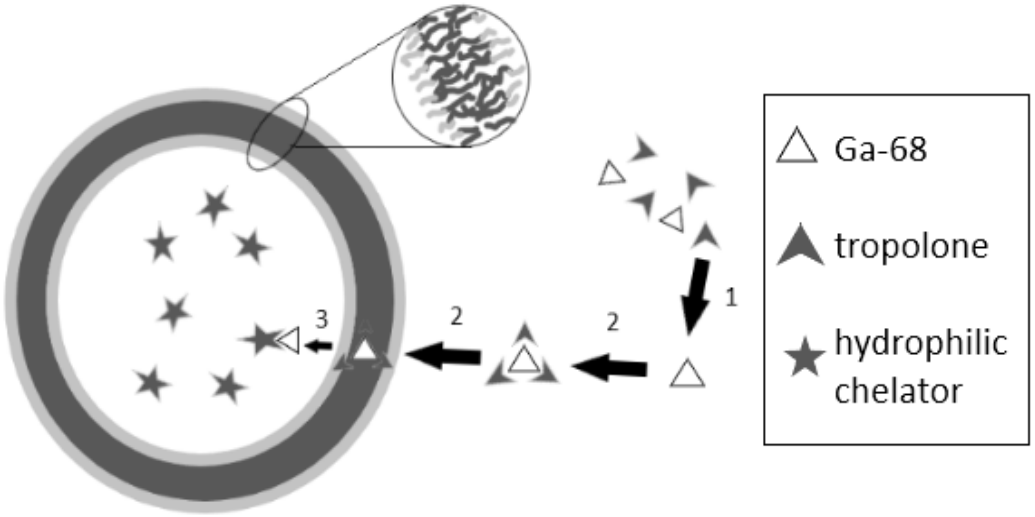

Figure 2. Illustration of polymersome (dark grey represents hydrophobic bilayer; light grey represents hydrophilic brush) with an overview of the required steps to load Ga-68 into the aqueous cavity of the polymersome.

The mechanism for the transport of Ga-68 through the bilayer is not well-known. However, two possible mechanisms for the transport of In-111 through the bilayer with tropolone was discussed by *Wang, G. et al.* [3]. The first proposition is that the complex of In-111 with tropolone (as a whole) diffuses through the hydrophobic bilayer to reach the DTPA. The second proposition is that tropolone is present in the hydrophobic bilayer where it forms an ion channel for the ^{111}In ion, in which the ^{111}In ion can jump from one tropolone molecule to another molecule until it reaches the DTPA in the cavity [3].

It is possible that one of both propositions for the transport mechanism of In-111 into polymersomes can also be applied to describe the loading of Ga-68 into polymersomes.

2.3. Tumour targeting

One could rely on an active and/or passive mechanism for the delivery of polymersomes to tumours. Tumours are known to have leaky blood vessels (gasps of 100 nm – 2 μm size have been established) [5], and therefore nanoparticles with a size less than 100 nm can pass through these blood vessels to accumulate in the tumour.

This passive targeting is known as the Enhanced Permeation and Retention (EPR) effect [5].

Alongside the EPR effect, the delivery of polymersomes to tumours can be assisted with an active targeting mechanism. The polymersome could be designed to actively seek specific tumours by conjugating a targeting vector to the hydrophilic part (outer shell) of the polymersome. Either way, the accumulation of sufficient nanoparticles requires a long blood circulation time.

However, the body's own immune system is the biggest enemy for the uptake of polymersomes in tumours. Opsonin proteins in the blood stream are able to cover particles that are foreign to the body. Opsonization makes foreign particles visible for macrophages, that can remove those particles from the blood stream, preventing a long circulation time. A known strategy for incorporating stealth properties to nanoparticles is through decorating the surface with PEG (poly(ethylene glycol)) chains, so called PEGylation. *{It should be noted that PEG is also known as PEO (poly(ethylene oxide))}* This increases the blood circulation half-life of the nanoparticles by creating a barrier to block the adhesion of opsonin proteins, and thereby slowing down opsonization, which makes the nanoparticles undetectable for macrophages [7].

2.4. Decay of Ge-68 and Ga-68

Gallium-68 is part of a decay chain in which it is a daughter radionuclide of germanium-68, and the parent radionuclide of Zinc-68:

$$^{68}\mathrm{Ge} \rightarrow {}^{68}\mathrm{Ga} \rightarrow {}^{68}\mathrm{Zn} \tag{2.2}$$

Germanium-68 decays ($T_{1/2}$ = 270.93 d) [8] by electron capture (100%) [8] to form gallium-68:

$$^{68}\mathrm{Ge} \rightarrow {}^{68}\mathrm{Ga} + \nu_e \tag{2.3}$$

Gallium-68 decays ($T_{1/2}$ = 67.71 min) [8] by positron emission (88.88%) [9] to form Zinc-68, which is a stable isotope:

$$^{68}\mathrm{Ga} \rightarrow {}^{68}\mathrm{Zn} + \beta^{+} + \nu_e \tag{2.4}$$

The remainder decays by electron capture (11.11%) [9]:

$$^{68}\mathrm{Ga} \rightarrow {}^{68}\mathrm{Zn} + \nu_e \tag{2.5}$$

2.5. ^{68}Ge/^{68}Ga generator: secular equilibrium

Ga-68 is obtained by elution of a germanium-68/gallium-68 generator. The generator that was used in this project consists of a glass column filled with titanium dioxide (TiO_2), onto which Ge-68 is adsorbed [10]. ^{68}Ge decays on this column to produce ^{68}Ga, which can be eluted from the generator while ^{68}Ge stays fixed on the column.

Since the half-life of Ge-68 (270.93 d) is much bigger than that of Ga-68 (67.71 min), a so-called secular equilibrium can be reached in the generator.

A secular equilibrium is defined as that condition in serial radioactive decay where the ratio of activities of the parent and daughter radionuclides is a constant and where there is no important decay of the parent nuclide during the time interval of interest [11]. In this section, a derivation is given to show that this definition applies to Ga-68. If the activity of Ga-68 is 0 at $t = 0$, it can be shown (see Appendix C) that:

$$A_{Ga}(t) = A_{Ge,0}\frac{\lambda_{Ga}}{\lambda_{Ga}-\lambda_{Ge}}(e^{-\lambda_{Ge}\cdot t} - e^{-\lambda_{Ga}\cdot t}) \tag{2.6}$$

where $A_{Ga}(t)$ is the time dependent activity of Ga-68 in the generator,
$A_{Ge,0}$ is the activity of Ge-68 at $t = 0$ in the generator,
λ_{Ga} is the decay constant of Ga-68,
λ_{Ge} is the decay constant of Ge-68.

Since $\lambda_{Ge} << \lambda_{Ga}$, equation (2.6) can be approximated by:

$$A_{Ga}(t) = A_{Ge,0}(e^{-\lambda_{Ge}\cdot t} - e^{-\lambda_{Ga}\cdot t}) \tag{2.7}$$

Given that $A_{Ge}(t) = A_{Ge,0}\cdot e^{-\lambda_{Ge}\cdot t}$, equation (2.7) is equal to:

$$A_{Ga}(t) = A_{Ge}(t) - A_{Ge,0}\cdot e^{-\lambda_{Ga}\cdot t} \tag{2.8}$$

2.5.1. Long timescales

At long timescales ($t \to \infty$) equation (2.8) becomes:

$$A_{Ga}(t) = A_{Ge}(t) \tag{2.9}$$

For long timescales, it is shown that the activity of gallium-68 in the generator becomes equal to the activity of germanium-68 in the generator. But because the activities of Ga-68 and Ge-68 are not a constant on this timescale (since they follow the decay of germanium-68), this cannot be considered a secular equilibrium.

$$A_{Ga}(t) = A_{Ge}(t) = A_{Ge,0}\cdot e^{-\lambda_{Ge}\cdot t} \tag{2.10}$$

2.5.2. Short timescales

Because the half-life of Ge-68 is very long (the decay constant of Ge-68 is very short), the activity of Ge-68 stays practically constant at short timescale:

$$A_{Ge}(t) = A_{Ge,0} \tag{2.11}$$

and equation (2.8) becomes:

$$A_{Ga}(t) = A_{Ge,0} - A_{Ge,0}\cdot e^{-\lambda_{Ga}\cdot t} \tag{2.12}$$

which can be rewritten into:

$$A_{Ga}(t) = A_{Ge,0}(1 - e^{-\lambda_{Ga} \cdot t}) \tag{2.13}$$

Since $\lambda_{Ga} = \frac{\ln 2}{T_{1/2,Ga}}$, where $T_{1/2,Ga}$ denotes the half-life of Ga-68, equation (2.13) is equal to:

$$A_{Ga}(t) = A_{Ge,0}(1 - e^{-\frac{\ln 2}{T_{1/2,Ga}} t}) \tag{2.14}$$

If the time t is expressed as the number (k) of half-lives of Ga-68:

$$t = k \cdot T_{1/2,Ga} \tag{2.15}$$

then the activity of Ga-68 can be expressed in terms of number of half-lives of Ga-68:

$$A_{Ga}(k) = A_{Ge,0}(1 - e^{-k \cdot \ln 2}) \tag{2.16}$$

or simplified:

$$A_{Ga}(k) = A_{Ge,0}(1 - 2^{-k}) \tag{2.17}$$

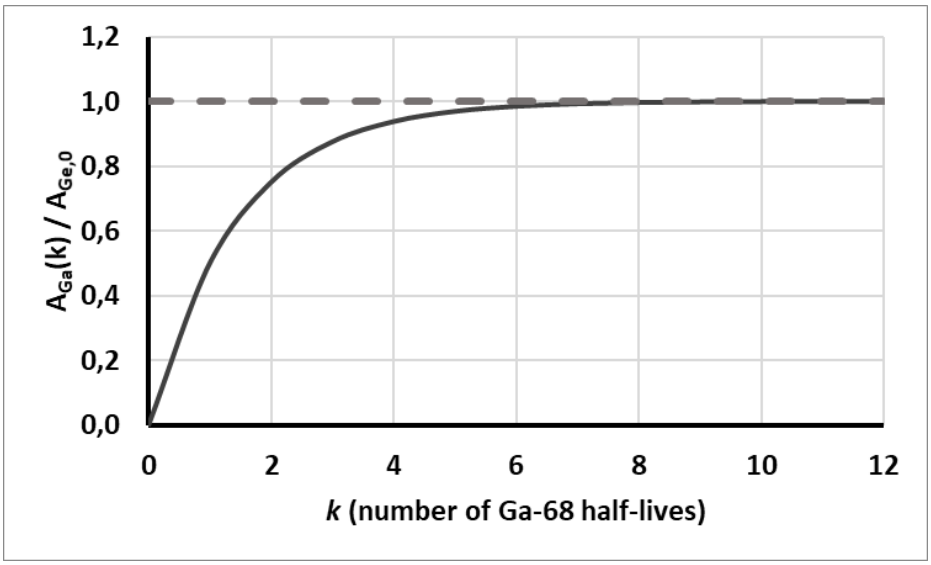

Figure 3. Time dependent activity of Ga-68 as fraction of the constant activity of Ge-68 (vs.) the time expressed as the number of Ga-68 half-lives.

In **Figure 3** the activity of gallium-68 is plotted as fraction of the (constant) activity of germanium-68: $\frac{A_{Ga}(k)}{A_{Ge,0}} = 1 - 2^{-k}$. After several half-lives of Ga-68, the activity of Ga-68 becomes indistinguishable from the activity of Ge-68. And since the activity of Ge-68 on this timescale is practically constant, a secular equilibrium is reached.

After only 4 half-lives of Ga-68 (≈ 4.5 h), the activity of Ga-68 in the generator already reaches 94% of its maximum activity. As a result of this observation, it can be concluded that the $^{68}Ge/^{68}Ga$ generator can be eluted more than once per day, which is useful from a practical point of view.

2.6. PET scanner

Positron emission tomography (PET) is an imaging technique that relies on labelling a tracer with an isotope that emits positrons (such as ^{68}Ga). It makes use of the property that an emitted positron annihilates with an electron to form two 511 keV γ photons that travel in opposite direction.

The PET scanner (see **Figure 4**) consists of a ring of detectors. These detectors are based on scintillation crystals that convert the energy of the γ photons into flashes of light, and subsequently, these light flashes are converted into electronic pulses by photomultiplier tubes [12].

When two detectors record an electric pulse simultaneously (they both detect a photon simultaneously), then this is called a 'coincidence' event [13]. Since both photons of one coincidence can travel slightly different lengths to reach a detector, it is necessary to have a coincidence timing window. When two electric pulses are detected within this timing window (typically up to ~12 ns [4][13]), then they are still considered to be 'simultaneous' and therefore recorded as a coincidence event.

The path between the two detectors of a coincidence event is known as the 'line of response' (LOR). It indicates that an annihilation occurred somewhere along the LOR [13]. An image of the distribution of the activity can be reconstructed by combining all the recorded LORs.

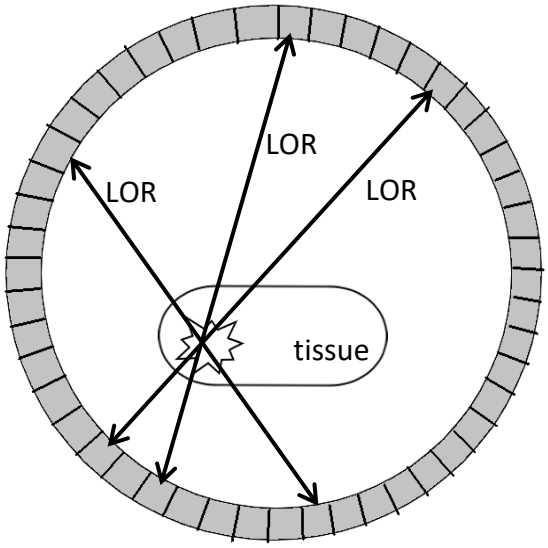

Figure 4. Coincidence events with corresponding LORs. Example of annihilation events at a local spot in some tissue.

Several factors can negatively impact the image quality of PET. Three of them will be discussed in this section.

Positron range

An emitted positron travels some distance through the tissue as it loses kinetic energy by Coulomb interactions with electrons [14] before it annihilates with an electron. So, there is a distance between the location of the source of positron emission and the location of annihilation: this distance is the positron range.

Angle between opposite traveling γ photons

The produced γ photon pair, as a result of positron annihilation, possibly do not travel in exact opposite direction, but at a small angle: 180° ± 0.25° [4]. This results in a LOR that slightly deviates from the location of annihilation. See **Figure 5**.

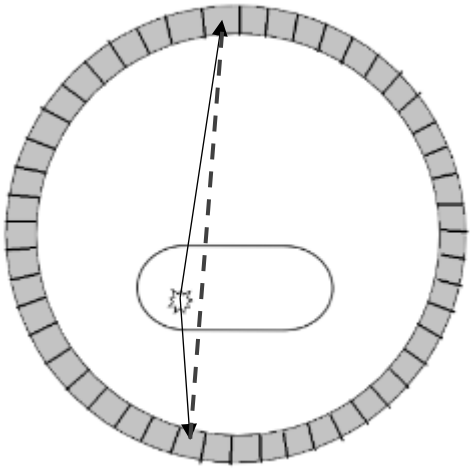

Figure 5. Inaccurate LOR (dashed line in figure) due to path of photon pair that deviates from 180°.

Compton scattering

A photon can interact with an electron (for example: an electron of an atom of the tissue) and transfer some of its energy to the electron, after which the photon is scattered through an angle θ relative to its incoming direction [15]. This could lead to an inaccurate LOR (see **Figure 6**).

The energy of the scattered photon (E_s) is given [15] by:

$$E_s = \frac{E_\gamma}{1 + \frac{E_\gamma}{m_0 c^2}(1 - \cos\theta)} \tag{2.18}$$

where E_γ is the energy of the incident photon, m_0 is the rest mass of the electron, and c is the speed of light.

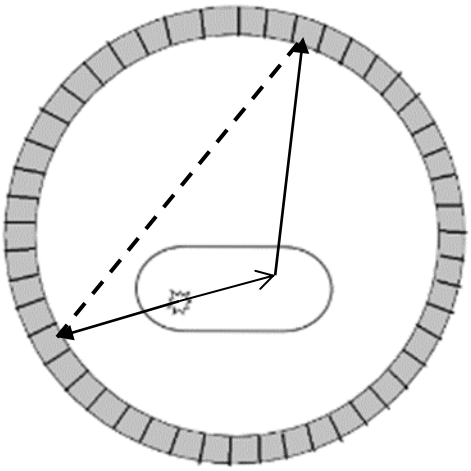

Figure 6. Incorrect LOR (dashed line in figure) caused by a changed pathway of the photon due to Compton scattering in the tissue.

2.7. Size-exclusion chromatography (SEC)

Size-exclusion chromatography (SEC) involves the separation of molecules in solution by their size. In this report, Sephadex columns were used to separate big polymeric particles from smaller molecules in solution. Sephadex is a porous, bead-like gel that acts as the stationary phase in the column. Smaller molecules can enter and exit the pores of the gel beads; the larger molecules cannot enter the pores and they travel passed the beads. This way, the smaller molecules effectively increase their pathways when they pass through the column and they will elute later from the column than the larger molecules.

2.8. Dynamic light scattering (DLS)

With Dynamic light scattering (DLS) it is possible to determine the size distribution of particles in solution. A laser beam passes through the solution where the light gets scattered due to interaction with the particles, which creates a speckle pattern. The intensity of the scattered light fluctuates over time because the particles undergo Brownian motion. This means that they are subjected to random forces from the thermal motion of the surrounding molecules [16]. Smaller particles cause the intensity to fluctuate more rapidly than larger ones [17], since smaller particles move faster than larger particles.

The information of the fluctuations of the intensity is used to determine the diffusion coefficients of the particles. The diffusion coefficients (D) can be used to determine the hydrodynamic radius of the particles using the Stokes-Einstein equation [16][17]:

$$D = \frac{k_b T}{6\pi\eta r_h} \tag{2.19}$$

where k_b is the Boltzmann's constant, T is the temperature, η is the dynamic viscosity, and r_h is the hydrodynamic radius.

The output of DLS measurements in this report is given as figures of intensity (vs.) hydrodynamic radius. (See Appendix A). It should be noted that the intensity of scattered light scales with the size of a particle to the power six:

$$I \sim r_h^6 \tag{2.20}$$

This means that a (1:1) ratio of ('small particles': 'large particles') in solution, will lead to a higher intensity for the 'large particles'.

A brief and more mathematically accurate explanation about DLS, and how to determine the diffusion coefficients is given by *Hamley, I.W.* [16]:

"DLS involves measuring the temporal fluctuations of the intensity of scattered light. The number of photons entering a detector are recorded and analysed by a digital correlator. The separation in time between photon countings is the correlation time. The autocorrelation function of the intensity at an angle θ can be analysed to yield the distribution of relaxation times. The decay rates of the relaxation modes provide translational diffusion coefficients. From these, the hydrodynamic radius of the constituent particles can be obtained using the Stokes-Einstein equation." [16]

2.9. Cryogenic transmission electron microscopy (CryoTEM)

In order to resolve structures on a nanometre scale, it is not possible to use light microscopes that relies on visible light (wavelength ~400 nm) to create an image. However, electrons can be accelerated to such high speeds, that their wavelengths decrease to a few picometres [18]. Therefore, by using an electron beam, electron microscopes (EM) are suitable to create images with a much better resolution than light microscopes.

There are two main types of electron microscopes: scanning electron microscope (SEM) and transmission electron microscope (TEM). SEM creates an image by detecting reflected or knocked-off electrons, and it provides information on the sample's surface and its composition. TEM uses transmitted electrons (that pass through the sample) to create an image, and it provides information about the inner structure of the sample, such as its morphology [19].

EM operates under vacuum, which requires sample preparation in the form of fixation and/or dehydration. This could be a huge disadvantage of EM, because these processes may affect the size and morphology of the sample of interest [20].

Cryogenic transmission electron microscopy (CryoTEM) involves analysing the sample in cryogenic conditions. However, if an aqueous sample is frozen too slowly, then ice crystals will be formed which disrupts the electron beam, and hence prevents good imaging.

Therefore, a CryoTEM sample is prepared [21] by:

i. Applying the (aqueous) liquid onto a perforated carbon film supported on a TEM copper grid.
ii. Blotting the grid with solvent-absorbent filter paper to remove excess solution; this creates a thin film on top of the grid.
iii. Rapidly plunging the sample into liquid ethane.

This last step ensures that the thin film is vitrified. This means that the liquid is in an amorphous, glass-like state, while no solid-like ice crystals are formed.

The most important advantage of CryoTEM is that the particles in the sample are trapped and can be seen in their native conformation [20].

2.10. Germanium gamma detector

A high-purity germanium detector can be used to measure the gamma spectrum of an isotope. Essentially, it consists of a piece of solid material (germanium, which is a semiconductor) in which electrons and holes are produced when a gamma ray is absorbed [22].

When a high-energy photon passes through the material, it can ionise the atoms (electrons get excited) of the semiconductor to produce the electron-hole pairs. The number of electron-hole pairs that are created is proportional to the energy of the photon. When an electric field is applied, the electrons and holes are collected to provide an electric pulse, which contains information about the energy of the photon [22][23].

The number of such pulses (per unit time) provides information about the intensity of the radiation [23]. An example of the gamma spectrum for Ga-68 is shown in **Figure 7**. Here the 511 keV annihilation peaks are clearly visible.

It is not possible to operate a germanium gamma detector at room temperature, since the thermal energy would generate too much electron-hole pairs (the band gap energy is only 0.7 eV), which would result in too much background noise. Therefore, it is operated at very low temperatures, usually using liquid nitrogen [22][23]

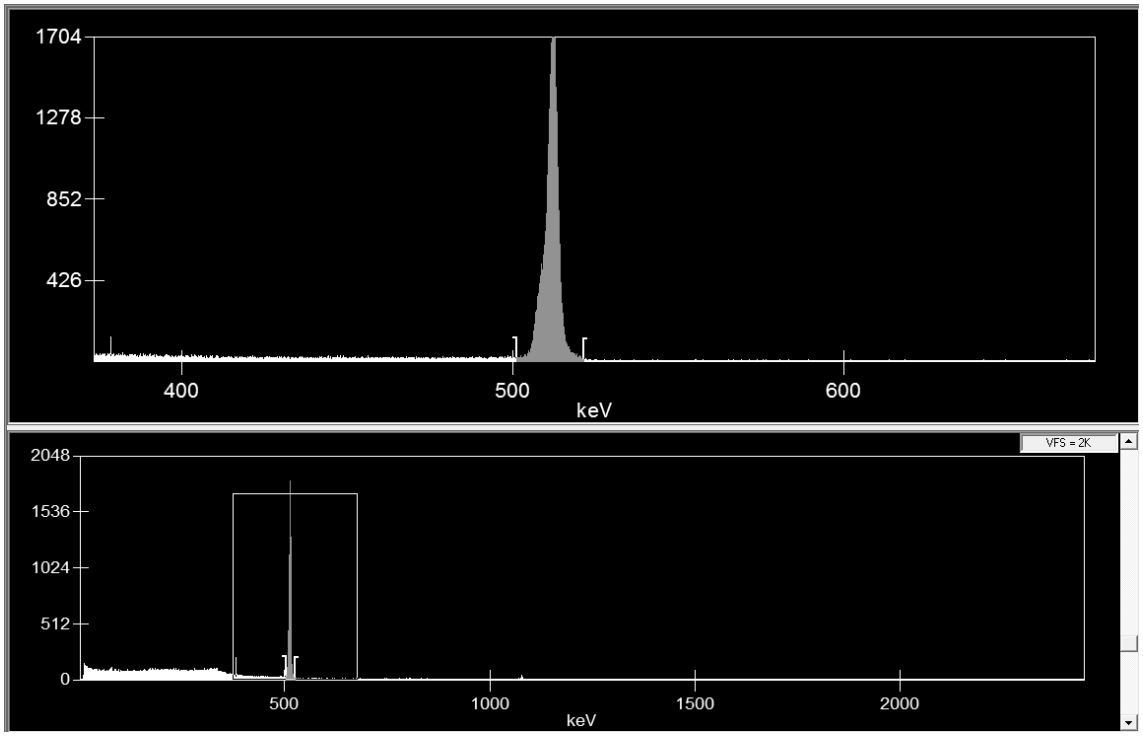

Figure 7. Number of pulses vs. energy. Example of a gamma spectrum of Ga-68.

2.11. Speciation of gallium in aqueous solution

Gallium in aqueous solution has a +3 oxidation state and it can form different complexes depending on pH, temperature and gallium concentration. Polynuclear species of gallium, such as $[Ga_{26}(OH)_{65}]^{13+}$, are reported to exist in solutions with more than 1.4 mM of gallium [24][25]. This is of no concern in radiochemistry since the gallium concentration in radiolabelling is several orders of magnitude lower than that.

Below 0.14 mM of gallium, only mononuclear complexes are reported to exist in solution, such as: $GaOH^{2+}$, $Ga(OH)_2^+$, $Ga(OH)_3$, $Ga(OH)_4^-$ [24][25]. Note that these are shorthand notations in which H_2O ligands are omitted.

Table 2. Overview of the speciation of gallium at 25°C as function of pH found throughout literature.

Speciation	**pH range and comment**	**reference**
$[Ga(H_2O)_6]^{3+}$	Practically not hydrolysed at pH < 1 (i.e. nearly 100% of gallium is in this form at pH < 1)	[26][27] [28][29]
	Dominating specie at pH below 3	[24][28]
	Exists between pH 1 and pH 4.5	[28]
	Exists at pH below 5. Dominating specie at pH below 4.	[30]
$[Ga(OH)(H_2O)_5]^{2+}$	Exists between pH 1 and pH 5. Dominating specie between pH 3 and pH 4.5	[28]
	Exists at pH > 1	[26]
	Exists at pH > 3	[24]
	Exists at pH below 5.	[30]
$[Ga(OH)_2(H_2O)_4]^+$	Exists between pH 3 and pH 5.5	[28]
	Exists at pH > 2.5	[26]
	Exists at pH > 3	[24]
	Exists between pH 3 and pH 6	[30]
$[Ga(OH)_3(H_2O)_3]$ or $Ga(OH)_3$ (s)	Exists between pH 3.5 and pH 6	[28]
	Precipitated between pH 3 and pH 7.5	[24]
	Exists between pH 3.5 and pH 8. Dominating specie between pH 4.5 and pH 6	[30]
$Ga(OH)_4^-$	Dominating specie at pH > 5-6	[25][27]
	Exists at pH > 3.5. Dominating specie at pH > 4.5	[28]
	Dominating specie at pH > 7.5	[24]
	Exists at pH > 4.5. Dominating specie at pH > 6.	[30]

At pH < 1, gallium is almost entirely present in its unhydrolyzed form as $[Ga(H_2O)_6]^{3+}$. [26][27][28][29]

At increasing pH values, it can hydrolyse successively to produce other octahedral complexes:

$$[Ga(H_2O)_6]^{3+} + H_2O \rightleftharpoons [Ga(OH)(H_2O)_5]^{2+} + H_3O^+ \quad (2.21)$$

$$[Ga(OH)(H_2O)_5]^{2+} + H_2O \rightleftharpoons [Ga(OH)_2(H_2O)_4]^+ + H_3O^+ \quad (2.22)$$

$Ga(OH)_2^+$ can hydrolyse further to $Ga(OH)_3$, which is known to be poorly soluble. Precipitation can be expected, so two equations are suggested:

$$[Ga(OH)_2(H_2O)_4]^+ + H_2O \rightleftharpoons [Ga(OH)_3(H_2O)_3] + H_3O^+ \quad (2.23)$$

or

$$[Ga(OH)_2(H_2O)_4]^+ + H_2O \rightleftharpoons Ga(OH)_3(s) + H_3O^+ + 3H_2O \quad (2.24)$$

$Ga(OH)_3(aq)$ can continue to hydrolyse into the negative $Ga(OH)_4^-$ ion. In contrary to the above mentioned octahedral complexes (with coordination number 6), it is reported [31] that it is not known how many water molecules are coordinated to $Ga(OH)_4^-$, so possible coordinating water molecules are omitted in the chemical equation:

$$Ga(OH)_3(aq) + H_2O \rightleftharpoons Ga(OH)_4^- + H^+ \quad (2.25)$$

Different gallium complexes are present simultaneously in solution at a certain pH value, since gallium partakes in multiple, competing equilibria. Several papers have described the speciation of gallium as function of pH, and an overview is given in **Table 2**. It can be seen that $[Ga(H_2O)_6]^{3+}$ is predominant at low pH, while $Ga(OH)_4^-$ becomes predominant around neutral and high pH values. Apart from that, however, there is no clear consensus about which complex is present or predominant at what pH range.

2.11.1. Precipitation of $Ga(OH)_3$

The pH of precipitation of $Ga(OH)_3$ can be predicted [32] with the following equation:

$$pH = \frac{1}{3}\log K_{sp} - \frac{1}{3}\log[Ga^{3+}] - \log K_w \quad (2.26)$$

where K_{sp} ($7.1 \cdot 10^{-36}$) [32][33] is the solubility product of $Ga(OH)_3$, $[Ga^{3+}]$ is the concentration of gallium, K_w ($1 \cdot 10^{-14}$) is the autoionization constant of water.
So, it is expected that the pH of precipitation is a function of the gallium concentration.

A derivation of equation (2.26) is given below. Consider the following equation:

$$Ga(OH)_3(s) \rightleftharpoons Ga^{3+}(aq) + 3OH^-(aq) \quad (2.27)$$

The solubility product (K_{sp}) is given by:

$$K_{sp} = [Ga^{3+}][OH^-]^3 \quad (2.28)$$

Note that the autoionization constant of water (K_w) is equal to:

$$K_w = [H_3O^+][OH^-] \quad (2.29)$$

and the solubility product can then be rewritten as:

$$K_{sp} = [Ga^{3+}]\left(\frac{K_w}{[H_3O^+]}\right)^3 \quad (2.30)$$

Taking the logarithm of both sides of the equation, and rearranging yields:

$$\log K_{sp} = \log[Ga^{3+}] + 3\log K_w - 3\log[H_3O^+] \quad (2.31)$$

$$pH = -\log[H_3O^+] = \frac{1}{3}\log K_{sp} - \frac{1}{3}\log[Ga^{3+}] - \log K_w \quad (2.32)$$

2.12. Speciation of tropolone in aqueous solution

Tropolone is a lipophilic, bidentate ligand with two oxygen atoms (in this section, these will be labelled as 'O1' and 'O2') that both can be (de)protonated. Its pK_a values [34] are pK_{a1} = 0.0, pK_{a2} = 6.7, and its structure is shown in **Figure 8**.

The speciation of tropolone as function of pH can be estimated using the equation for the ratio of a base and its conjugate acid (see Appendix D):

$$\left(\frac{[A^-]}{[HA]}\right) = 10^{pH-pK_a} \tag{2.33}$$

where $[A^-]$ denotes the concentration of a base, and [HA] its conjugate acid.

- If pH << pK_{a1} = 0.0, then both oxygen atoms are completely protonated, and "tropH_2^+" is the dominating tropolone specie in solution.
- If pH = pK_{a1} = 0.0, then O1 is expected to be 50% protonated, while O2 is completely protonated. An equal mixture of "tropH_2^+" and "tropH" is expected to be present in solution.
- If pH = pK_{a2} = 6.7, then O1 is expected to be completely deprotonated, while O2 is expected to be 50% deprotonated. An equal mixture of "tropH" and "trop$^-$" is expected to be in solution.
- If pH >> pK_{a2} = 6.7, then both oxygen atoms are completely deprotonated, and "trop$^-$" is the dominating tropolone specie in solution.
- If 0 < pH < 6.7, then O1 is mostly deprotonated, while O2 is mostly protonated. In this pH range, "tropH" is expected to be the dominating tropolone specie in solution.

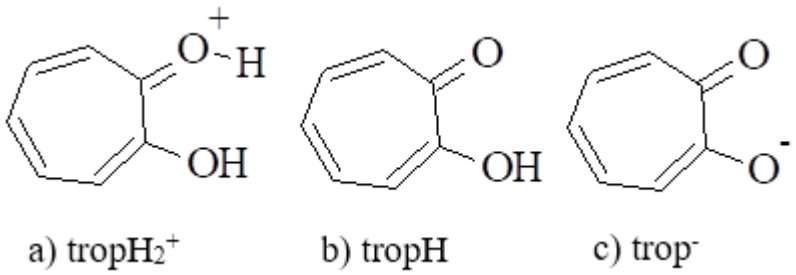

Figure 8. Structures of tropolone in its a) positively charged, b) neutral, and c) negatively charged form.

2.13. HEPES buffer characteristics

4-(2-hydroxyethyl)piperazine-1-ethanesulfonic acid (HEPES) is a zwitterion that is mainly used for its buffer capacity. See **Figure 9**.

It is reported [35] that the sulfonate group of HEPES is completely dissociated over almost the whole pH range.

The buffer capacity comes from the two nitrogens of the piperazine ring at position 1 (labelled N_1) and position 4 (labelled N_4). The *pKa* of N_1 is 3.0, and the *pKa* of N_4 is 7.5 [35][36][37].

The reported isoelectric point of HEPES is 5.0 [35][36], which is close to the predicted value (5.25) using the calculation of Appendix E. It should be noted that HEPES does not have any buffer capacity around this pH value.

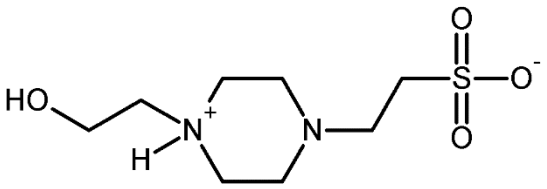

Figure 9. Structure of HEPES in its zwitterionic form. In this figure N_1 is deprotonated, while N_4 is protonated.

3. Materials & Methods

3.1. Materials

For the preparation of buffer solutions:

Milli-Q® water (Merck Millipore).
HEPES, ≥99.5% (4-(2-hydroxyethyl)piperazine-1-ethanesulfonic acid); NaOH pellets; HCl, fuming, ≥37 w%; acetic acid, glacial, ≥99.85%; sodium acetate anhydrous, >99% were all purchased from Sigma Aldrich, the Netherlands.

For tropolone extraction:

Tropolone (2-hydroxy-2,4,6-cycloheptatrien-1-one) was purchased from Merck, Germany; chloroform, ≥99.8%, containing ethanol as stabilizer, was purchased from Sigma Aldrich, the Netherlands.

Hydrophilic chelators:

DOTA (1,4,7,10-Tetraazacyclododecane-N,N',N'', N'''-tetraacetic acid; 98%) was purchased from abcr, Germany; NOTA (2,2′,2”-(1,4,7-triazacyclononane-1,4,7-triyl)triacetic acid) was purchased from CheMatech, France; DTPA (diethylenetriaminepentaacetic acid) Titriplex® V was purchased from Merck, Germany.

For polymersome preparation:

The diblock copolymer poly(1,2-butadiene)-b-poly(ethylene oxide) {PBd(1800 g mol^{-1})-b-PEO(600 g mol^{-1})} (M_w/M_n = 1.09) was purchased from Polymer Source, Canada.

Equipment

A GalliaPharm® $^{68}Ge/^{68}Ga$ generator from Eckert & Ziegler was used to obtain gallium-68. A peristaltic pump was used for the elution.

A High-Purity Germanium detector (Princeton Gamma-Tech, model: LG 22) was used for measuring gamma annihilation peaks. Glass scintillation vials (20 mL) from PerkinElmer Nederland B.V. (the Netherlands) were used during these measurements.

A pH meter (Metrohm 744) was used to measure the pH.of buffers and solutions.

A vortex mixer (Vortex Genie 2) was used for extraction to mix phases.

The Lipex Extruder (Northern Lipids Inc, Canada) was used for extrusion of polymersomes. Whatman® Nuclepore™ Track-Etch Membrane polycarbonate filters of diameter 800 nm, 400 nm and 200 nm were used during extrusion.

Sephadex G-25 (Sigma Aldrich, the Netherlands) and PD10 Desalting Columns (GE Healthcare, UK) were used for size exclusion chromatography (SEC).

Dynamic Light Scattering (DLS) was used to determine the hydrodynamic radius of polymersomes. The setup consisted of a JDS Uniphase 633 nm 35 mW laser, a fiber detector, an ALV-5000/epp correlator, an ALV sp 125 s/w 93 goniometer and a Perking Elmer photon counter. ALV-5000 software was used for this setup.

Cryogenic transmission electron microscopy (CryoTEM) was used to characterize the prepared nanoparticles. The setup consists of carbon, holey films (Quantifoil 1.2/1.3, Cu 200 mesh grids) on which solution was pipetted. This was rapidly plunged in liquid ethane, and then placed in a Cryo Transfer Holder (Gatan 626). Images were obtained with a Jeol JEM-1400 Transmission Electron Microscope at an acceleration voltage of 120 keV.

3.2. Methods

3.2.1. Elution of gallium-68

A GalliaPharm® $^{68}Ge/^{68}Ga$ generator of Eckert & Ziegler (1.11 GBq, on calibration date 19/5/2015) was used to obtain ^{68}Ga. A peristaltic pump was used to pass through 5 mL HCl (0.1 M) eluent at a rate of about 1 mL per minute through the generator. The eluate ([^{68}Ga]gallium chloride) was retrieved in one fraction of 5 mL.

With a calibrated detector, the activity of 5 mL eluate was determined to be 25 MBq at the start of the project. This is equivalent to 100 kBq per 20 µL. During the course of the project this decreased to roughly 60 kBq per 20 µL due to decay of the parent radionuclide Ge-68.

The generator was eluted once or twice per day. In case it was used twice per day, there was at least 4 hours between the first and second elution. When the generator had not been used for a few days, the generator was eluted with 10 mL HCl (0.1M) and the eluate was considered waste.

3.2.2. ^{68}Ga count rate measurement

The count rate measurements of activity of ^{68}Ga were carried out with a germanium gamma detector. A vial with activity was placed at a fixed distance from the detector, after which the total counts (N) of the gamma spectrum with energy levels between 501 keV and 521 keV were measured during a 90 second interval. All further mentioned counting experiments of ^{68}Ga in this report refer to this procedure of measuring the gamma energy annihilation peak.

3.2.3. Preparation of buffer solutions

HEPES (50 mM) buffers {pH = 2.0, 3.0, 3.5, 4.0} were prepared by dissolving HEPES powder in Milli-Q, and the pH was adjusted by adding a solution of HCl 1M under stirring, while measuring the pH with a pH meter. Once the right pH was obtained, a volume of Milli-Q was added to obtain a concentration of 50 mM HEPES.

HEPES (50 mM) buffers {pH = 6.5, 7.5, 8.5} were prepared by dissolving HEPES powder in Milli-Q, and the pH was adjusted by adding a solution of NaOH 1M under stirring, while measuring the pH with a pH meter. Once the right pH was obtained, a volume of Milli-Q was added to obtain a concentration of 50 mM HEPES.

Acetic acid / acetate buffer (pH 4.9) was created by adding 167 µL of CH_3COOH (l) to 435.3 mg CH_3COONa (s), and diluting it by adding 26.36 mL Milli-Q. The solution was stirred, and the pH was measured with a pH meter and determined to be 4.9.

3.2.4. Determining the pH dependency of tropolone binding to ^{68}Ga

3.2.4.1. Formation of the [^{68}Ga]Ga-tropolone complex

1.00 mL of buffer solution (various pH, see §3.2.3) was pipetted into a glass liquid scintillation vial, after which 10.0 µL tropolone (2.0 mM) was added. Note that this creates a solution with a tropolone concentration of 20 µM.
Then 20.0 µL (approx. 60-100 kBq of ^{68}Ga) of eluate of the ^{68}Ge/^{68}Ga generator was pipetted into the solution. The vial was gently swirled by hand for a few seconds and was left to incubate for 10 minutes at room temperature (20 ± 1 °C) to allow the formation of the [^{68}Ga]Ga-tropolone complex.

Some experiments were performed with 10.0 µL of tropolone (0.2 mM) or (2 µM), instead of (2.0 mM), to determine formation of the Ga-tropolone complex at lower concentration of tropolone.

3.2.4.2. Liquid-liquid extraction of the [^{68}Ga]Ga-tropolone complex

After formation of the [^{68}Ga]Ga-tropolone complex, 1.00 mL chloroform was pipetted into the solution using a prewetted pipette tip. The immiscible (aqueous and organic) phases were mixed thoroughly using a vortex mixer for 20 seconds, after which the mixture was left standing to allow the two phases to separate by gravity.

Subsequently, a fraction (0.80 mL) of the (bottom) organic phase was transferred to a second glass vial using a prewetted pipette tip, leaving behind the aqueous phase and the remainder of the organic phase in the first vial. See **Figure 10**.

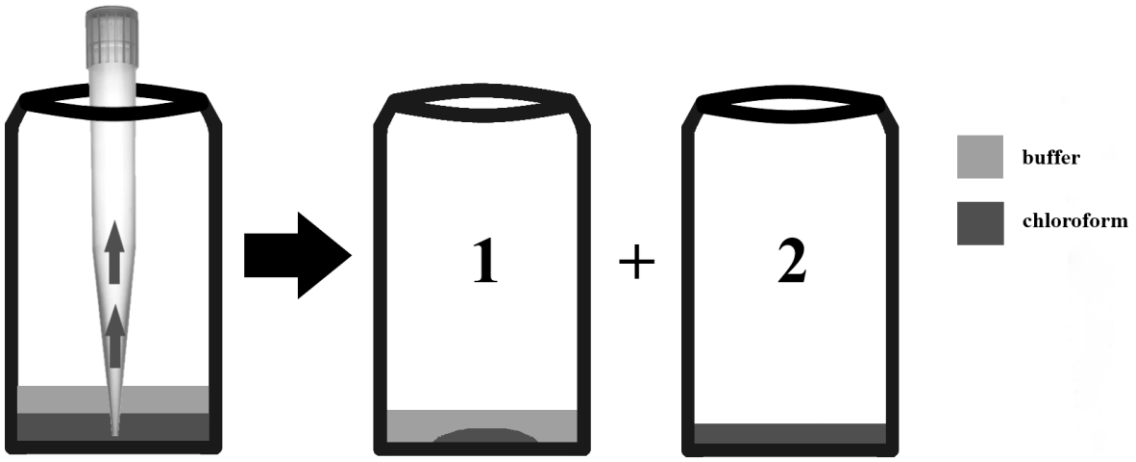

Figure 10. Separation of a fraction of the organic phase (chloroform) to a second vial. The remainder of the organic phase stays in vial 1, together with the aqueous phase (buffer).

Finally, the number of counts of the gamma energy annihilation peak of both vials was measured using a germanium gamma detector. This data was used in equation (3.4) as a measure of what percentage of ^{68}Ga was bound to tropolone.

3.2.4.3. Control experiment: liquid-liquid extraction of ^{68}Ga without tropolone

Liquid-liquid extraction control experiments were performed to validate the assumption that all unbound ^{68}Ga (not bound to tropolone) stays in the aqueous phase. These experiments were performed at each pH using the exact same method as described in §3.2.4.2, but without the addition of tropolone.

3.2.5. *Calculation of RCY of ^{68}Ga bound to tropolone*

The radiochemical yield (*RCY*) of ^{68}Ga bound to tropolone can be defined as:

$$RCY = \frac{A_{Ga-trop}}{A_{Ga-trop} + A_{Ga-unbound}} \cdot 100\% \quad (3.1)$$

where $A_{Ga\text{-}trop}$ is the activity of ^{68}Ga bound to tropolone; $A_{Ga\text{-}unbound}$ is the activity of ^{68}Ga not bound to tropolone.

If the assumption is made that all [^{68}Ga]Ga-tropolone complex gets extracted from the aqueous phase and is transferred to the organic phase, and if all unbound ^{68}Ga stays in the aqueous phase, then eq. (3.1) is equal to:

$$RCY = \frac{A_c}{A_c + A_a} \cdot 100\% \quad (3.2)$$

where A_c is the activity of ^{68}Ga in the organic phase; A_a is the activity of ^{68}Ga in the aqueous phase.

Furthermore, if a homogeneous distribution of all activity of ^{68}Ga in the organic phase is assumed, then the activity of a volume fraction of the organic phase can be used as a measure to calculate the activity of the total volume of the organic phase:

$$A_c = \frac{A_2}{\phi} \quad (3.3)$$

where φ is a volume fraction of the organic phase; A_2 is the activity of ^{68}Ga of this volume fraction.

With the experimental set-up of measuring the number of counts produced by the 511 keV annihilation peaks at a constant distance from the germanium gamma detector (§3.2.2), it is expected that the measured number of counts (*N*) is proportional to the activity :

$$N \sim A$$

After separating a volume fraction of organic phase to 'vial 2' (see **Figure 10**), the *RCY* was calculated using the measured number of counts of 'vial 2' and the number of counts of the remaining content in 'vial 1':

$$RCY = \frac{N_2^{corr}}{\phi \cdot (N_2^{corr} + N_1)} \cdot 100\% \quad (3.4)$$

where N_2^{corr} is the time-corrected number of counts in the volume fraction (φ) of transferred organic phase ('*vial 2*');
N_1 is the measured number of counts in the aqueous phase plus the remainder of the non-transferred organic phase ('*vial 1*'); and:

$$N_2^{corr} = N_2 \cdot 2^{\Delta t / T_{1/2}} \quad (3.5)$$

where N_2 is the actual measured number of counts in the volume fraction of transferred organic phase;
Δt is the time between the measurement of N_1 and N_2;
$T_{1/2}$ is the half-life of ^{68}Ga (67.71 min).

It should be noted that the formulation of eq. (3.4) and eq. (3.5) holds the implication that the measurement of N_1 took place before the measurement of N_2.

3.2.6. The substitution of tropolone in the [^{68}Ga]Ga-tropolone complex with a hydrophilic chelator

In this section the term 'hydrophilic chelator' refers to
DOTA (1,4,7,10-Tetraazacyclododecane-N,N',N'', N'''-tetraacetic acid),
NOTA (2,2′,2''-(1,4,7-triazacyclononane-1,4,7-triyl)triacetic acid)
or **DTPA** (diethylenetriaminepentaacetic acid).

3.2.6.1. Control experiment: binding ^{68}Ga to hydrophilic chelator

1.00 mL of HEPES (50 mM) buffer solution (pH 4.0, 6.5 or 7.5) was pipetted into a glass liquid scintillation vial, after which 20.0 µL of hydrophilic chelator (1.0 mM) was added. Then 20.0 µL (approx. 60-100 kBq of ^{68}Ga) of eluate of the ^{68}Ge/^{68}Ga generator was pipetted into the solution. The vial was gently swirled by hand for a few seconds and was left to incubate for 10 minutes at room temperature (20 ± 1 °C) to allow the formation of the [^{68}Ga]Ga-hydrophilic chelator complex. Subsequently, 10.0 µL tropolone (2.0 mM) was pipetted into this solution. Again, the vial was gently swirled by hand for a few seconds and was left to incubate for 10 minutes at room temperature to allow the formation of the [^{68}Ga]Ga-tropolone complex.

After this, 1.00 mL chloroform was pipetted into this vial using a prewetted pipette tip, and the same extraction experiment and counting experiment were performed as described in §3.2.4.2.

3.2.6.2. The exchange of tropolone for hydrophilic chelator

First [^{68}Ga]Ga-tropolone complex was formed at room temperature in 1 mL buffer solution in a glass vial as described in §3.2.4.1. Then 20.0 µL of hydrophilic chelator (1.0 mM) was pipetted into solution, after which the vial was swirled for few seconds. Subsequently, this vial was heated in an oven (60-90°C) or water bath (30-60°) and left to incubate for times, ranging 10 to 60 minutes. After this, the vial was removed from the oven or water bath and cooled down at room temperature for 15-20 minutes. Then 1.00 mL chloroform was pipetted into this solution using a prewetted pipette tip, and the same extraction experiment and counting experiment were performed as described in §3.2.4.2.

3.2.7. The loading of ^{68}Ga into polymersomes

3.2.7.1. Formation of polymersomes

Polymersomes were formed by dissolving PBd_{33}-PEO_{14} (1800-600 g mol^{-1}) block copolymer at various polymer concentration (2 mg/mL or 5 mg/mL) in solutions containing DTPA(1mM) / HEPES buffer at various pH (4.0, 6.5 and 7.4). See **Table 4**, §4.3.5 for an overview of polymersome solutions used in this report.

Procedure: The polymer (soft, gel-like structure) was added to a glass vial and weighted. A volume of DTPA (1 mM) / HEPES buffer solution was pipetted into the vial to create 2 mg/mL or 5 mg/mL polymer concentration. A magnetic stirrer was added, and the mixture was stirred at 500 rpm in a closed vial for 1 week. Upon stirring the polymer gets dissolved, and within 1 or 2 days it was observed that the solution becomes whitish.

3.2.7.2. Extruding the polymersomes

Double layer of 800 nm filter was placed in the extruder. Then the polymersome solution was passed through the filters twice with a pressure of 200 psi.

Then a double layer of 400 nm filter was placed in the extruder and the solution was passed through the filters twice with a pressure of 200 psi.

After this a double layer of 200 nm filter was placed in the extruder and the solution was passed through the filters 4 times with a pressure of 300 psi.

3.2.7.3. Removing DTPA outside of the polymersomes

DTPA outside of polymersomes was removed from solution by using a Sephadex G-25 column (D = 1 cm, L = 28-31 cm). 1 mL polymersome solution was added to the column, and the 1 mL volume fraction exiting the column was collected. Then the same procedure was repeated with 1 mL HEPES (10 mM) buffer {pH = 4.0, 6.5 or 7.5} and a total of 13 fractions of 1 mL were collected.

It was observed that fractions 9-12 were whitish (contains polymersomes), depending on the column length.

The column was rinsed with 150 mL buffer solution before reusing.

3.2.7.4. The loading of ^{68}Ga into polymersomes

200 µL HEPES buffer (500 mM, pH 4.0 or pH 6.5) was pipetted into a glass vial. Then 10.0 µL tropolone (2.0 mM) was added. Then 20.0 µL (approx. 60-100 kBq of ^{68}Ga) of eluate of the ^{68}Ge/^{68}Ga generator was pipetted into the solution. The vial was gently swirled by hand for a few seconds and was left to incubate for 10 minutes at room temperature (20 ± 1 °C) to allow the formation of the [^{68}Ga]Ga-tropolone complex.

Then 0.80 mL polymersome solution, of which the DTPA outside the polymersomes was removed, was added to the vial. This was heated in an oven (50-90°C) or in a water bath (50-60°C) for variable time (10-60 minutes). Then the sample was removed from the heat source and cooled down at room temperature for 15-20 minutes.

3.2.8. Determining the loading efficiency

The initial number of counts of the vial with loaded polymersomes was measured with the germanium gamma detector, and the exact time of the measurement was noted.

1 mL sample was passed through a PD10 column, and a 1 mL fraction was collected. Then the same procedure was repeated with 1 mL HEPES (10 mM) buffer {pH = 4.0, 6.5 or 7.5} and a total of 8 fractions of 1 mL were collected. The number of counts of each vial, including the 'empty' vial with potentially leftover initial solution, was measured using the germanium gamma detector. The maximum loading efficiency (LE_{max}) was calculated using equation (4.11), and the 'lower bound estimate of the loading efficiency' (LE_{low}) was calculated using equation (4.12).

3.2.9. Standard deviation and standard error

The sample standard deviation (*SD*) was calculated with:

$$SD = \sqrt{\frac{1}{n-1}\sum_{i=1}^{n}(x_i - \bar{x})^2} \tag{3.6}$$

where n is the number of data values; x_i is a data value; $\bar{x}$ is the mean.

The standard error of the mean (*SE*) was estimated by dividing the sample standard deviation by the square root of n:

$$SE \approx \frac{SD}{\sqrt{n}} \tag{3.7}$$

In this report, values or error bars in figures are represented as (mean ± 1 *SD*), **unless stated otherwise.**

3.2.10. Control experiment: elution profiles PD10 column

3.2.10.1. Elution profile of 'free' Ga-68 in buffer {pH 4.0 or pH 6.5}

200 µL HEPES buffer (500 mM, {pH 4.0 or pH 6.5}) was pipetted into a glass vial. Then 20.0 µL (approx. 60-100 kBq of ^{68}Ga) of eluate of the ^{68}Ge/^{68}Ga generator was pipetted into the solution. Then 800 µL HEPES buffer (50 mM, {pH 4.0 or pH 6.5}) was added, and the vial was gently swirled by hand for a few seconds. After the initial number of counts of this solution was measured, a 1 mL sample was passed through a PD10 column and the same procedure as described in §3.2.8 was followed to collect 8 fractions to create the PD10 elution profile.

3.2.10.2. Elution profile of Ga-tropolone in buffer {pH 4.0 or pH 6.5}

200 µL HEPES buffer (500 mM, {pH 4.0 or pH 6.5}) was pipetted into a glass vial. Then 10.0 µL tropolone (2.0 mM) was added. Then 20.0 µL (approx. 60-100 kBq of ^{68}Ga) of eluate of the ^{68}Ge/^{68}Ga generator was pipetted into the solution. The vial was gently swirled by hand for a few seconds and was left to incubate for 10 minutes at room temperature (20 ± 1 °C) to allow the formation of the [^{68}Ga]Ga-tropolone complex. After this, 800 µL HEPES buffer (50 mM, {pH 4.0 or pH 6.5}) was added, and the vial was gently swirled by hand for a few seconds. After the initial number of counts of this solution was measured, a 1 mL sample was passed through a PD10 column and the same procedure as described in §3.2.8 was followed to collect 8 fractions to create the PD10 elution profile.

3.2.10.3. Elution profile of Ga-DTPA in buffer {pH 4.0 or pH 6.5}

200 µL HEPES buffer (500 mM, {pH 4.0 or pH 6.5}) was pipetted into a glass vial. Then 10.0 µL tropolone (2.0 mM) was added. Then 20.0 µL (approx. 60-100 kBq of ^{68}Ga) of eluate of the ^{68}Ge/^{68}Ga generator was pipetted into the solution. The vial was gently swirled by hand for a few seconds and was left to incubate for 10 minutes at room temperature (20 ± 1 °C) to allow the formation of the [^{68}Ga]Ga-tropolone complex.

After this, 800 µL HEPES buffer (50 mM, {pH 4.0 or pH 6.5})/DTPA (1 mM) was added, and the vial was gently swirled by hand for a few seconds. This was heated in a heat source for 10 minutes, after which it got removed from the heat source and cooled down at room temperature for 15 minutes. (For the experiment with pH 6.5, the heat source was an oven at 70 °C. For the experiment with pH 4.0, the heat source was a water bath at 50 °C)

After the initial number of counts of this solution was measured, a 1 mL sample was passed through a PD10 column and the same procedure as described in §3.2.8 was followed to collect 8 fractions to create the PD10 elution profile.

3.2.10.4. Elution profile of Ga-tropolone in buffer {pH 6.5} after heating

This control experiment follows the same steps as described in §3.2.10.2. The only difference was that after the [^{68}Ga]Ga-tropolone formation step, the solution was placed in an oven at 70 °C for 10 minutes, after which the solution was cooled down at room temperature for 10 minutes. Then the PD10 elution profile was created following the same procedure as described in §3.2.10.2.

3.2.11. Additional control experiments

3.2.11.1. Control experiment Sephadex column: determining whether all DTPA outside of the polymersomes was removed

1 mL DTPA (1 mM, pH 4.0) was added to a Sephadex column (DxL = 1x30 cm), and 12 fractions of 1 mL were collected using HEPES (10 mM, pH 4.0) as eluent.

200 µL HEPES (500 mM, pH 4.0) was pipetted into a vial, after which 10 µL tropolone (2 mM) was added, and 20 µL of Ga-68 eluate was added. This was left to incubate for 10 minutes to allow the formation of Ga-tropolone complex.

Then 0.80 mL of 'Sephadex fraction 1' was added. The solution was heated for 10 minutes at 50 °C.

After this, 1 mL chloroform was added to perform an extraction experiment similar to §3.2.4.2, and the percentage of activity in the organic phase was determined.

These extraction experiments were also done with 'Sephadex fraction number 9, 10, 11, 12'.

3.2.11.2. Removing DTPA outside of the polymersomes, modified method

Additional experiments were performed using a modified method to remove DTPA outside of polymersomes. It follows the exact same procedure of §3.2.7.3, but after collecting 1 mL of whitish polymersome containing fraction, this fraction was passed through another Sephadex column, to completely ensure the removal of DTPA.

3.2.11.3. Control experiment: loading Ga-68 into polymersomes, after acidifying the sample before passing it through PD10 column

Polymersome sample 'PS-D' (2 mg/mL, pH 7.4) see §4.3.5, was used for this one control experiment.

First DTPA outside of polymersomes was removed following the procedure of §3.2.11.2

200 µL HEPES (500 mM, pH 6.5) was pipetted into a vial, after which 10 µL tropolone (2 mM) was added, and 20 µL of Ga-68 eluate was added. This was left to incubate for 10 minutes to allow the formation of Ga-tropolone complex.

Then 0.80 mL of polymersome sample without DTPA outside, was added. The solution was heated for 60 minutes at 70 °C. Then the initial number of counts was determined.

After a PD10 column was washed with 25 mL HCl 1M (pH 0.0), 200 µL of HCl (1 M, pH 0.0) was added to the polymersome sample to acidify it. Then 1 mL of this sample was passed through the PD10 column using 1 M HCl as eluent.

After this, the maximum loading efficiency was determined.

4. Results and Discussion

4.1. Liquid-liquid extraction [^{68}Ga]Ga-tropolone complex

In this experiment the formation of [^{68}Ga]Ga-tropolone complex as function of pH and tropolone concentration was investigated.

The complex forming of tropolone with Ga-68 was performed in an aqueous buffer, using the property that tropolone can dissolve in water. It was chosen to allow only 10 minutes for the formation of Ga-tropolone complex to keep the loss of activity as small as possible (half-life of Ga-68 is only 67.71 minutes). A liquid-liquid extraction with chloroform was chosen as the experimental method to separate Ga-tropolone complex from unbound gallium. This makes use of the property that tropolone is more hydrophobic than hydrophilic, so that Ga-tropolone complex should be present in the organic layer after extraction.

By separating the aqueous and organic phase, it is possible to determine how much Ga-68 is bound to tropolone by measuring the number of counts of 511 keV gamma energy annihilation peaks of the organic phase compared to the aqueous phase, using the fact that Ga-68 is a positron emitter. However, it is practically impossible to perfectly separate the organic phase from the aqueous phase. So only a fraction of the organic phase was separated. This was done by pipetting a volume fraction of chloroform (using a prewetted pipette tip to prevent dripping) out of the organic phase. The number of counts in the volume fraction was used as a measure of the number of counts in the total volume of the organic phase, and the radiochemical yield was calculated using eq. (3.4). The results are found in **Figure 11**.

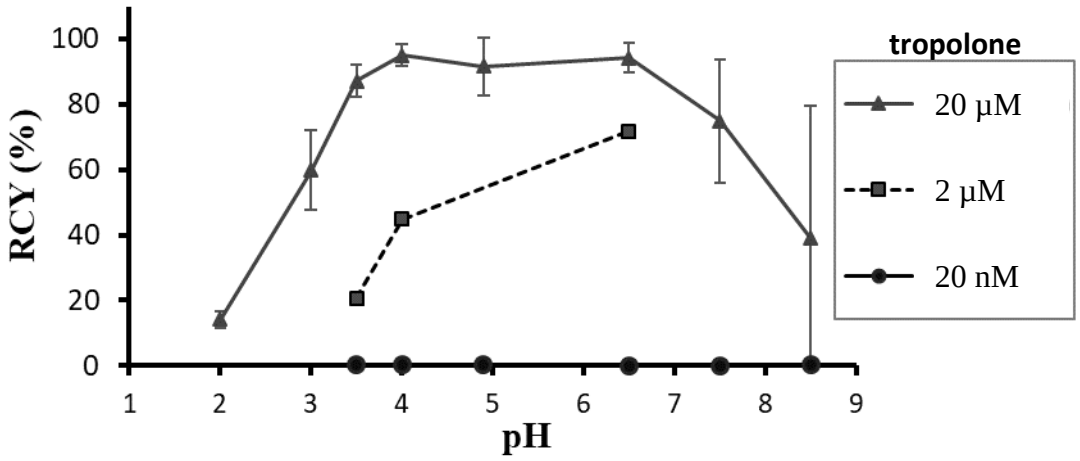

Figure 11. Radiochemical yield of Ga-68 bound to tropolone as function of pH at three different tropolone concentrations. The activity of Ga-68 was approx. 60-100 kBq, corresponding to a gallium concentration of (0.6 – 1) x 10^{-12} M.
Error bars represent (**mean ± 2 SE**). *n* =1 for tropolone (2 µM) and tropolone (20 nM).
For trop (20 µM), *n* is {4, 4, 13, 12, 4, 6, 7, 4} at pH is {2.0, 3.0, 3.5, 4.0, 4.9, 6.5, 7.5, 8.5} respectively.

It can be observed that tropolone (20 µM) binds well to gallium (0.6 - 1 pM) at pH between 4.0 and 6.5. Note that the concentration of tropolone (20 µM) is 20 million times higher than that of gallium. A 10 times lower concentration of tropolone (2 µM) leads to much lower RCY, and tropolone (20 nM) leads to no higher measured activity in the organic phase compared to experiments without tropolone.

4.1.1. Discussion

The eluate that is retrieved from the $^{68}Ge/^{68}Ga$ generator consists of a $GaCl_3$ solution at pH 1. It is reasonable to neglect complexation between Ga^{3+} and Cl^-, since this only becomes significant at very high chloride ion concentration [38][39][40]. Therefore it is presumed that gallium in the eluate exists as the $[Ga(H_2O)_6]^{3+}$ specie, similar to gallium in aqueous solution at pH 1 as described in chapter §2.11.

When the eluate is pipetted into the tropolone containing buffer solution, the formation of the Ga-tropolone complex is the desired reaction.

Since the presence of tropolone can make gallium soluble in chloroform in extraction experiments, it is suggested that the Ga-tropolone complex must have a neutral charge [41], because chloroform is practically a nonpolar solvent [42]. Therefore, it is proposed that tropolone acts as a bidentate ligand, in such a way that three tropolone molecules form a six-coordinate complex with one Ga^{3+} ion:

$$[Ga(H_2O)_6]^{3+} + trop^- \rightleftharpoons [Ga(trop)(H_2O)_4]^{2+} + 2H_2O \quad (4.1)$$

$$[Ga(H_2O)_4]^{2+} + trop^- \rightleftharpoons [Ga(trop)_2(H_2O)_2]^{+} + 2H_2O \quad (4.2)$$

$$[Ga(H_2O)_2]^{+} + trop^- \rightleftharpoons [Ga(trop)_3] + 2H_2O \quad (4.3)$$

However, one should be careful in assuming that *all* activity in the organic phase comes from $[Ga(trop)_3]$. Since it is possible that $[Ga(H_2O)_6]^{3+}$ can hydrolyse into $[Ga(OH)(H_2O)_5]^{2+}$ and $[Ga(OH)_2(H_2O)_4]^{+}$, it is not unthinkable that neutral species such as $[Ga(OH)(trop)_2(H_2O)]$ or $[Ga(OH)_2(trop)(H_2O)_2]$ could also be formed and be detectable in the organic phase.

Additionally, the possibility that some activity in the organic phase comes from charged complexes, such as $[Ga(trop)(H_2O)_4]^{2+}$ or $[Ga(trop)_2(H_2O)_2]^{+}$, should not be disposed. It is expected that these complexes majorly favour to stay in the aqueous phase, because they are charged. But this statement cannot be made with complete certainty because the partition coefficients from these complexes are unknown.

As observed in **Figure 11**, the *RCY* drops at pH < 4, and it also drops around neutral pH and higher pH, which suggests that less $[^{68}Ga]$Ga-tropolone complex is formed at these pH ranges. This could be explained by considering the speciation of gallium and tropolone, in aqueous solution as function of the pH.

Low pH range

At increasingly lower pH, it is likely that the protonation of tropolone becomes more dominant (see §2.12), which competes with the complexation of gallium with tropolone.

Also, the estimated isoelectric point of tropolone (pKa_1 = 0.0, pKa_2 = 6.7) is 3.35. (See Appendix E). This means that on average, tropolone is positively charged at a pH below 3.35. It could be more difficult for the positively charged tropolone molecule to react with the positively charged species of gallium $\{Ga^{3+}, Ga(OH)^{2+}, Ga(OH)_2^{+}\}$.

At low pH (but above pH 1), the formation of $Ga(OH)^{2+}$ (see §2.11) might compete with the formation of $[Ga(trop)_3]$.

Neutral / high pH range

At neutral pH and upwards, tropolone becomes more negatively charged (see §2.12), which should make it more susceptible for complex formation. However, it is

not unexpected that the formation of Ga-tropolone faces severe competition with the formation of the $Ga(OH)_4^-$ specie (see §2.11).

Furthermore, one should be aware of the possibility that the poorly soluble $Ga(OH)_3$ specie can precipitate. It is shown in §2.11.1 that the pH of precipitation is a function of gallium concentration. Using equation (2.26), it is predicted that precipitation can be expected at pH ≥ 6.3 for a gallium concentration of $1 \cdot 10^{-12}$ M.

4.1.2. Discussion of measurement errors and assumptions

Several assumptions had to be made to justify the calculation of the *RCY* as described in §3.2.5. This section will discuss measurement errors and assumptions that are associated with this calculation and corresponding experiment.

- **Systematic error at pipetting volume fraction out of organic phase.**

A minor systematic error is made when pipetting a volume fraction containing Ga-68 activity. A small amount of activity (estimation: less than 1%) stays behind in the pipette tip that was tossed away. This leads to a minor underestimation of the *RCY*.

- **Assumption: all Ga-68 that is not bound to tropolone, stays in the aqueous phase.**

This seems to be a practically correct assumption. The result of control experiments (§3.2.4.3), at which an extraction with chloroform at each pH was performed without the presence of tropolone, confirms that almost no activity (< 0.2%) is found in the organic phase.

- **Assumption: all Ga-tropolone complex is present in the organic phase after extraction with chloroform.**

This assumption cannot be true since extraction efficiency will never be 100%. So, the *RCY* as shown in **Figure 11**, can only be an underestimation.

Literature suggests [34] that the partition coefficient of tropolone in a chloroform/water system is equal to 50, which means that a notable amount (2 percent point) of tropolone stays in the aqueous phase. However, it is not valid to assume that also 2 percent point of the Ga-tropolone complex stays in the aqueous phase, because the partition coefficient of tropolone says nothing about the partition coefficient of the Ga-tropolone complex. Therefore, no quantification for the underestimation of the RCY can be given. Furthermore it should be noted that different Ga-tropolone species could be formed (see §4.1.1) with different corresponding partition coefficients.

- **Assumption: all Ga-tropolone complex in the organic phase is homogeneously distributed.**

This assumption is not necessarily true. By only separating a fraction of chloroform from the rest of the mixture, the implicit assumption is made that an absence of activity in this fraction of the organic phase, would mean that all activity is present in the aqueous phase. The possibility of a system in which molecules are mostly located in the interface of the aqueous and organic layer, is not excluded by the applied measuring method in this project. This hypothesis could be tested by separating a fraction of both the organic phase, and the aqueous phase. A lack of activity in both fractions would indicate that the Ga-tropolone complex is located at the interface of both layers.

- **Systematic error: influence of volume of liquid on count rate measurement**

Figure 12 represents count rate measurements of vials with activity at a fixed distance from a germanium gamma detector. The detector is located underneath the vials similar to the experiments conducted in §3.2.4.2, of which the results were used to calculate the *RCY* (§3.2.5).

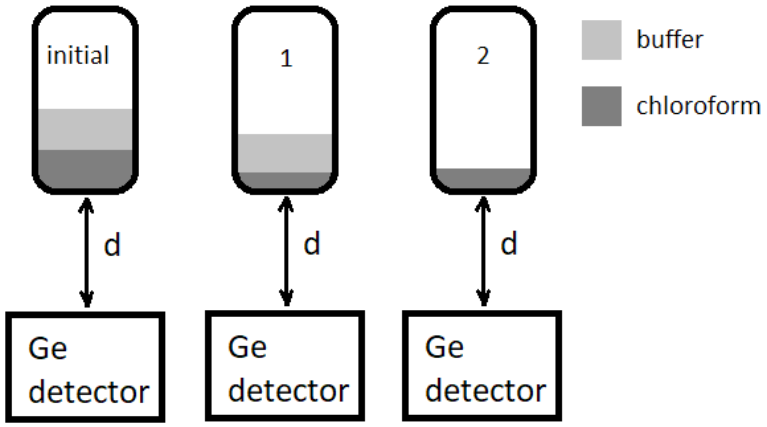

Figure 12. Schematic representation of measuring the count rate, at which the vials are placed at a fixed distance, *d*, from the germanium gamma detector

Consider a vial with an initial volume, which is the sum of an aqueous buffer layer and a chloroform layer. Vial 2 represents a volume fraction of the chloroform layer of the initial vial, while vial 1 represents the remainder of the total initial volume, such that:

$$V_{initial} = V_1 + V_2 \tag{4.4}$$

In theory, the activity (A) of the content within the initial vial is equal to the sum of the activity of the contents of vial 1 and vial 2:

$$A_{initial} = A_1 + A_2 \tag{4.5}$$

In practice however, such equality cannot be applied to the measured number of counts (N) with this experimental setup:

$$N_{initial} \neq N_1 + N_2 \tag{4.6}$$

It is necessary to keep the source of activity at a fixed distance from the detector, since only a small fraction of all emitted γ-photons is detected. However, by keeping the distance of the vials to the detector constant, the change in volume itself has an effect on the distance of the activity to the detector, because the volume of the liquid in vial 1 and vial 2 respectively is different compared to the initial situation. Therefore the inequality of (4.6) is true in theory.

In the actual experiments, the distance, *d*, is relatively large and the chloroform layer is relatively thin. Therefore, it is justified to say that:

$$N_{initial} \approx N_1 + N_2 \tag{4.7}$$

and for this reason, the systemic error due to this 'volume effect' in the calculation of the *RCY* is small.

4.2. The substitution of tropolone ligand in the [^{68}Ga]Ga-tropolone complex with a hydrophilic chelator

In chapter §4.1 conditions were found at which it is possible to form the [^{68}Ga]Ga-tropolone complex. This is just one step to enable the active loading of gallium through the hydrophobic bilayer of the polymersome.

In this chapter, conditions are researched at which the substitution of tropolone with a hydrophilic chelator can take place. This step is another important requirement to make the active loading of gallium possible. One example of such an exchange reaction is:

$$Ga(trop)_3 + \text{chelator} \rightleftharpoons \text{Ga-chelator} + 3\ \text{trop} \qquad (4.8)$$

As discussed in §4.1.1, other Ga-tropolone complexes besides $Ga(trop)_3$ can be formed. So, consequently, several other exchange reactions in which the ligands in the Ga-tropolone complex is substituted by the hydrophilic chelator, are possible.

In this report, experiments were conducted with three hydrophilic chelators: DOTA, NOTA and DTPA (see **Figure 13**).

DOTA was chosen, because DOTA derivatives are already clinically used with Ga-68 for PET scan imaging. NOTA was chosen, because it has a very high stability constant with gallium (see **Table 3**) and literature suggests that it can bind to gallium quickly at room temperature [47]. And DTPA was chosen, because it is already used in the active loading of In-111 into polymersomes. It would be interesting to determine whether a similar method with DTPA could be used to load Ga-68 instead of In-111 into polymersomes.

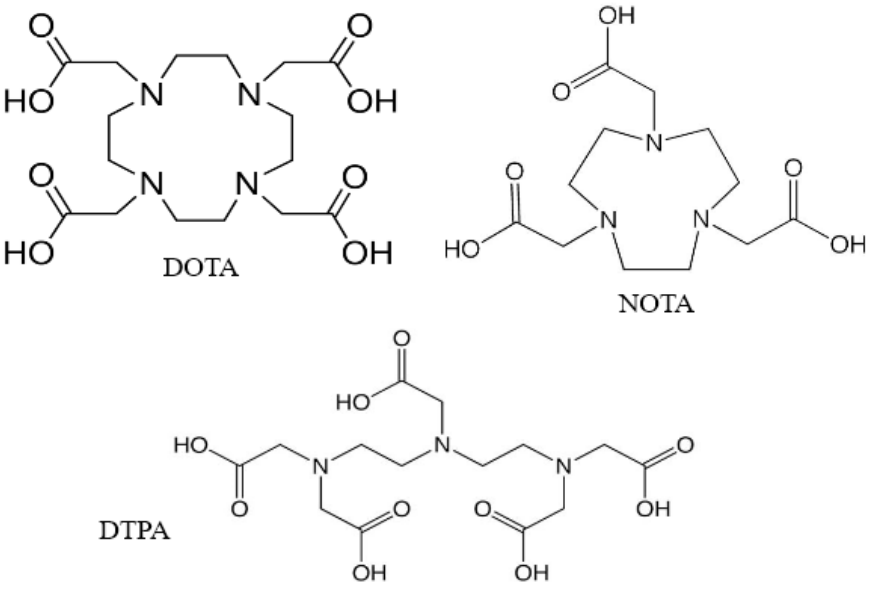

Figure 13.Chemical structures of DOTA, NOTA and DTPA. These are all polydentate ligands. DOTA and NOTA are macrocyclic chelators, DTPA is an acyclic chelator.

Table 3. Stability constants of chelators with gallium.

chelator	log (K_{ML})	reference
DOTA	21.3	[43][44]
NOTA	31.0	[43][44]
DTPA	25.5	[43][45]

The stability constant K_{ML} plays an important role in the exchange reaction. If: $\mathrm{M+L} \rightleftharpoons \mathrm{ML}$, where *M* denotes a metal and *L* denotes the ligand, then:

$$K_{ML} = \frac{[ML]}{[M][L]} \tag{4.9}$$

It should be noted that the stability constant is an *equilibrium* constant. It says nothing about the association rate and the dissociation rate of a metal-ligand complex, so it provides no information about how quickly the equilibrium is reached.

Even though the stability constant of gallium with tropolone is unknown, it is expected to be much lower than the stability constants of gallium with the hydrophilic chelators of **Table 3**. The reasoning behind this is that the complex of a metal with a polydentate ligand is typically much more stable than with a monodentate or bidentate ligand.

The equilibrium constant (K_{ex}) of the ligand exchange reaction can be estimated with:

$$\log K_{ex} = \log(K_{MC}) - \log(K_{ML}) \tag{4.10}$$

where K_{MC} is the stability constant of gallium with the hydrophilic chelator, and K_{ML} is the stability constant of gallium with tropolone. A derivation is given in Appendix F.

So, if the stability constant of the Ga-chelator complex is higher than the stability constant of Ga-tropolone (which is presumably true), then the tropolone ligand in the [^{68}Ga]Ga-tropolone complex should be able to be substituted by the hydrophilic chelator.

4.2.1. *Control experiment: binding ^{68}Ga to hydrophilic chelator*

The goal of this control experiment is to determine whether the hydrophilic chelator can bind to gallium. If this would not succeed, it would be pointless to use this chelator for the ligand exchange reaction with tropolone in the Ga-tropolone complex. In this control experiment, the chelator was first allowed to bind to Ga-68 within 10 minutes at room temperature. Only then tropolone was added to show that binding to chelator was (un)successful. The idea is that if any Ga-68 is unbound to the chelator, then tropolone can form a complex with the free gallium, resulting in activity that can be found in the organic phase after extraction with chloroform, as shown in §4.1.

The results are presented in **Figure 14**. A lack of activity in the organic phase is used as an indicator that the hydrophilic chelator has formed a complex with gallium. The figure suggests that DTPA and NOTA can easily form complex with gallium at room temperature, while DOTA is only somewhat effective at pH 4.

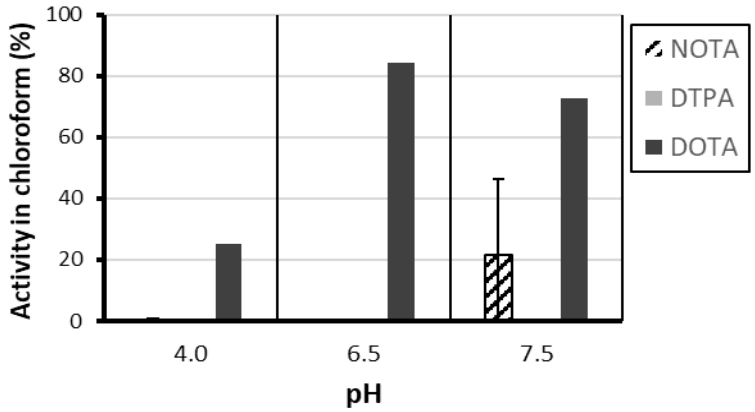

Figure 14. Activity in chloroform (%) vs. pH. NOTA and DTPA are barely visible in the graph because the activity is close to 0%. n = 2 for NOTA at each pH, n = 1 for DTPA and DOTA at each pH.

4.2.2. *The substitution of tropolone ligand in the Ga-tropolone complex with DOTA, NOTA or DTPA*

Extraction experiments were conducted to indirectly determine whether tropolone in [^{68}Ga]Ga-tropolone complex could be substituted with a hydrophilic chelator. First the Ga-tropolone complex was created (**Figure 11** indicates that this can be done reliably at pH 4.0-6.5), after which the hydrophilic chelator was added. The absence of activity in the organic phase, after extraction with chloroform, was used as a measure of complexation of gallium with the hydrophilic chelator. If no activity was found in the organic phase, then it is likely that the complex of Ga-68 with the hydrophilic complex was formed, indicating the successful exchange of ligands.

In the next section the results of extraction experiments with DOTA, NOTA and DTPA are shown. These experiments were conducted in a well-structured manner.

First the attempt was made to perform the ligand exchange reaction at room temperature. If this failed at room temperature, then experiments were performed at elevated temperature. And if this were successful, additional experiments were conducted to determine at what minimalized incubation time and temperature the ligand exchange reaction would still succeed.

4.2.2.1. Substitution of tropolone in Ga-tropolone complex with DOTA

- **<u>Room temperature / variable pH / 60 minutes</u>**

After the Ga-tropolone complex was formed, DOTA was added and the solution was left to incubate to allow the exchange with tropolone at room temperature. After 60 minutes incubation time, an extraction was performed with chloroform. **Figure 15** indicates that no Ga-DOTA complex was formed at room temperature.
This is not surprising, since gallium does not easily form a complex with DOTA at room temperature in the absence of tropolone. (See §4.2.1).

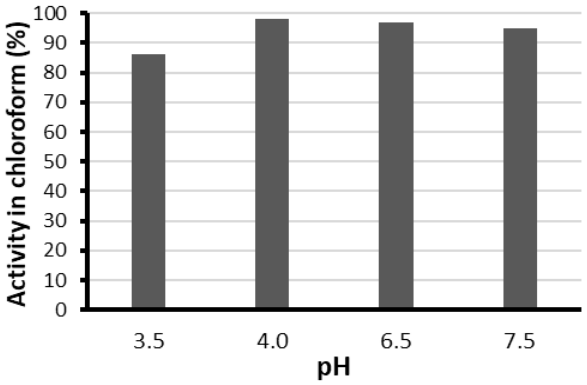

Figure 15. Activity in chloroform (%) vs. pH. The ratio (DOTA: tropolone) was (60 µM: 20 µM).

- **<u>90 °C / variable pH / 30 minutes</u>**

After the Ga-tropolone complex was formed, DOTA was added and the solution was left to incubate to allow the exchange with tropolone at 90 °C. After 30 minutes incubation time, an extraction was performed with chloroform. **Figure 16** indicates that Ga-DOTA was formed with high yield at pH 3.5 and pH 4.0.

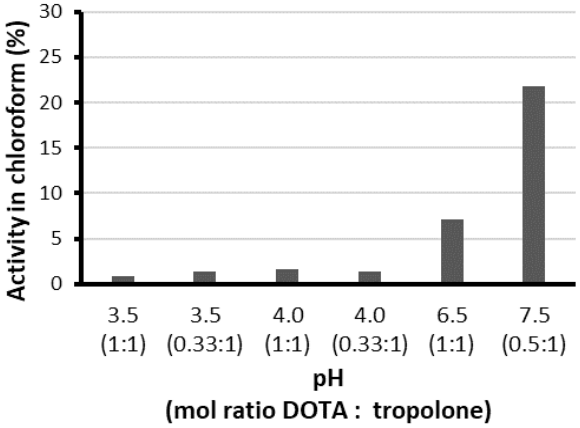

Figure 16. Activity in chloroform (%) vs. pH.
The ratio (1:1) refers to (20 µM DOTA: 20 µM tropolone). The ratio (0.33:1) refers to (6.7 µM DOTA: 20 µM tropolone)
The ratio (0.5:1) refers to (10 µM DOTA: 20 µM tropolone)

The experiment was repeated with variable incubation time to determine the shortest time possible at which the ligand exchange reaction will take place.

- **<u>90 °C / pH 4.0 / variable time</u>**

After the Ga-tropolone complex was formed in pH 4.0 buffer, DOTA (equimolar with tropolone) was added and the solution was left to incubate to allow the exchange with tropolone at 90 °C. After 10-30 minutes incubation time, extraction was performed with chloroform. **Figure 17** indicates that Ga-DOTA complex will be formed with high yield at pH 4.0, after incubating for at least 20 minutes at 90 °C.

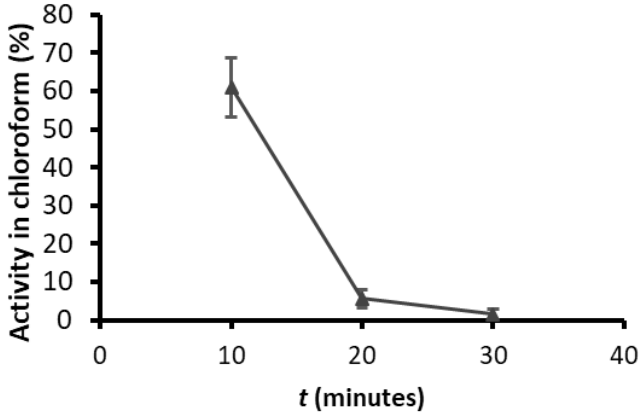

Figure 17. Activity in chloroform (%) vs. time. The ratio (DOTA: tropolone) was (20 µM: 20 µM). n = 3 for all data points.

4.2.2.2. Substitution of tropolone in Ga-tropolone complex with NOTA

- **Room temperature / variable pH / 60 minutes**

After Ga-tropolone complex was formed, NOTA was added, and the solution was left to incubate to allow the exchange with tropolone at room temperature. After 60 minutes incubation time, extraction was performed with chloroform. **Figure 18** indicates that no Ga-NOTA complex was formed at room temperature.

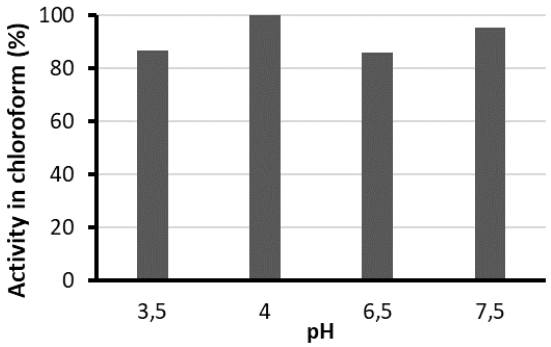

Figure 18. Activity in chloroform (%) vs. pH. The ratio (NOTA: tropolone) was (20 µM: 20 µM).

Even though NOTA on its own can form a very stable complex with gallium (see **Table 3**), gallium will not transfer from tropolone to NOTA at room temperature. This is remarkable, since it was shown in §4.2.1 that NOTA can easily form a complex with gallium at room temperature. It is possible that the activation energy of the exchange of tropolone for NOTA is too high. Raising the temperature should be able to tackle this problem.

- **Variable temperature / variable pH / 10 minutes**

After the Ga-tropolone complex was formed, NOTA was added, and the solution was left to incubate to allow the exchange with tropolone at variable temperature. After 10 minutes incubation time, extraction was performed with chloroform. The results are seen in **Figure 19**.

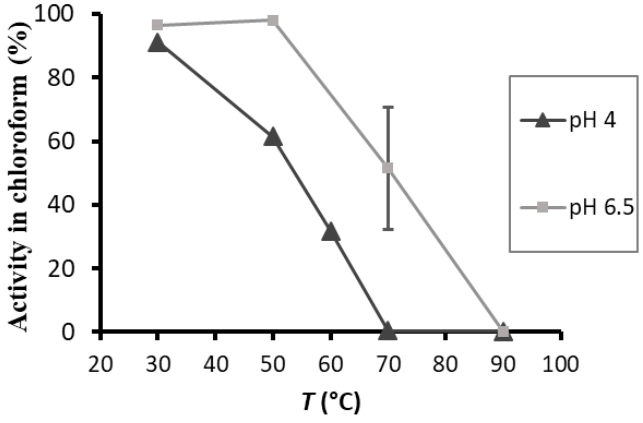

Figure 19. Activity in chloroform (%) vs. temperature. The ratio (NOTA: tropolone) was (20 µM: 20 µM) n = 2 for data points with error bar, otherwise n = 1.

No activity is found in chloroform for pH 4.0 at 70 °C, which indicates that the Ga-NOTA complex is formed at these conditions.

It appears that the exchange of tropolone for NOTA occurs faster and at a lower temperature compared to the exchange of tropolone for DOTA (20 minutes, 90 °C).

4.2.2.3. Substitution of tropolone in Ga-tropolone complex with DTPA

All experiments in this section were performed with (DTPA 20 µM: tropolone 20 µM).

- **Room temperature / variable pH / variable time**

After Ga-tropolone complex was formed, DTPA was added, and the solution was left to incubate to allow the ligand exchange of tropolone for DTPA at room temperature. After 10-60 minutes incubation time, extraction was performed with chloroform.

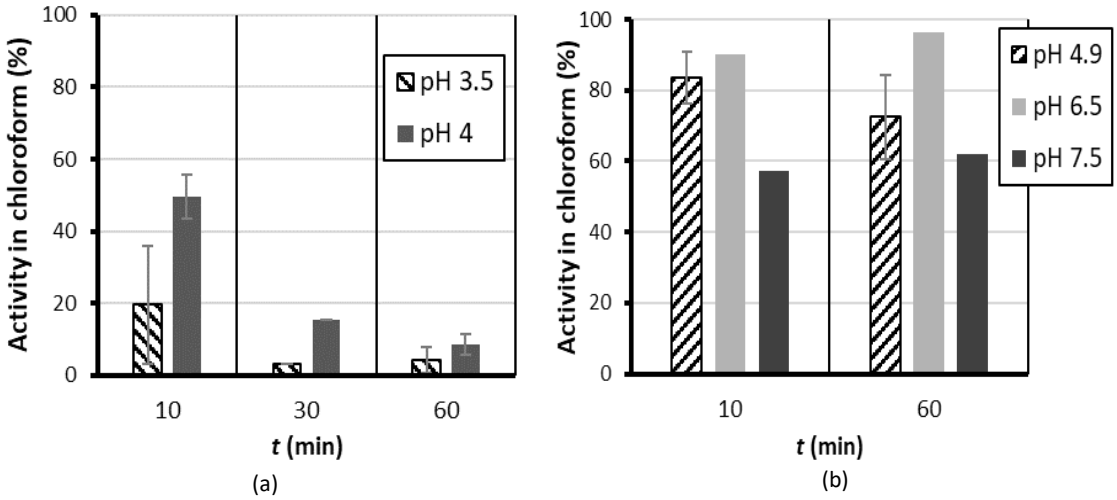

Figure 20. Activity in chloroform (%) vs. time. **(a)** pH 3.5 and pH 4.0, **(b)** pH 4.9, pH 6.5 and pH 7.5. n = 2 for data points with error bar, otherwise n = 1.

Figure 20(a) indicates that Ga-DTPA is formed at room temperature at pH 3.5 and pH 4.0 if one waits long enough.

Figure 20(b) shows that the exchange of tropolone for DTPA does not work well at room temperature at higher pH values, which is remarkable. It is expected that DTPA is less protonated at higher pH, which should make it easier to form a complex with gallium. This same logic also applies to DOTA (§4.2.2.1) and NOTA (§4.2.2.2). Therefore, it is presumed that the dissociation rate of the Ga-tropolone complex decreases at higher pH, which would explain why the ligand exchange of tropolone for DTPA is inhibited.

- **10 minutes / variable pH / variable temperature**

After Ga-tropolone complex was formed, DTPA was added and the solution was left to incubate to allow the exchange with tropolone at various temperatures. After 10 minutes incubation time, extraction was performed with chloroform.

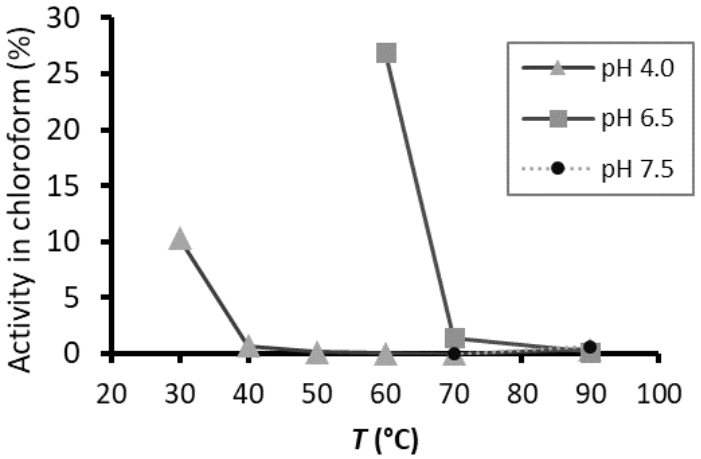

Figure 21. Activity in chloroform (%) vs. temperature. Experiment with pH 7.5 was only performed at 70 °C and 90 °C.

Figure 21 indicates that Ga-DTPA is formed after 10 minutes incubation time at pH 6.5 at 70 °C, and that the same can be achieved for pH 4.0 after 10 minutes at a much lower temperature (40 °C). This is a much milder condition than what was found for NOTA (§4.2.2.2), which required heating to 70 °C.

For this reason, DOTA and NOTA were rejected in the remainder of this project, and DTPA was chosen to be used as the hydrophilic chelator in the preparation of polymersomes. This means that all experiments in this project concerning the loading of Ga-68 into polymersomes were conducted with DTPA filled polymersomes.

4.3. The loading of Ga-68 into polymersomes

This chapter builds further on the knowledge gained in the previous sections, where two requirements were tested to make the active loading mechanism of Ga-68 into polymersome possible. In §4.1 it was found that Ga-68 (approx. $1 \cdot 10^{-12}$ M) could bind to 20 µM tropolone with the highest radiochemical yield at pH range 4.0 - 6.5. In §4.2 three hydrophilic chelators at different conditions (pH, temperature, time) were tested in their ability to form a complex with Ga-68 in the ligand exchange for tropolone of the Ga-tropolone complex. DTPA appeared to be the best choice to make this possible.

But fulfilling both requirements under the right conditions (pH, temperature) does not necessarily mean that loading Ga-68 into polymersomes will work.

In this chapter the method of loading is discussed, and results of loading experiments are shown.

4.3.1. Preparation of polymersomes

This section contains some reasoning about the chosen method of the preparation of the polymersomes.

Polymersomes of PBd-PEO 1800-600 (PBd_{33}-PEO_{14}) diblock copolymer were prepared by dissolving polymer in a DTPA (1 mM) / HEPES buffer solution upon stirring it for 1 week. This way, the polymersomes entrap DTPA in the aqueous cavity. It was observed that the solution already became whitish within one or two days, but the stirring was continued for a week to ensure that all polymer got dissolved.

The polymersomes were extruded through 800, 400 and 200 nm filters to get polymersomes of smaller size. It was observed that the polymersome solutions slowly passed through the 200 nm filters; therefore, for this filter size, the pressure was increased from 200 psi to 300 psi. DLS data is given in Appendix A.

An overview of the polymersomes in this report is given in **Table 4** (p.42).

Size-exclusion chromatography (SEC) was used to remove the DTPA in solution outside of polymersomes by passing the polymersomes through a Sephadex G-25 column using HEPES buffer as eluent. Fractions of 1 mL were collected. It was observed that the polymersomes always came out in two fractions, since these fractions were white and cloudy instead of a clear solution. The most whitish fraction of the two was used for the loading experiment, because this indicates a higher concentration of polymersomes. In case both fractions were visually equally whitish, then both fractions were used to perform loading experiments on.

4.3.2. Loading method and calculation maximum loading efficiency

Tropolone solution was added to 200 µL of HEPES buffer (500 mM). Then 20 µL of Ga-68 eluate was added and the solution was left to incubate to allow the formation of Ga-tropolone complex. An increased concentration of HEPES (compared to the 50 mM HEPES buffers of §3.2.3 that were used thus far) was necessary to have enough buffer capacity to maintain pH after adding the Ga-68 eluate (pH 1) in such a small volume.

After this, 800 µL of polymersome solution was added to start the loading of Ga-68 into polymersomes at variable time and temperature. (See **Table 5** for an overview).

It should be noted that for the loading of Ga-68 into pH 7.4 polymersomes, HEPES buffer (0.5 M, pH 6.5) was used for the Ga-tropolone formation, resulting in slightly lower pH outside of the pH 7.4 polymersomes. In all other loading experiments, the formation of Ga-tropolone complex was performed in the same pH as its corresponding polymersome sample (pH 4.0 or pH 6.5).

After the loading process the initial number of counts (N_{ini}) was measured with the germanium gamma detector (and the exact point of time of the measurement was noted), after which 1 mL of polymersomes were passed through a PD-10 column. 8 fractions of 1 mL were collected, using HEPES buffer as eluent. It was observed that fractions 4 and 5 were very whitish (containing polymersomes), while fraction 3 was sometimes slightly whitish.

Therefore, the maximum loading efficiency (LE_{max}) was determined by:

$$LE_{\max} = \frac{N_3^{corr} + N_4^{corr} + N_5^{corr}}{N_{ini} - N_{empty}^{corr}} \times 100\% \qquad (4.11)$$

where $N_3^{corr}, N_4^{corr}, N_5^{corr}$ are the time corrected number of counts in PD10 fraction 3, 4 and 5 respectively, N_{in} is the initial number of counts, N_{empty}^{corr} is the time corrected number of counts of the 'empty' vial containing leftover activity.

If PD10 fractions 3-5 contain no other Ga-68 activity outside of the polymersomes, then this definition of the maximum loading efficiency is equal to the 'real' loading efficiency. So, elution profiles were made of free Ga-68 in buffer, Ga-tropolone and Ga-DTPA to determine whether it is reasonable to assume that the maximum loading efficiency is close to the 'real' loading efficiency.

4.3.3. Control experiment: elution profiles PD10 column

Elution profiles were made of free Ga-68 in buffer, Ga-tropolone and Ga-DTPA in a pH 4.0 and pH 6.5 buffer, respectively. See **Figure 22** and **Figure 23**.

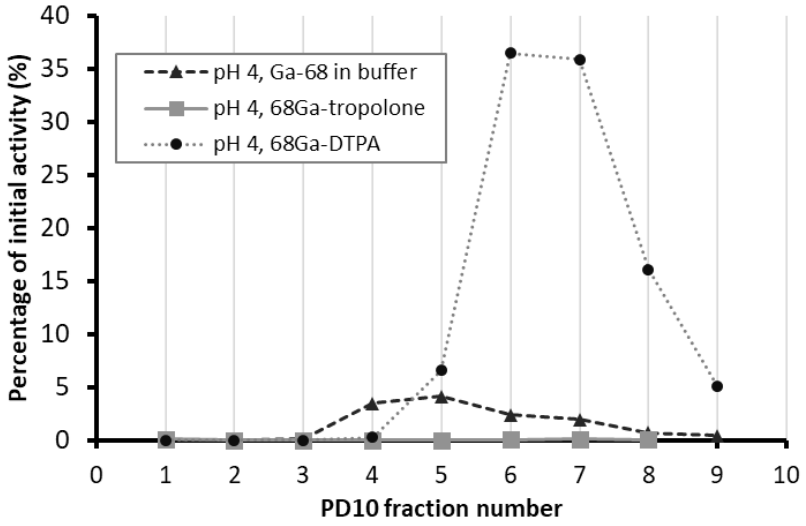

Figure 22. Percentage of initial activity (%) vs. PD10 fraction number (1 mL fractions). Elution profiles of free Ga-68, Ga-tropolone and Ga-DTPA in a pH 4 environment.

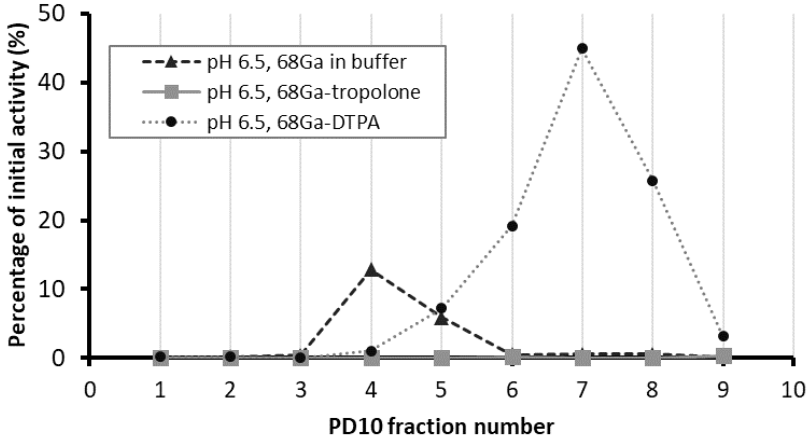

***Figure 23*.** Percentage of initial activity (%) vs. PD10 fraction number (1 mL fractions). Elution profiles of free Ga-68, Ga-tropolone and Ga-DTPA in a pH 6.5 environment.

In both figures it can be observed that when unbound Ga-68 in buffer is passed through the PD10 column, a notable amount of Ga-68 will be found in the collected fractions.

However, when tropolone is added to the Ga-68 containing buffer solution to form a [^{68}Ga]Ga-tropolone complex, after which this is passed through the PD10 column, then no Ga-68 is present in the collected fractions. This is an important observation, because it means that if any activity is found in the collected PD10 fractions of the actual loading experiments, then this activity cannot originate from ^{68}Ga bound to tropolone.

An elution profile was also made for the Ga-DTPA complex. This was done by performing a ligand exchange reaction in which the tropolone ligand in the Ga-tropolone complex got replaced by DTPA. The Ga-DTPA containing solution was then passed through the PD10 column. As observed in both figures, Ga-DTPA elutes from the column in fractions 5-9.

Additionally, another elution profile was made of Ga-tropolone, after the Ga-tropolone containing solution was heated and cooled down back again to room temperature (not shown in the figures). The idea was to exclude the possibility that any unexpected process might have occurred due to the heating process, which could have led to the dissociation of the Ga-tropolone complex. No difference was observed for the PD10 elution profile of Ga-tropolone, whether such solution was heated before or not. This result reaffirms the idea that the activity in PD10 fractions 6-8 must (only) come from Ga-DTPA.

4.3.4. Lower bound estimate of the loading efficiency

There is an overlap between the PD10 fraction numbers in which polymersomes are present (fractions 3-5), and in which Ga-DTPA can be found (fractions 5-9).

Consequently, the activity that is found in PD10 fraction number 5 could come from Ga-68 loaded into polymersomes, but also from [^{68}Ga]Ga-DTPA that might be present outside of the polymersomes. This gives reason to define a lower bound estimate of the loading efficiency (LE_{low}):

$$LE_{low} = \frac{N_3^{corr} + N_4^{corr}}{N_{ini} - N_{empty}^{corr}} \times 100\% \qquad (4.12)$$

In this definition of LE_{low}, the measured number of counts in fraction number 5 is omitted, compared to the definition of the LE_{max} (see §4.3.2).

4.3.5. Overview of polymersome solutions

An overview of the polymersome solutions is given in **Table 4**. They are referenced in this report by their label as mentioned in the column '*Polymersome label*'. Only PBd_{33}-PEO_{14} (1800-600) polymer was used in this report.

Note that 'PS-E**a**' and 'PS-E**b**' are polymersome solutions from the exact same batch, with the difference that 'PS-E**b**' is unfiltered. The same principle holds true for the polymersome solutions 'PS-F**a**' and 'PS-F**b**'.

Table 4.Overview of the prepared polymersome solutions.

Polymersome label	**Polymer concentration**	**pH**	**Chelator / buffer (concentration)**	**Extruder filter**
PS-A	2 mg/mL	4.0	DTPA (1mM) / HEPES (50 mM)	200 nm
PS-B	5 mg/mL	4.0	DTPA (1mM) / HEPES (50 mM)	200 nm
PS-C	5 mg/mL	6.5	DTPA (1mM) / HEPES (50 mM)	200 nm
PS-D	2 mg/mL	7.4	DTPA (1mM) / HEPES (10 mM)	200 nm
PS-Ea	2 mg/mL	7.4	DTPA (1mM) / HEPES (10 mM)	200 nm
PS-Eb	2 mg/mL	7.4	DTPA (1mM) / HEPES (10 mM)	none
PS-Fa	5 mg/mL	7.4	DTPA (1mM) / HEPES (10 mM)	200
PS-Fb	5 mg/mL	7.4	DTPA (1mM) / HEPES (10 mM)	none

4.3.6. Overview of loading experiments and loading efficiencies

An overview of the loading experiments is given in **Table 5**. They are referenced in this report by their label as mentioned in the column '*Experiment label*'.

In this table, the values for the 'maximum loading efficiency' (LE_{max}) and the 'lower bound estimate of the loading efficiency' (LE_{low}) are reported in the last two columns.

Several different Sephadex columns were used in this project with slightly different lengths, so the polymersomes were found in different fraction numbers (9-12). In **Table 5** it is mentioned in which fraction number the polymersomes that were used for the experiment were found. Since the polymersomes usually came out in two whitish fractions, it is also mentioned whether it is the 1st or 2nd whitish fraction. (For example: if fraction 9 and 10 were whitish, then fraction 9 would be labelled '1st' in this column, and fraction 10 would be labelled '2nd'. But because several different Sephadex columns were used, all 1st's and all 2nd's cannot be compared with each other).

'Eb3-90-10-1-trop' and 'Eb3-90-10-2-trop' refer to loading experiments where a tropolone concentration of 200 µM was used for the loading experiment. (In all other loading experiments the tropolone concentration was 20 µM).

Table 5. Overview of the loading experiments and their experimental conditions.

Experiment label	**Polymersome label**	**Loading temp. [°C]**	**Loading time [min]**	**Sephadex fraction [1st or 2nd]**	**LE_{low} [%]**	**LE_{max} [%]**
A1-50-10-2	PS-A	50	10	2nd, 11	1.8	5.5
A2-50-60-2	PS-A	50	60	2nd, 11	7.4	25
B1-50-10-2	PS-B	50	10	2nd, 11	7.5	18
B2-60-10-1	PS-B	60	10	1st, 10	9.0	24
B2-60-10-2	PS-B	60	10	2nd, 11	0.5	14
B3-60-10-1	PS-B	60	10	1st, 9	28	36
B3-90-10-2	PS-B	90	10	2nd, 10	7.0	29
C1-70-10-1	PS-C	70	10	1st, 11	1.3	2.9
C1-70-10-2	PS-C	70	10	2nd, 12	0.9	12
C2-70-30-1	PS-C	70	30	1st, 10	2.2	5.8
C2-70-30-2	PS-C	70	30	2nd, 11	5.8	27
Eb1-90-10-1	PS-Eb	90	10	1st, 9	29	35
Eb1-90-10-2	PS-Eb	90	10	2nd, 10	16	20
Eb2-90-10-1	PS-Eb	90	10	1st, 9	18	22
Eb2-90-10-2	PS-Eb	90	10	2nd, 10	22	26
Eb3-90-10-1-trop	PS-Eb	90	10	1st, 9	0.6	0.9
Eb3-90-10-2-trop	PS-Eb	90	10	2nd, 10	0.6	0.7
Fa1-90-10-1	PS-Fa	90	10	1st, 10	26	32
Fa1-90-10-2	PS-Fa	90	10	2nd, 11	13	22
Fb1-90-10-2	PS-Fb	90	10	2nd, 10	77	90
Fb2-90-10-1	PS-Fb	90	10	1st, 9	57	71
Fb2-90-10-2	PS-Fb	90	10	2nd, 10	53	63
(See §4.3.13.1)	PS-A	50	60	modified	4.8	7.3
(See §4.3.13.2)	PS-D	70	60	modified	13	19
(See §4.3.13.3)	PS-D	70	60	modified	17	23

4.3.7. Loading experiments in 2 mg/mL PBd-PEO 1800-600, pH 4

Two loading experiments were performed with polymersome solution 'PS-A' at a constant loading temperature of 50 °C (see **Figure 24**). The idea was to compare the effect of the loading time (10 minutes vs. 60 minutes) on the loading efficiency.

The results were rather remarkable. Activity was found in PD10 fraction numbers 6-8, even though it was expected to only find activity in PD10 fraction numbers 3-5. The graph resembles the elution profile of DTPA as discussed in §4.3.3. This strongly suggests that DTPA was also present in solution outside the polymersomes. It is plausible that this has a negative influence on the loading efficiency.

It does give rise to the question of why there is DTPA outside of the polymersomes. It is possible that the Sephadex columns that were used in these experiments do not separate the polymersomes and the DTPA in solution outside of the polymersomes well enough. It is plausible that some Sephadex columns were poorly packed, leading to poor separation performance. (A control experiment was conducted to investigate this idea, see §4.3.12).

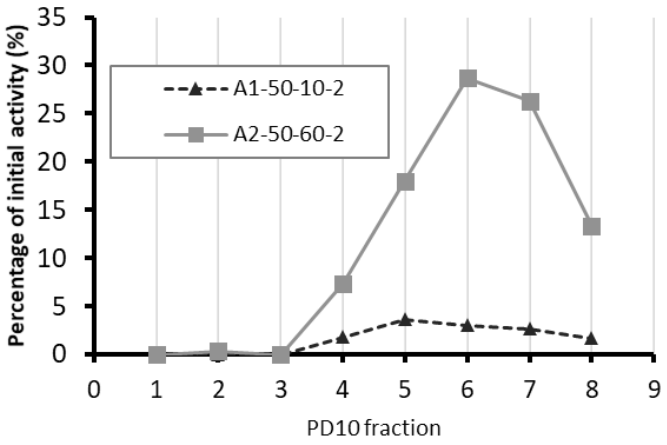

Figure 24. Percentage of initial activity (%) vs. PD10 fraction number (1 mL fractions).

Nonetheless, it appears that some gallium was loaded successfully. For experiment 'A2-50-60-2', the LE_{low} is 7.4% and the LE_{max} is 25%. In this experiment, the LE_{max} could be a huge overestimation of the loading efficiency, due to the uncertainty of the origin of the activity in PD10 fraction number 5. (It could be gallium loaded into polymersomes, but it might as well be from Ga-DTPA complex outside of the polymersomes).

For experiment 'A1-50-10-2', the LE_{low} is 1.8% and the LE_{max} is 5.5%. The shorter loading time might be an explanation for the lower loading efficiency compared to 'A2-50-60-2'. Also for this experiment, DTPA outside of polymersomes appears to be present. It looks like there was a lower DTPA concentration outside of polymersomes at experiment 'A1-50-10-2', compared to experiment 'A2-50-60-2', resulting in a lower DTPA peak. This difference of DTPA concentration could be explained by the fact that two different Sephadex columns were used for these two experiments.

4.3.8. Loading experiments in 5 mg/mL PBd-PEO 1800-600, pH 4

A few loading experiments were performed with polymersome solution 'PS-B' at a constant loading time of 10 minutes (see **Figure 25**). The idea was to compare the effect of the loading temperature (50 °C, 60 °C, 90 °C) on the loading efficiency. However, unexpected DTPA peaks (see discussion of §4.3.7) were also observed at these experiments. Therefore, no good comparison about the effect of the temperature could be made.

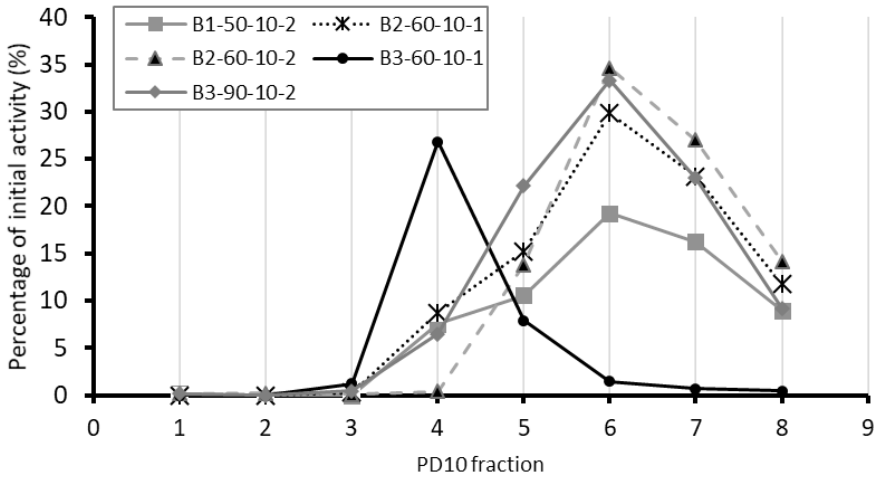

Figure 25. Percentage of initial activity (%) vs. PD10 fraction number (1 mL fractions).

It is noteworthy to compare experiment 'B2-60-10-1' with 'B2-60-10-2', which both contain polymersomes from the same Sephadex column in the separation step to separate DTPA from the polymersomes; experiment 'B2-60-10-1' was performed with the 1st whitish fraction, and experiment 'B2-60-10-2' was performed with the 2nd whitish fraction. The graphs for both loading experiments show a DTPA peak. However, the LE_{low} (9.0%) for 'B2-60-10-1' is much higher than the LE_{low} (0.5%) for 'B2-60-10-2'. It is apparent that DTPA separation from the polymersomes was not completely successful. It is possible that the 2nd whitish polymersome fraction contained a higher DTPA concentration, which could explain the difference in loading efficiency.

Most remarkable is the graph of loading experiment 'B3-60-10-1'. No DTPA profile is visible, and it appears that the loading of Ga-68 was quite successful. The LE_{low} is 28% and the LE_{max} is 36%. Based on the shape of the graph of 'B3-60-10-1', and due to the lack of activity in fraction numbers 6 and 7, it is presumed that the activity from fraction 5 is not from DTPA. If this is true, then the maximum loading efficiency of 36% is the better representation for the 'real' loading efficiency than the lower bound estimate of 28%.

4.3.9. Loading experiments in 5 mg/mL PBd-PEO 1800-600, pH 6.5

A few loading experiments were performed with polymersome solution 'PS-C' at a constant loading temperature of 70 °C (see **Figure 26**). The idea was to compare the effect of the loading time (10 minutes vs. 30 minutes) on the loading efficiency. However, also at these loading experiments, unexpected DTPA peaks were observed (see discussion of §4.3.7), which may have influenced the loading of gallium into polymersomes. Therefore, no reliable comparison can be made between the experiments with different loading time.

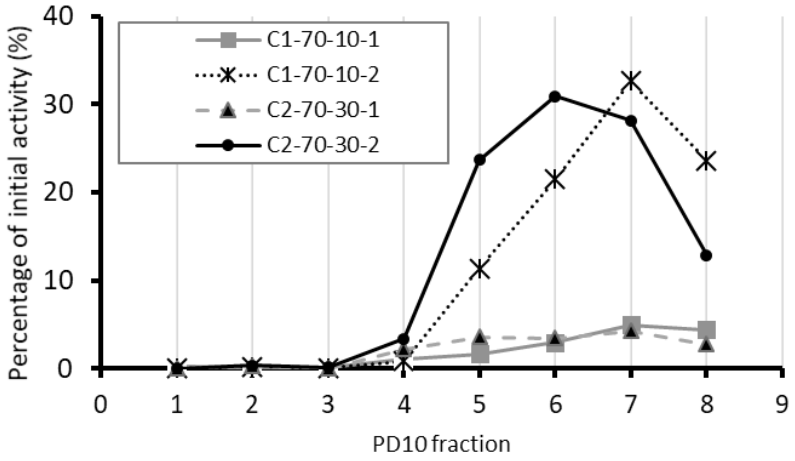

Figure 26. Percentage of initial activity (%) vs. PD10 fraction number (1 mL fractions).

Experiment 'C1-70-10-1' and 'C1-70-10-2' were conducted at the exact same conditions using the same polymersome solution that eluted from the same Sephadex column, but it led to notably different results. The only difference is that 'C1-70-10-1' was done with the 1st whitish Sephadex fraction, while 'C1-70-10-2' was done with the 2nd whitish Sephadex fraction (which eluted 1 fraction later from the column). And the same holds true, when comparing experiment 'C2-70-30-1' with 'C2-70-30-2'.

It is remarkable that in both cases where the 2nd whitish Sephadex fraction was used, the apparent DTPA peak is much higher. It could mean that the DTPA concentration outside of polymersomes was significantly higher in the fraction that eluted one fraction later from the Sephadex column.

4.3.10. Loading experiments in 2 mg/mL PBd-PEO 1800-600, pH 7.4

Several loading experiments were performed with polymersome solution 'PS-Eb' at a constant loading temperature of 90 °C and a constant loading time of 10 minutes (see **Figure 27**).

Note that these were all experiments with an unfiltered polymersome solution. Therefore, it is likely that this polymersome solution contained polymersomes that were larger than 200 nm. Larger polymersomes encapsulate more DTPA in its aqueous cavity, which could lead to a higher loading efficiency than a filtered polymersome solution. Also, filtering/extruding the polymersome solution effectively decreases the polymersome concentration, which is another reason why an unfiltered polymersome solution could lead to a higher loading efficiency.

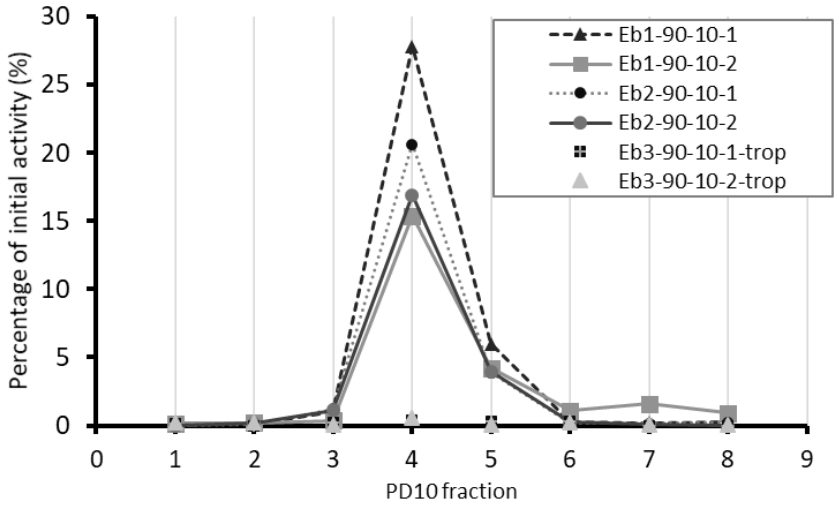

Figure 27. Percentage of initial activity (%) vs. PD10 fraction number (1 mL fractions).

The graphs show (barely) no peaks that are associated with [^{68}Ga]Ga-DTPA, unlike the loading experiments from the previous sections. So, it appears that the Sephadex column that was used for the experiments from **Figure 27** was packed well. The LE_{max} of these experiments is: (26 ± 7) %, (n = 4).

Additionally, two loading experiments ('Eb3-90-10-1-trop' and "Eb3-90-10-2-trop') were conducted with 200 µM tropolone, instead of 20 µM tropolone as lipophilic ligand. It can be observed that practically all activity stays in the PD10 column, which indicates that no Ga-68 was loaded into polymersomes. This can be explained by the presumption that the encapsulated DTPA is simply outnumbered by tropolone, which prevents the substitution of the tropolone ligand in the [^{68}Ga]Ga-tropolone complex with DTPA. The conclusion can be drawn that an upper limit for the concentration of the lipophilic ligand exists for which the active loading of Ga-68 into polymersomes works best.

4.3.11. Loading experiments in 5 mg/mL PBd-PEO 1800-600, pH 7.4

A few loading experiments were performed with polymersome solutions 'PS-Fa' and 'PS-Fb' at a constant loading temperature of 90 °C and a constant loading time of 10 minutes (see **Figure 28**).

It is not unexpected to observe a higher loading efficiency in loading experiments with polymersome 'PS-Fb' compared to 'PS-Fa', since 'PS-Fb' is an unfiltered polymersome solution, while 'PS-Fa' is the filtered solution of the exact same batch. (See discussion §4.3.10 about loading efficiency of filtered solution vs. unfiltered solution).

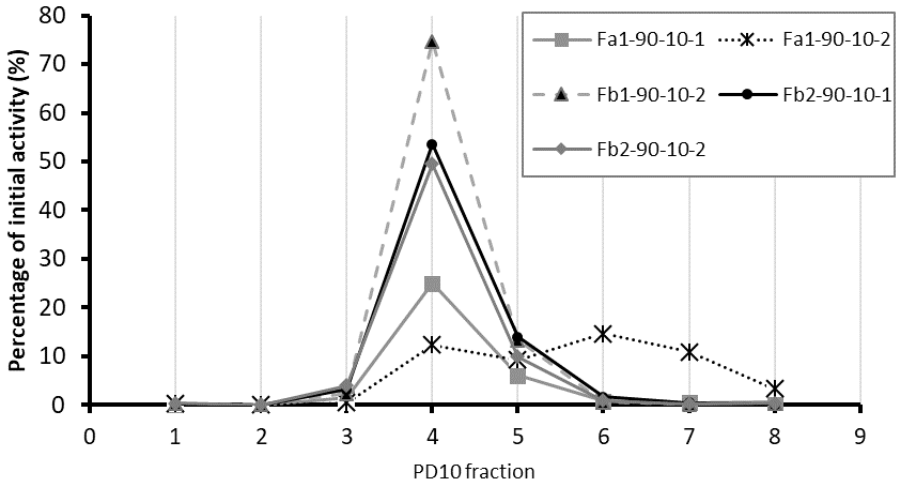

Figure 28. Percentage of initial activity (%) vs. PD10 fraction number (1 mL fractions).

The three loading experiments with the unfiltered solution show no DTPA peaks, and the LE_{max} for these experiments is (75 ± 14)%, (n = 3).

Coincidentally, another Sephadex column was used for the loading experiments ('Fa1-90-10-1' and 'Fa1-90-10-2') with the filtered polymersome solutions, and it appears that this Sephadex column was not packed well, because of the presence of DTPA in one experiment.

It is noteworthy to compare these two loading experiments, because'Fa1-90-10-1' was done with the 1st whitish Sephadex fraction, while 'Fa1-90-10-2' was done with the 2nd whitish Sephadex fraction (which eluted 1 fraction later from the column). Also, in this case, it was the second whitish fraction that clearly showed the DTPA peaks. It is imaginable that fractions that eluted later from the column, contained higher DTPA concentration.

The loading experiment with the first whitish fraction ('Fa1-90-10-1') shows no DTPA signature and the LE_{max} of this experiment is 32%. As expected, this is a lower loading efficiency compared to the experiments with unfiltered polymersome solution.

4.3.12. Control experiment Sephadex column: determining whether all DTPA was removed outside of polymersomes

Many loading experiments show unexpected peaks in the PD10 fractions 5-8. It is presumed that (some) Sephadex columns that were used for the experiments during this project did not completely remove DTPA from the solutions containing polymersomes. It is suspected that some Sephadex columns were not packed well.

A control experiment was conducted to investigate this presumption. A Sephadex column was chosen of which it was known that polymersomes would elute from the column in fraction number 11.

1 mL of DTPA (1 mM, pH 4.0) solution was added to this Sephadex column (DxL = 1x30 cm), and 12 fractions of 1 mL were collected using HEPES (10 mM, pH 4.0) as eluent. After Ga-tropolone was formed in a solution, one of the collected Sephadex fractions was added, after which the solution was heated at 50 °C for 10 minutes. Subsequently, an extraction with chloroform was performed.

The idea of these control experiments was two-fold:

- If the Sephadex fraction contains no DTPA, then Ga-68 stays bound to tropolone, and activity stays in the organic phase.
- If the Sephadex fraction does contain DTPA, then Ga-68 will form a complex with DTPA, and no/less activity stays in the organic phase.

The results from the extraction experiments are shown in **Table 6**.

Table 6. Overview of the results of the extraction experiments with different Sephadex fractions. 'Activity (%)' is the percentage of the initial (total) activity.

Sephadex fraction	**Activity (%) in organic phase**
1	94
9	75
10	78
11	32
12	0.2

The percentage of the initial total activity that is found in the organic phase decreases significantly at fraction number 11, which is exactly the fraction number in which polymersomes would elute from this particular column. The results indicate that this Sephadex column does not separate the DTPA from polymersomes well enough. This could explain the DTPA peaks that were found in the fractions of the PD10 column in the loading experiments of previous sections.

The results also indicate that the DTPA concentration in fraction number 12 of this Sephadex column is higher than in fraction number 11. It is possible that only a small concentration of DTPA is present in Sephadex fraction 11, but it could be enough to interfere with an even smaller concentration of Ga-68.

4.3.13. Additional loading experiments: modified method

Additional loading experiments were done, using a modified method to separate DTPA outside of polymersomes: two Sephadex columns were used to separate DTPA, instead of only one. This was done by collecting the 1 mL polymersome fraction that eluted from one Sephadex column, and then passing this fraction through a second Sephadex column to ensure more removal of DTPA.

By passing these samples through an extra Sephadex column, the polymersome solutions get more diluted. This effectively decreases the polymersome concentration, which could lead to a slightly decreased loading efficiency.

4.3.13.1. Loading experiment (modified method), 2 mg/mL PBd-PEO 1800-600, pH 4.0

A loading experiment was performed using the 'modified method' with polymersome solution 'PS-A' with a loading temperature of 50 °C and a loading time of 60 minutes. The result can be seen in **Figure 29**.

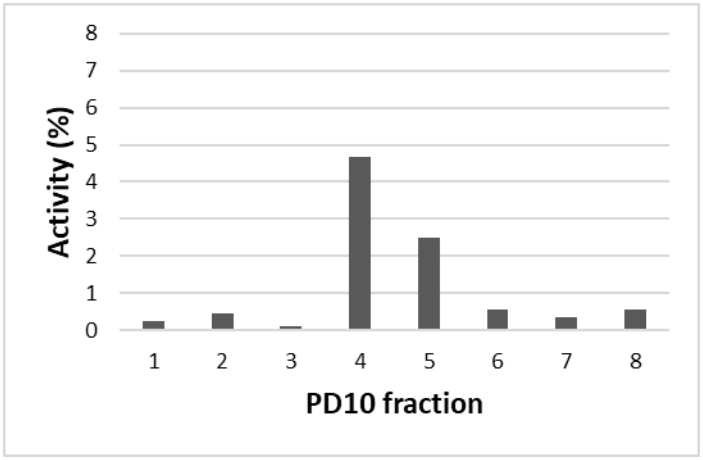

Figure 29. Percentage of initial activity (%) vs. PD10 fraction number (1 mL fractions).

No clear DTPA peaks are observed (in contrary to **Figure 24**, where loading experiments with the same polymersome solution was performed), so it appears that the modified method was quite successful in removing the DTPA that was outside of the polymersomes from the polymersome solution.

Despite that, the maximum loading efficiency (LE_{max}) is only 7.3%, which is quite low. Given the results from §4.3.7, it was not expected to get high loading efficiency with this polymersome sample. On top of that, the decreased polymersome concentration due to dilution by implementing the second Sephadex column step, could have had some negative impact on the loading efficiency.

4.3.13.2. Loading experiment (modified method), 2 mg/mL PBd-PEO 1800-600, pH 7.4

Another loading experiment was performed using the 'modified method' with polymersome solution 'PS-D' with a loading temperature of 70 °C and a loading time of 60 minutes. The result can be seen in **Figure 30**.

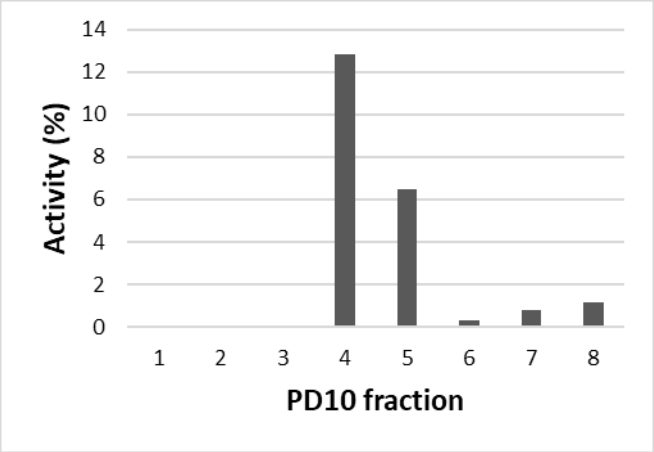

Figure 30. Percentage of initial activity (%) vs. PD10 fraction number (1 mL fractions).

Again, the goal of removing the DTPA that was outside of the polymersomes from the polymersome solution was accomplished with the 'modified method'. A maximum loading efficiency of 19% was observed.

4.3.13.3. Loading experiment (modified method + acidifying step), 2 mg/mL PBd-PEO 1800-600, pH 7.4

Another loading experiment with the same loading time and temperature as §4.3.13.2 was conducted (60 min, 70 °C) with polymersome solution 'PS-D'. But here an attempt was made to ensure that no activity in fraction 3, 4, and 5 contained Ga-68 outside polymersomes, in case there is any doubt about that.

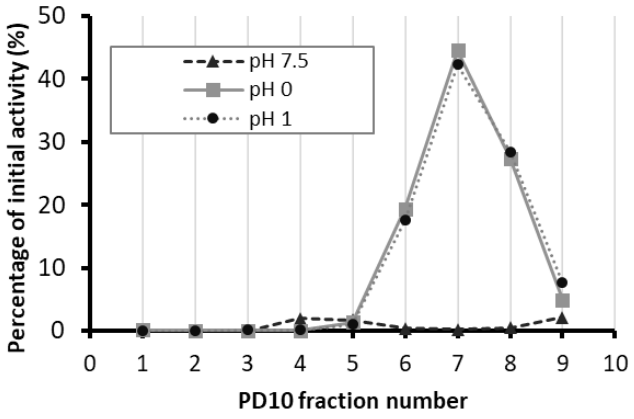

Figure 31. Percentage of initial activity (%) vs. PD10 fraction number (1 mL fractions). Elution profile of free Ga-68 in pH 7.5, pH 1 and pH 0.

First, an elution profile was made to evaluate where Ga-68 would end up in extreme low pH (see **Figure 31**). There is practically no difference between the elution profile of ^{68}Ga in a pH 1 or pH 0 environment, and all activity ends up in fraction numbers 6-9.

Then the loading experiment was performed. The polymersome solution was acidified (to a pH smaller than 1) just before it was passed through the PD10 column. The idea behind this acidifying step is to break any bonds of ^{68}Ga with any ligand, such as Ga-DTPA, Ga-tropolone or any possible hydrolysed specie of gallium {such as $Ga(OH)_3$ precipitate or $Ga(OH)_4^-$}.

The result of this experiment is shown in **Figure 32**. The peaks at fraction number 6, 7 and 8 must be the result of acidifying, as demonstrated by the elution profile of free Ga-68 in pH 0 and pH 1. It is probable that the gallium in these fractions exists as the $[Ga(H_2O)_6]^{3+}$ specie, since it is expected that this is the only speciation of gallium to be present at such a low pH (see §2.11).

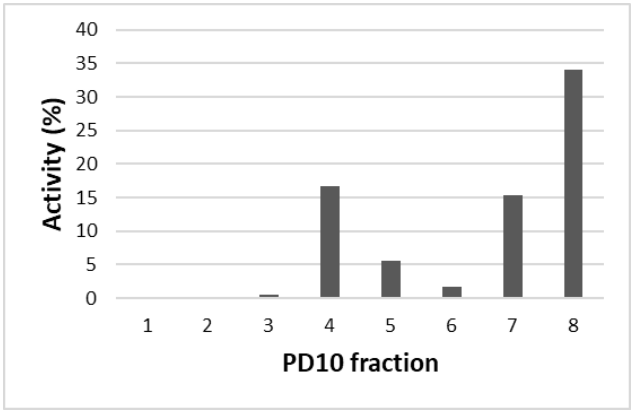

Figure 32. Percentage of initial activity (%) vs. PD10 fraction number (1 mL fractions). Loading experiment with acidifying. Loading time 60 minutes. *T* = 70 °C.

The peaks at fraction number 3, 4 and 5 are assigned to ^{68}Ga loaded into polymersomes, since it is presumed that the acidifying step ensures that no ^{68}Ga outside of polymersomes is present in these fractions. It can be observed that LE_{max} = 23%.

4.3.14. Discussion loading efficiency

When the results of the loading experiments with the unfiltered polymersome solutions are omitted, it can be observed that the maximum loading efficiency of the loading experiments did not exceed 36%.

The most important explanation for the small loading efficiencies can be found in the CryoTEM images (Appendix B). The thickness (*a*) of the hydrophobic bilayer of the prepared polymersome solutions in this report ranges from 10 nm to 19 nm, which is unexpectedly thick for a PBd_{33} (1800 g mol^{-1}) polymer. This could lead to a lower permeability of the hydrophobic bilayer.

A comparison can be made with the paper of *Bermudez et al.* (2002) [46], in which polymersomes were prepared with several PBd-PEO polymers with different molecular weights. It was found that the thickness scales with the hydrophobic molecular weight (M_h) with the following relationship:

$$a \sim (M_h)^{0.5} \tag{4.13}$$

With the data of [46] (**Table 7**), the following empirical equation is proposed, using a linear fit with *Microsoft Excel*:

$$a \approx 1.35 \cdot (n_{PBd})^{0.5} \tag{4.14}$$

where *a* is the thickness of the hydrophobic bilayer in nm, n_{PBd} is the number of PBd units in the PBd-PEO polymer.

Using this equation, it is expected that PBd_{33}-PEO_{14} (1800-600) should form a hydrophobic bilayer with a thickness of around 8 nm. In the paper of *Wang et al.* (2013) [3] it is found that the PBd_{33}-PEO_{21} polymer forms polymersomes with a PBd bilayer of around 7 nm thickness. This is in accordance with the empirical equation.

Since the polymersomes that were prepared for this project are much thicker than expected, it is questionable whether the polymer batch consisted of PBd(1800)-PEO(600) polymer.

Table 7. PBd-PEO polymersomes and their corresponding hydrophobic bilayer thickness (*a*). Data retrieved from [46]

Polymer	*a* (nm)
PBd_{46}-PEO_{26}	9.6
PBd_{55}-PEO_{50}	10.6
PBd_{125}-PEO_{80}	14.8
PBd_{250}-PEO_{150}	21.0

A comparison can be made between loading efficiencies of this project with a loading experiment of *Wang et al.* (2013) [3] in which ^{111}In was loaded with tropolone (20 µM) into PBd_{120}-PEO_{89} polymersomes (0.5 mg mL^{-1}) with a hydrophobic bilayer that had a thickness of 13 nm. There, after a loading time of 1 hour, the loading efficiency was only around 22%.

That result is somewhat comparable with the maximum loading efficiency for Ga-68 after 1 hour loading time that was found in this report in §4.3.13.2 (19%) and §4.3.13.3 (23%). The polymersomes that were used in this report had a membrane thickness of 15 nm ± 3 nm. (See Appendix B).

Another reason for the low loading efficiencies could be found in the ratio of the applied amount of tropolone and the amount of encapsulated DTPA. This ratio ($ratio_{trop/DTPA}$) is given by:

$$ratio_{trop/DTPA} = \frac{n_{tropolone}}{n_{DTPA}} \tag{4.15}$$

where $n_{tropolone}$ is the applied amount of tropolone (mol) used for the loading process, and n_{DTPA} is the amount of encapsulated DTPA (mol). Note that $n_{tropolone}$ is a constant.

The calculation of the estimated encapsulated DTPA is given in Appendix G, and the result is given below:

$$n_{DTPA} = \frac{C_{tot} \cdot V_{sample} \cdot (D-2a)^3 \cdot c_{DTPA}}{\rho_{bi} \cdot (D^3 - (D-2a)^3)} \cdot \frac{MW_{hydrophobic}}{MW_{tot}} \tag{4.16}$$

where n_{DTPA} is the amount of encapsulated DTPA (mol),
C_{tot} is the mass concentration of the polymer (kg m^{-3}),
V_{sample} is the volume of the sample (solution, containing polymersomes) (m^3)
ρ_{bi} is the density of polymersome membrane (hydrophobic bilayer) (kg m^{-3})
c_{DTPA} is the concentration of DTPA in the cavity (mol m^{-3})
$MW_{hydrophobic}$ is the molecular weight of the hydrophobic part of the polymer (kg mol^{-1}),
MW_{tot} is the molecular weight of the polymer (kg mol^{-1})
a is the thickness of the polymersome membrane (hydrophobic bilayer) (m)
D is the diameter of the polymersome (m).

Of all these symbols, only a and D are variables. An overview of the (converted) constants that were used for the calculation of n_{DTPA} is given in **Table 8**.

Table 8. Overview of constants that were used for the calculation of the amount of encapsulated DTPA.

Symbol	Value (unit)	Value (unit) for calculation
C_{tot}	2 mg/mL or 5 mg/mL	2 kg m^{-3} or 5 kg m^{-3}
V_{sample}	0.8 mL	$0.8 \cdot 10^{-6}$ m^3
ρ_{bi}	0.9 g cm^{-3}	900 kg m^{-3}
c_{DTPA}	1 mM	1 mol m^{-3}
$MW_{hydrophobic}$	1800 g mol^{-1}	1.8 kg mol^{-1}
MW_{tot}	2400 g mol^{-1}	2.4 kg mol^{-1}
$n_{tropolone}$	$20 \cdot 10^{-9}$ mol	$20 \cdot 10^{-9}$ mol

Example. For a polymersome solution (2 mg/mL) with membrane thickness of 15 nm and polymersome diameter of 200 nm, it can be calculated that n_{DTPA} = 2 nmol. This is about 2 million times more than the amount of gallium-68 ($1 \cdot 10^{-15}$ mol) used during the loading experiments. Therefore, the absolute amount of encapsulated DTPA does not provide an explanation for low loading efficiencies.

However, it is possible that the ligand exchange reaction does not take place effectively, if the $ratio_{trop/DTPA}$ is too high. This will be discussed using **Figure 33** and **Figure 34**, in which eq. (4.16) serves as the base for the calculations.

The effect of the membrane thickness on $ratio_{trop/DTPA}$ is explored in **Figure 33**. Two plots (2 mg/mL and 5 mg/mL polymer concentration) are shown for which the polymersome diameter was set as a constant (200 nm). It makes sense that $ratio_{trop/DTPA}$ increases for increasing membrane thickness, since the volume of the cavity (and therefore, also the amount of DTPA) decreases. However, the 2 mg/mL sample suffers a lot from the unexpected 15 nm thickness. The $ratio_{trop/DTPA}$ increases from 4 (at 8 nm thickness) to more than 9 (at 15 nm thickness).

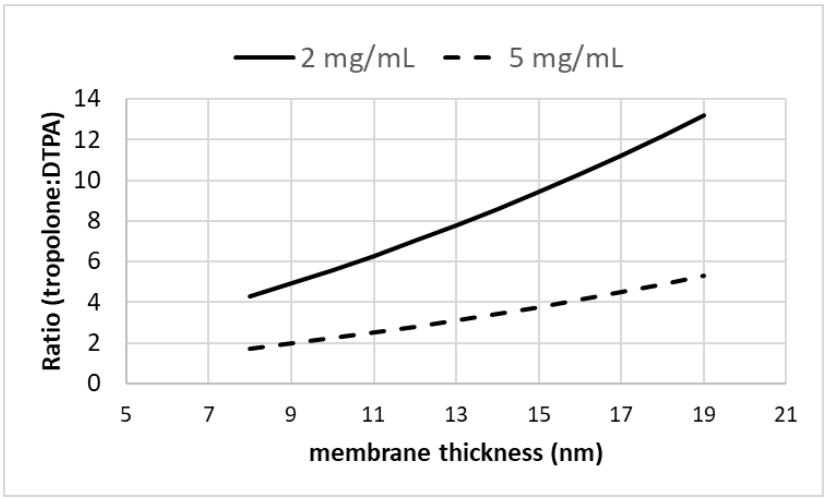

Figure 33. ratio tropolone:DTPA vs. membrane thickness (nm). Polymersome diameter is 200 nm.

In **Figure 34**, $ratio_{trop/DTPA}$ is plotted against the polymersome diameter. It is remarkable that the 5 mg/mL (15 nm thick) graph is very similar to the 2 mg/mL (8 nm thick) graph. Apparently, a slight increase of polymer concentration (from 2 mg/mL to 5 mg/mL) can compensate for the increased membrane thickness, in terms of $ratio_{trop/DTPA}$. Even though it does not solve the negative effect of the increased thickness on the permeability of the membrane, it might explain why the experiments with the unfiltered 5 mg/mL sample showed relatively good loading efficiencies.

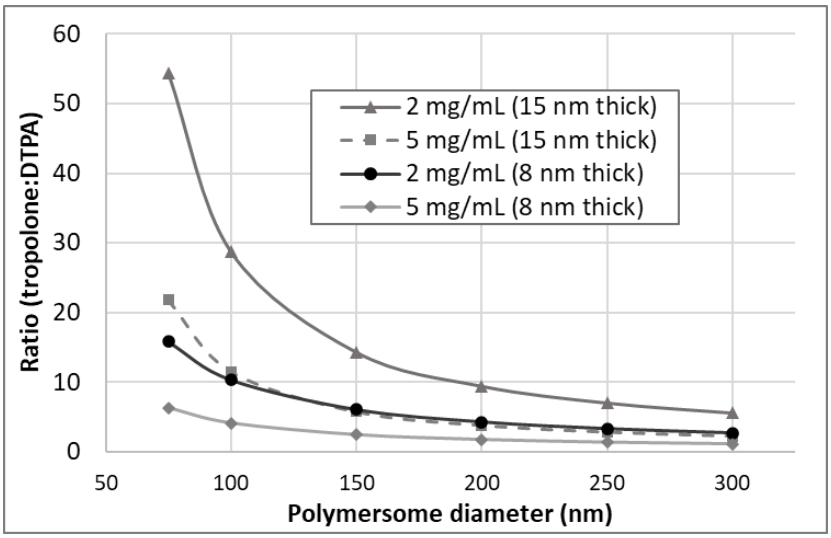

Figure 34. ratio tropolone:DTPA vs.polymersome diameter (nm). Data markers are not actual data points but are used as visual guidance.

Another explanation for the small loading efficiencies can also be found in the cryoTEM images. In some images it can be observed that many spherical micelles and worm-like micelles were formed besides polymersomes. Since the polymersome solutions are reported as polymer concentration, it means that if a substantial fraction of the polymer is formed as micelles, then it also means that the polymersome concentration is much less than the reported polymer concentration. Less polymersome vesicles in solution leads to a higher $ratio_{trop/DTPA}$, and therefore possibly a lower loading efficiency.

5. Conclusions

It is possible to load Ga-68 into polymersomes using an active loading mechanism with tropolone as the lipophilic ligand, and DTPA as the hydrophilic chelator that is encapsulated in the polymersomes.

A tropolone concentration of at least 20 µM is required to bind to $1 \cdot 10^{-12}$ M of Ga-68 with high efficiency at a pH between 4.0 and 6.5.

But the tropolone concentration cannot be raised too high to load Ga-68 into polymersomes because this can negatively impact the loading efficiency.

It is not possible to load Ga-68 into polymersomes at room temperature; an elevated temperature is required.

Ga-68 was loaded successfully into polymersomes with maximum loading efficiencies of up to 36%. It is argued that the unexpectedly thick hydrophobic bilayer of the polymersomes could have led to low loading efficiencies. It is also mentioned that a possible low amount of encapsulated DTPA compared to the applied amount of tropolone, could be a reason for the low efficiencies. But more research needs to be done to confirm these observations.

6. Recommendations

The unexpectedly thick membrane of the polymersomes was mentioned as the main reason for the low loading efficiencies. It is therefore strongly recommended to perform the same loading experiments with a polymersome batch, of which it is confirmed that the polymersomes have a 'thin' membrane, to test this idea.

A low amount of encapsulated DTPA compared to the applied amount of tropolone was mentioned as another possible reason for low loading efficiencies. It could be worthwhile to determine the effect on the loading efficiency of using a higher encapsulated DTPA concentration or using a higher polymersome concentration.

It was shown that some experiments failed due to poor separation performance of some Sephadex columns. It is recommended to first make elution profiles of the used Sephadex columns to determine at which fraction polymersomes and at which fraction DTPA are collected to confirm whether they are separated.

When the *RCY* for the binding of tropolone to Ga-68 is performed with extraction experiments by measuring the count rate of a fraction of the volume of the organic phase, it is recommended to fill up the volume to its initial volume to negate the systematic error due to the influence of the volume difference on the count rate experiment. (See discussion §4.1.2).

Only very small amounts of lipophilic ligand or hydrophilic chelator are used for radiolabelling with Ga-68. In case low *RCY*s are observed, it could be worthwhile to investigate the effect on possible metal impurities on the *RCY*, since this could be caused by competition with other metals.

It was shown in §2.11.1 that the pH of precipitation of $Ga(OH)_3$ is a function of gallium concentration. One should be aware that this decreases at increasing gallium concentration. This should be considered, when working with higher concentration of gallium.

During this project, the $^{68}Ge/^{68}Ga$ generator was eluted with 5 mL HCl, and only one fraction of 5 mL eluate was collected. It could be recommended to collect smaller volume fractions and determine which fraction contains the highest activity of Ga-68. The pH of the eluate is quite low (pH 1), and from a practical point of view, it could be worthwhile to be capable of getting the same amount of activity in less volume, since this requires less buffer capacity to maintain pH of the loading solution.

Acknowledgements

This project could not have been brought to a successful conclusion by me without the help and support of numerous other people.

I would like to express my gratitude towards **Antonia Denkova** for giving me the opportunity to do my research at the Applied Radiation & Isotopes research group. I am mainly thankful for the time, space, freedom, and responsibility that you gave me during my project. It has helped me to rekindle my joy in performing science again.

I would like to thank **Adrie Laan** for your assistance and advice during experimental work in the lab, and I would like to acknowledge you for the CryoTEM images of my polymersome samples that you have taken for me. These images were important for the final conclusions in this report.

I would like to thank **Baukje Terpstra** for assisting me in setting up the $^{68}Ge/^{68}Ga$ generator and teaching me how to use a peristaltic pump for the elution of gallium-68.

I appreciate the help of **Josette Moret** in rightfully suggesting that a faulty batch of HCl in the chemical storage cabinet could have been the cause for initially not getting any activity out of the $^{68}Ge/^{68}Ga$ generator, and thereby saving me one or two days of headaches.

I am thankful to **Folkert Geurink** for giving me advice about the use of the high-purity germanium detector, and for hosting online chess tournaments.

I would like to thank **Huanhuan Liu** for assisting me with the DLS measurements to characterise my polymersome samples.

I am thankful to **Jan Willem van Dorp** for some discussions about chemistry, which has given me some useful insights.

Surprisingly, I am somewhat thankful for **social distancing** measures against Covid-19. Working from home and attending online meetings have forced me to overcome my camera shyness.

I am thankful to **Henk van Doorn**, **Koos van Kammen** and **Rogier van Oossanen** for teaching me something about beer, and for introducing me to (non-alcoholic) IPA, and thereby helping me in finding a drink that does not taste like water and not like lemonade.

I would like to thank the **SBD** (radiation protection service) for giving me radiation safety advice and approving my internal permit. Traditionally, I would also like to thank them for checking the countless of wipe tests for contamination.

And above all, I am thankful to **Robin de Kruijff** for teaching me how to create polymersomes, teaching me how to use the extruder, teaching me how to use Sephadex columns, introducing me to operating the DLS apparatus and the high-purity germanium detector, taking CryoTEM images of a polymersome solution for me, retraining me in working safely and confidently with radioactivity, and your patience at my reintroduction into generic lab work. I am exceedingly grateful for all your positive encouragements when I was at my lowest. Not only has this supported me in finishing my thesis, it has helped me a lot in my life. Thank you.

Literature

[1] Wang, G., de Kruijff, R. M., *et al.*, (2016). Pharmacokinetics of Polymersomes Composed of Poly(Butadiene-Ethylene Oxide); Healthy versus Tumor-Bearing Mice. *J Biomed Nanotechnol, 12(2)*, 320-328.

[2] de Kruijff, R.M. (2018). *Alpha Radionuclide Therapy Using Polymeric Nanocarriers: Solution to the Recoil Problem?*. (Accessed on 2020, October 9). Retrieved from https://doi.org/10.4233/uuid:5c23f3d4-c331-4d1f-bf9d-ca37b5fb2436 .

[3] Wang, G., de Kruijff, R.M., *et al*. (2013). Polymersomes as radionuclide carriers loaded via active ion transport through the hydrophobic bilayer. *Soft Matter, 9(3)*, 727-734.

[4] Rahmim, A., Zaidi, H. (2008). PET versus SPECT: strengths, limitations and challenges. *Nucl Med Commun, 29*, 193-207.

[5] Anajafi, T., Mallik, S. (2015). Polymersome-based drug-delivery strategies for cancer therapeutics. *Ther Deliv 6(4)*, 521-534.

[6] Discher, D.E., Ahmed, F. (2006). Polymersomes. *Annual Review of Biomedical Engineering, 8*, 323-341.

[7] Owens III, D. E., Peppas, N. A. (2006). Opsonization, biodistribution, and pharmacokinetics of polymeric nanoparticles. *Int J Pharm, 307(1)*, 93-102.

[8] McCutchan, E.A. (2012). Nuclear Data Sheets for A = 68. *Nuclear Data Sheets, 113*, 1735-1870

[9] Bé, M-M., Schönfeld, E. (2012). *Table de Radionucleídes*. (Accessed on 2020, October 9). Retrieved from http://www.lnhb.fr/nuclear-data/nuclear-data-table/ .

[10] (2014, October 28). *Public Assessment Report Scientific discussion Galliapharm.* (Accessed on 2020, October 9). Retrieved from https://mri.cts-mrp.eu/Human/Downloads/DK_H_2294_001_PAR_2of2.pdf

[11] Prince, J.R. (1979). Comments on Equilibrium, Transient Equilibrium, and Secular Equilibrium in Serial Radioactive Decay. *The Journal of Nuclear Medicine, 20*, 162-164.

[12] Schaart, D. *Time-of-Flight Positron Emission Tomography*. (Accessed on 2020, October 9). Retrieved from https://www.tudelft.nl/tnw/over-faculteit/afdelingen/radiation-science-technology/research/research-groups/medical-physics-technology/research/tof-pet/ .

[13] Turkington, T.G. (2001). Introduction to PET Instrumentation. *Journal of Nuclear Medicine Technology, 29*, 1-8.

[14] Szirmay-Kalos, L., Magdics M. *et al.* (2012). Fast Positron Range Calculation in Heterogeneous Media for 3D PET Reconstruction. *Conference Paper*. DOI: 10.1109/NSSMIC.2012.6551492

[15] Zaidi, H. Montandon, M-L. (2007). Scatter Compensation Techniques in PET. *PET Clinics, 2(2)*, 219-234.

[16] Hamley, I.W. *Introduction to Soft Matter – Revised Edition*: *Synthetic and Biological Self-Assembling Materials*. John Wiley & Sons, Ltd, Chichester, (2007).

[17] Malvern Instruments Limited (2017). Dynamic Light Scattering: An Introduction in 30 Minutes. *Technical note*, 1-17.

[18] *Electron Microscopy Tutorial*. (Accessed on 2020, October 9). Retrieved from https://advanced-microscopy.utah.edu/education/electron-micro/ .

[19] *Transmission Electron Microscopy vs Scanning Electron Microscopy*. (Accessed on 2020, October 9). Retrieved from https://www.thermofisher.com/nl/en/home/materials-science/learning-center/applications/sem-tem-difference.html .
[20] Cizmar, P., Yuana, Y. (2017). Detection and Characterization of Extracellular Vesicles by Transmission and Cryo-Transmission Electron Microscopy. *Methods in Molecular Biology (1660),* 221-232.
[21] Cui, H., Hodgdon, T.K. *et al.* (2007). Elucidating the assembled structure of amphiphiles in solution via cryogenic transmission electron microscopy. *Soft Matter, 3*, 945-955.
[22] Pehl, R. (1977). Germanium gamma-ray detectors. *Physics Today, 30(11),* 50-61.
[23] Connor, N. (2019, December 14). *What is High Purity Germanium Detector – HPGE – Definition*. (Accessed on 2020, October 9). Retrieved from https://www.radiation-dosimetry.org/what-is-high-purity-germanium-detector-hpge-definition/ .
[24] Dumortier, R., Weber, M.E., Vera, J.H. (2005). Removal and recovery of gallium from aqueous solutions by complexation with sodium di-(n-octyl) phosphinate. *Hydrometallurgy, 76,* 207-215.
[25] Baes, C.F., Mesmer Jr., R.E. *The Hydrolysis of Cations*. Wiley Interscience publication, New York, (1976).
[26] van Gaans, P.F.M. (1990). The Pitzer model applied to aqueous $GaCl_3$ solutions with evaluation of regression methods. *Geologica Ultraiectina, 73,* 1-155.
[27] Diakonov, I.I., Pokrovski, G.S., *et al.* (1997). Gallium speciation in aqueous solution. Experimental study and modelling: Part 1. Thermodynamic properties of $Ga(OH)_4^-$ to 300°C. *Geochimica et Cosmochimica Acta, 61(7),* 1333-1343.
[28] Bénézeth, P., Diakonov, I.I., *et al.* (1997). Gallium speciation in aqueous solution. Experimental study and modelling: Part 2. Solubility of α-GaOOH in acidic solutions from 150 to 250°C and hydrolysis constants of gallium (III) to 300°C. *Geochimica et Cosmochimica Acta, 61(7),* 1345-1357.
[29] Wood, S.A., Samson, I.M. (2006). The aqueous geochemistry of gallium, germanium, indium and scandium. *Ore Geology Reviews, 28*, 57-102.
[30] Jackson, G.E., Byrne, M.J., (1996). Metal Ion Speciation in Blood Plasma: Gallium-67-Citrate and MRI Contrast Agents. *The Journal of Nuclear Medicine, 37(2),* 379-386.
[31] Bernstein, L.R., (1998). Mechanisms of Therapeutic Activity for Gallium. *Pharmacological Reviews, 50(4),* 665-682.
[32] Moerlein, S. M., Welch, M. J. (1981). The chemistry of gallium and indium as related to radiopharmaceutical production. *Int J Nucl Med Biol. 8(4),* 277-287.
[33] Meites, L. *Handbook of Analytical Chemistry.* McGraw-Hill, New York, (1963).
[34] Dyrssen, D. (1954). Studies on the Extraction of Metal Complexes. XVIII. The Dissociation Constants and Partition Coefficient of Tropolone. *Acta Chemica Scandinavica, 8,* 1394-1397.
[35] Al-Ghobashy, M.A. (2014). Electrophoretic behavior of charge regulated zwitterionic buffers in covalently and dynamically coated fused silica capillaries. *Bulletin of Faculty of Pharmacy, Cairo University, 52*, 71-78.
[36] Good, N.E., Winget, G.D., *et al.* (1966). Hydrogen Ion Buffers for Biological Research. *Biochemistry, 5(2),* 467-477.

[37] Sokołowska, M., Bal, W. (2005). Cu(II) complexation by ‘‘non-coordinating’’*N*-2-hydroxyethylpiperazine-*N*’-2-ethanesulfonic acid (HEPES buffer). *Journal of Inorganic Biochemistry, 99*, 1653-1660.
[38] Hacht, B. (2008). Gallium(III) Ion Hydrolysis under Physiological Conditions. *Bulletin of the Korean Chemical Society, 29(2),* 372-376.
[39] Das, B., Roy, R.N., *et al*. (2000). Thermodynamics of the $GaCl_3$-HCl-H_2O System at 25°C. *Journal of Solution Chemistry, 29(3),* 289-297.
[40] van Gaans, P.F.M., (1993). Thermodynamics of aqueous gallium chloride: Activity coefficients in dilute and high chloride solutions with consideration of the effects of hydrolysis and chloride complex formation. *Chemical Geology, 104*, 139-157.
[41] Henderscott, L., Gentilcore, R., *et al.* (1982). Tropolone: A Lipid Solubilizing Agent for Cationic Metals. *European Journal of Nuclear Medicine, 7*, 234-236.
[42] Ashenhurst, J. (2020, February 12). *Polar Protic? Polar Aprotic? Nonpolar? All About Solvents*. (Accessed on 2020, October 9). Retrieved from https://www.masterorganicchemistry.com/2012/04/27/polar-protic-polar-aprotic-nonpolar-all-about-solvents/ .
[43] Wadas, T. J., Wong, E. H., *et al.* (2010). Coordinating radiometals of copper, gallium, indium, yttrium, and zirconium for PET and SPECT imaging of disease. *Chem Rev., 110(5),* 2858-2902.
[44] Martell, A. E., Motekaitis, R. J., *et al*. (1996). Stability constants of metal complexes of macrocyclic ligands with pendant donor groups. *Supramolecular Chemistry, 6(3-4),* 353-363.
[45] Smith, R. M.; Martell, A. E. (1989). *Critical Stability Contants*; Plenum Press, New York, (1989).
[46] Bermudez, H., Brannan, A.K., *et al.* (2002). Molecular Weight Dependence of Polymersome Membrane Structure, Elasticity, and Stability. *Macromolecules, 35*, 8203-8208.
[47] Tsionou, M. I., Knapp, C. E., *et al*. (2017). Comparison of macrocyclic and acyclic chelators for gallium-68 radiolabelling. *RSC Adv, 7(78),* 49586-49599.
[48] Lux, P. *Secular and Transient Equilibrium Formula*. (Accessed on 2020, October 9). Retrieved from http://www.plux.co.uk/secular-and-transient-equilibrium-formula/ .
[49] *Topic 4 – Sources of Radiation | Decay Chains*. (Accessed on 2020, October 9). Retrieved from https://courses.ecampus.oregonstate.edu/ne581/four/decay_chains.htm .

Appendix A

DLS measurements

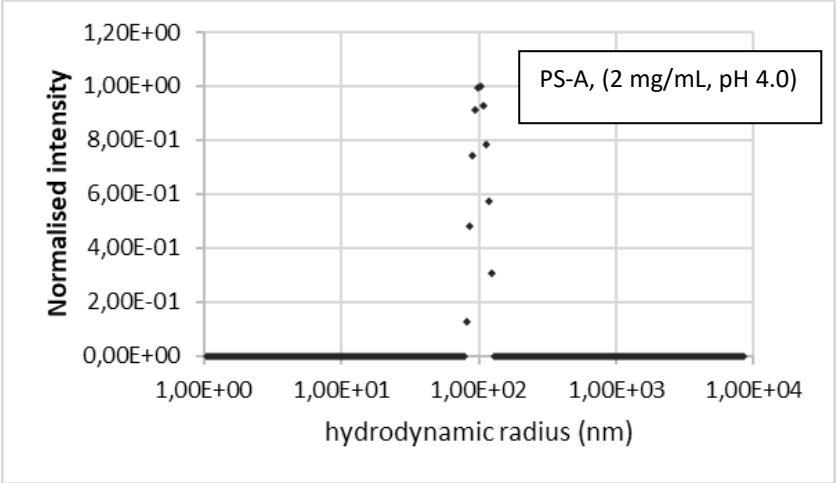

Figure A 1. Normalised intensity vs. hydrodynamic radius (nm). 200 nm extrusion.

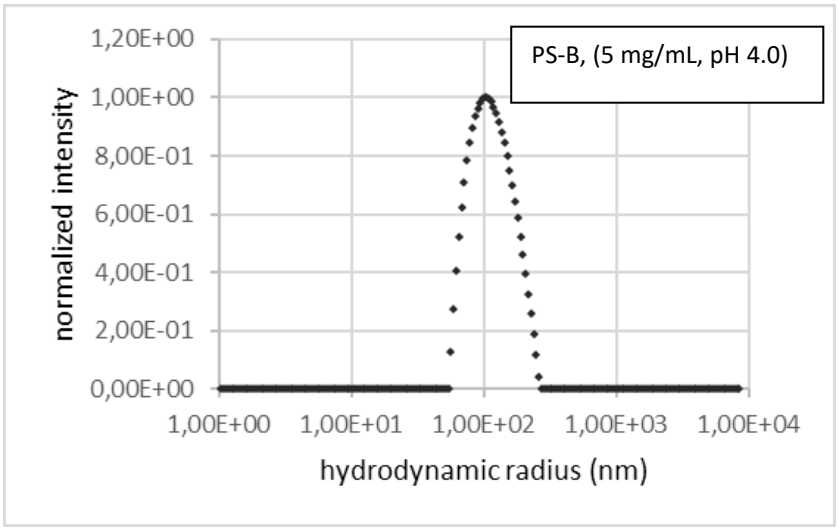

Figure A 2. Normalised intensity vs. hydrodynamic radius (nm). 200 nm extrusion.

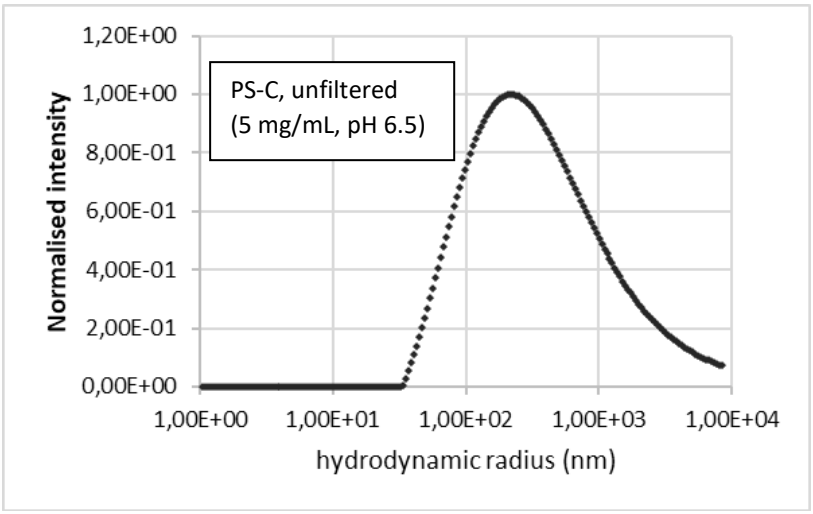

Figure A 3. Normalised intensity vs. hydrodynamic radius (nm). No extrusion step was performed.

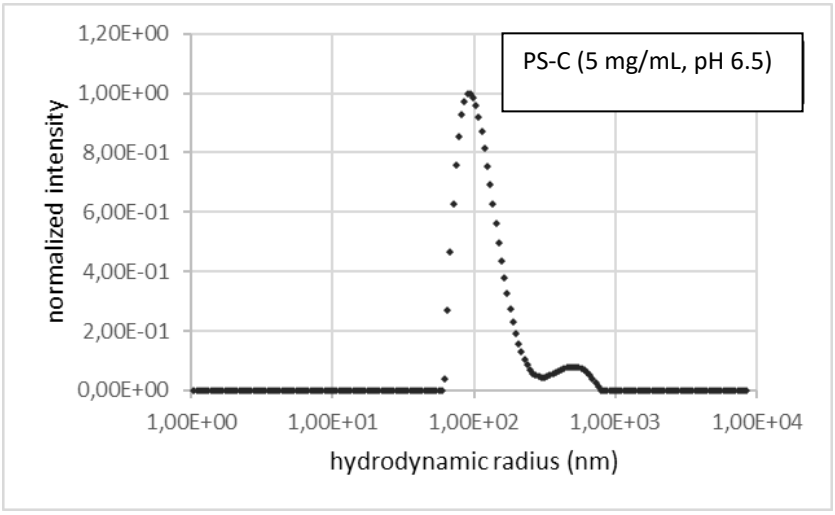

Figure A 4. Normalised intensity vs. hydrodynamic radius (nm). 200 nm extrusion.

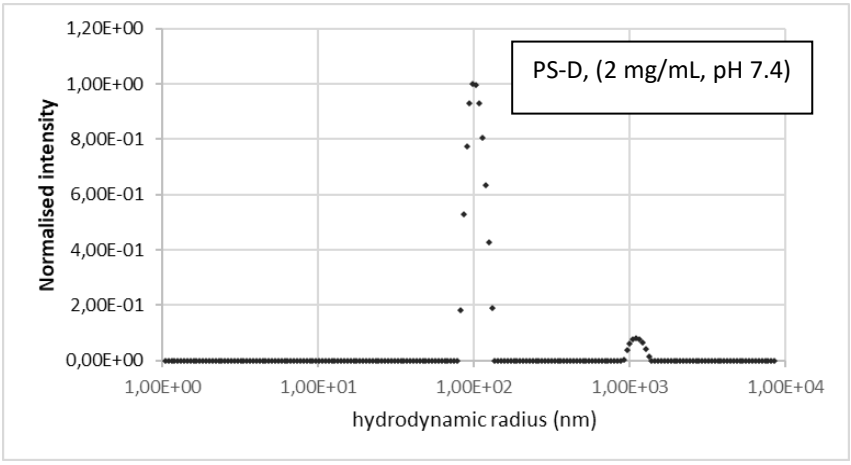

***Figure A 5*.** Normalised intensity vs. hydrodynamic radius (nm). 200 nm extrusion.

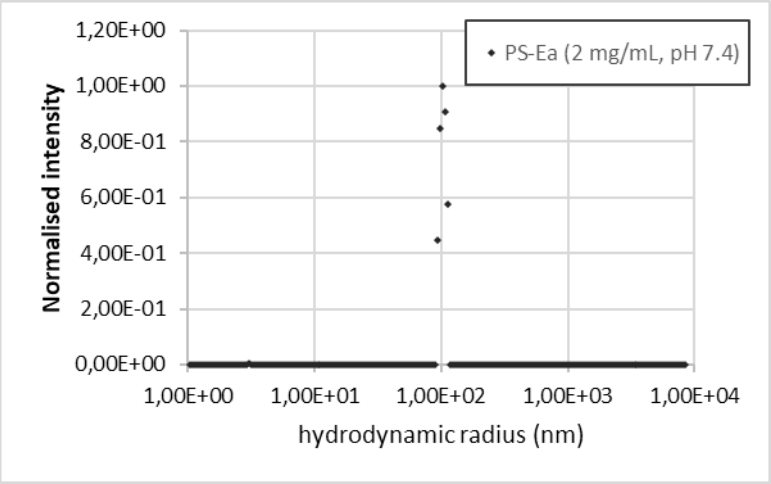

***Figure A 6*.** Normalised intensity vs. hydrodynamic radius (nm). 200 nm extrusion.

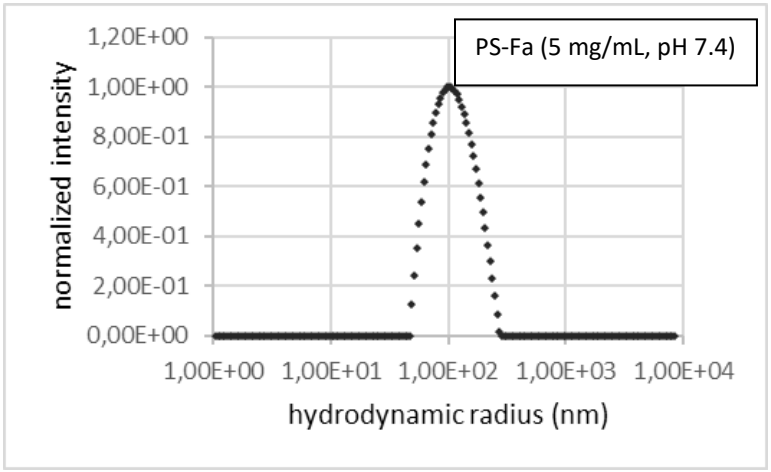

Figure A 7. Normalised intensity vs. hydrodynamic radius (nm). 200 nm extrusion.

Appendix B

CryoTEM images

The polymersome samples were characterised by taking CryoTEM images. The thickness of the hydrophobic bilayer of the polymersomes were measured, and the average thickness was determined. The results are found in **Table B 1**. A selection of the CryoTEM images is found on the following pages.

Table B 1. Overview of the measurements of the thickness of the membrane of the polymersomes.

Polymersome sample	Thickness (nm)		Polymersome sample	Thickness (nm)
PS-A	15		PS-C	13
	16			15
	13			19
	12			17
	11			18
	10			18
	14			18
	15			17
	16			19
PS-B	12			19
	17			17
	14			18
	14			18
	11			15
	16			15
	11		PS-D	17
	12			14
	15			12
	16			13
	13		PS-Ea	19
	15			19
	14			18
	16			18
	17			14
	12		PS-Fa	10
	13			17
	14			12
				18
				17
				11
Thickness = 15 nm ± 3 nm (mean ± 1 SD)				

PS-A: 2 mg /mL PBd(1800)-PEO(600), pH 4.0, 200 nm filter

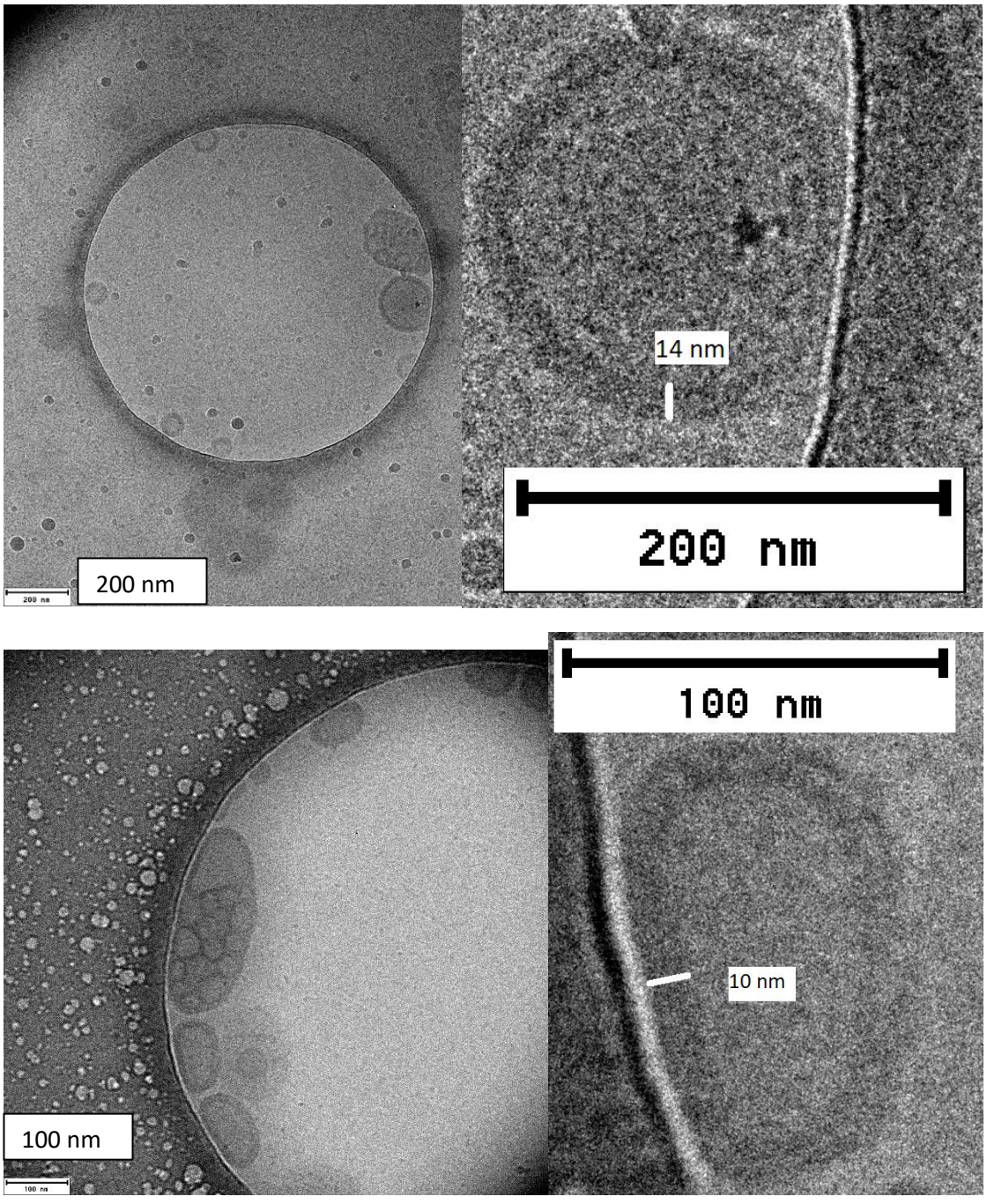

PS-B: 5 mg /mL PBd(1800)-PEO(600), pH 4.0, 200 nm filter

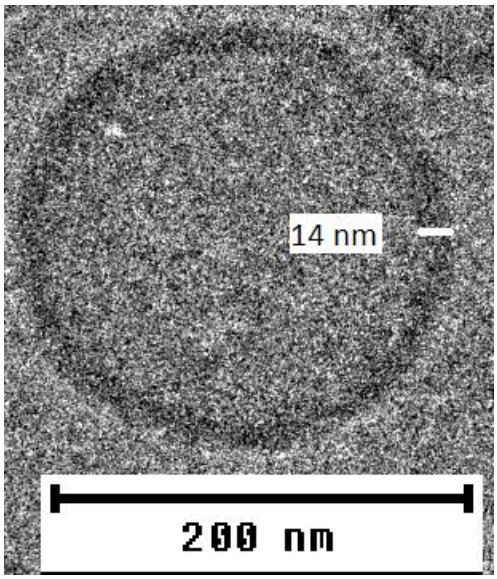

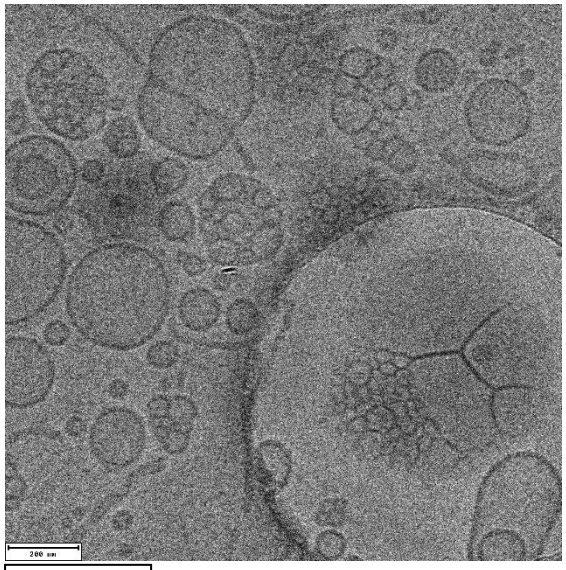

200 nm

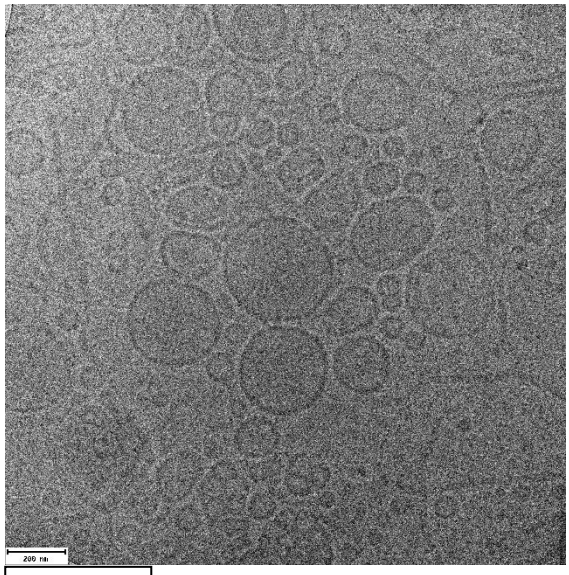

200 nm

PS-C: 5 mg /mL PBd(1800)-PEO(600), pH 6.5, 200 nm filter

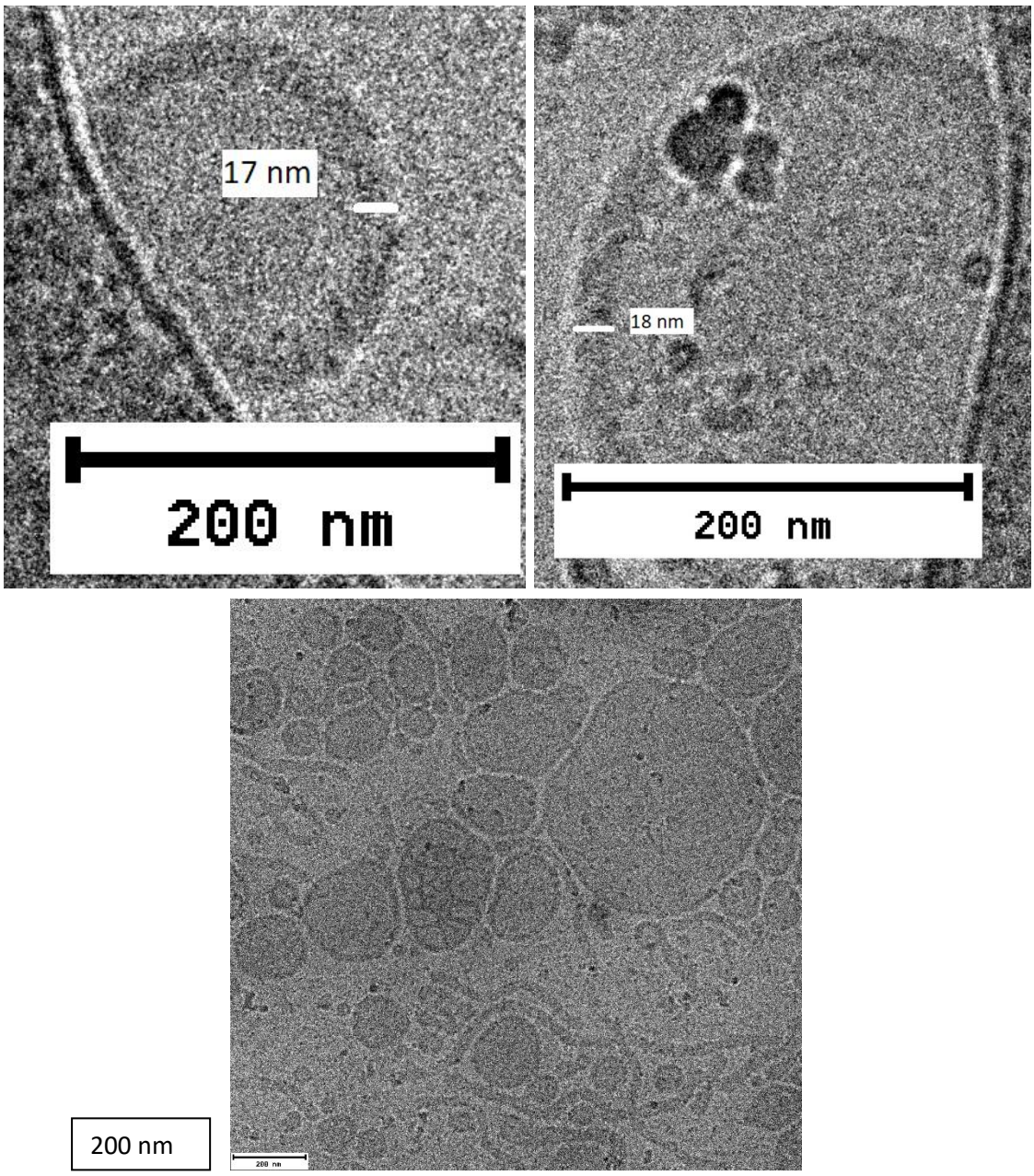

PS-C: 5 mg /mL PBd(1800)-PEO(600), pH 6.5, <u>unfiltered</u>

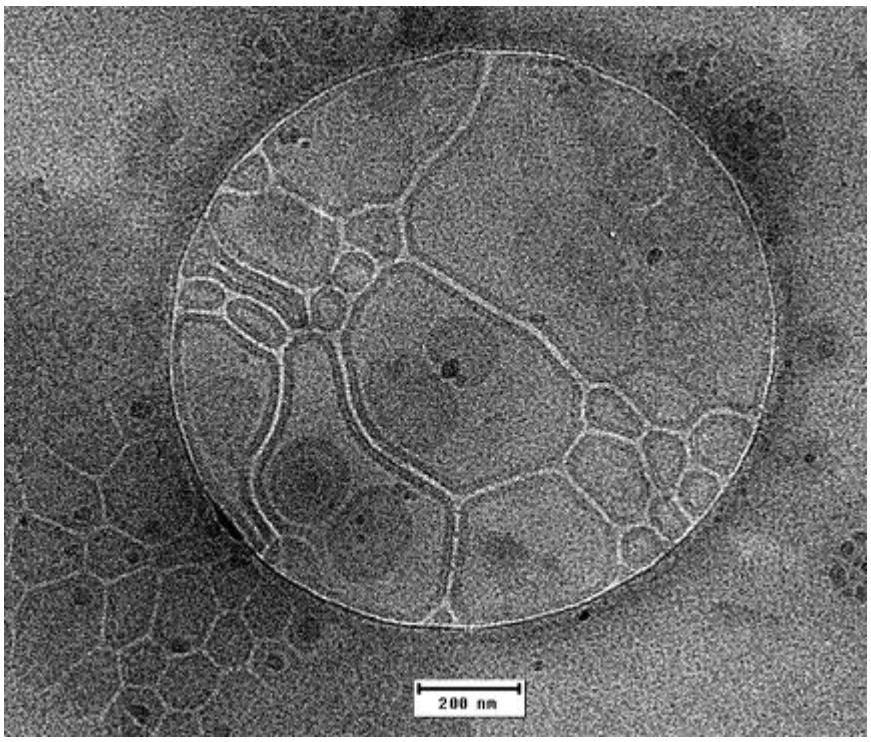

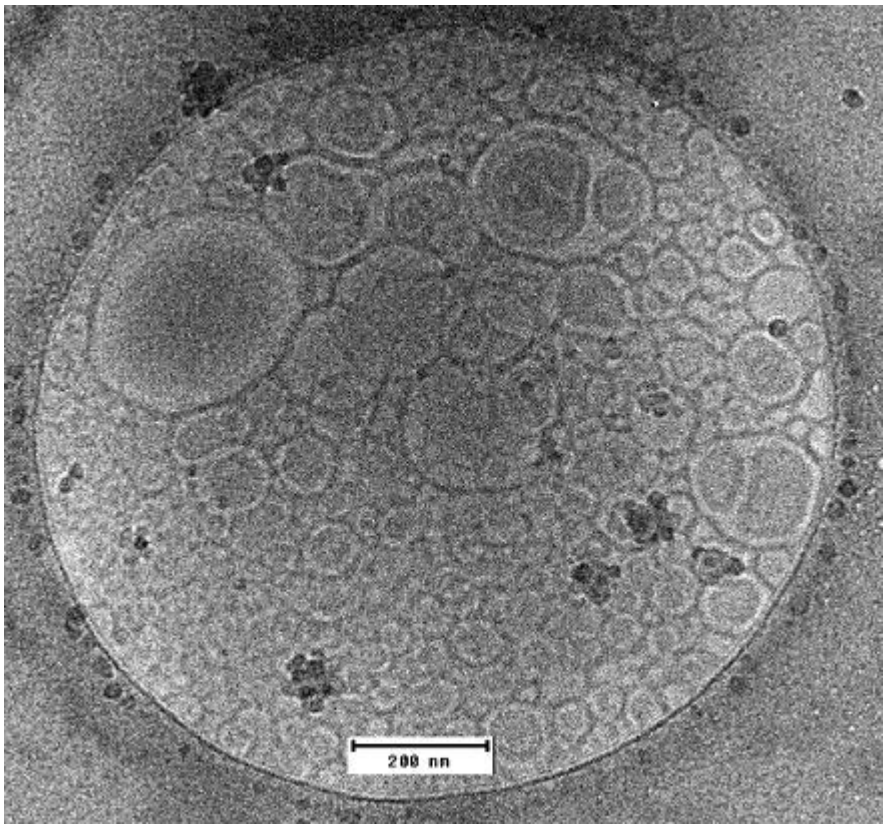

PS-D: 2 mg /mL PBd(1800)-PEO(600), pH 7.4, 200 nm filter

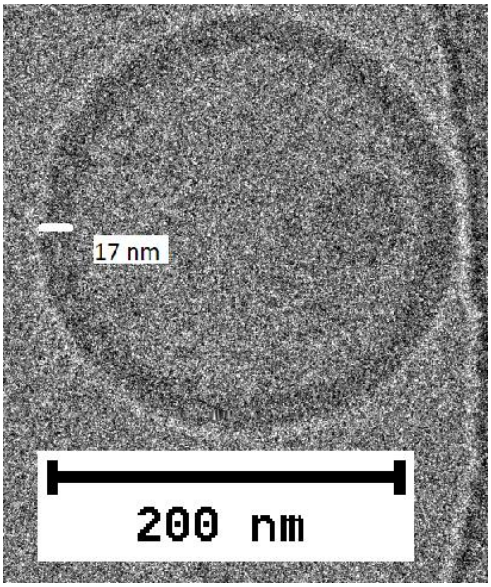

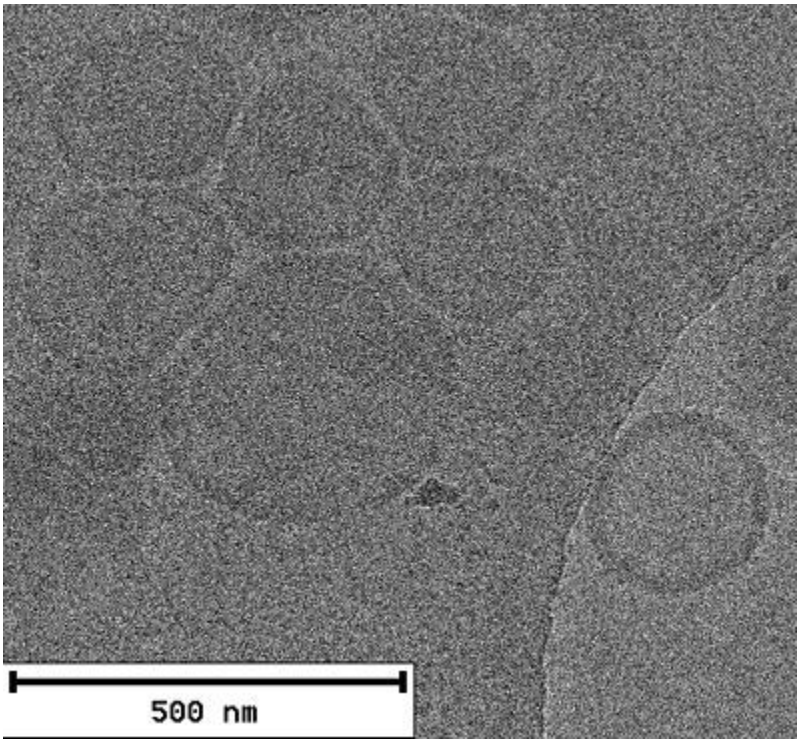

PS-Ea: 2 mg /mL PBd(1800)-PEO(600), pH 7.4, 200 nm filter

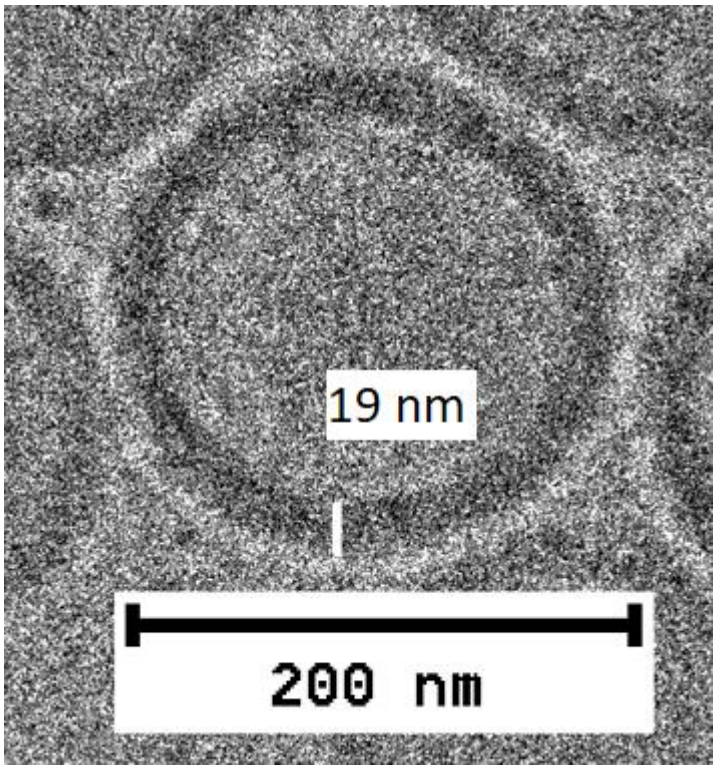

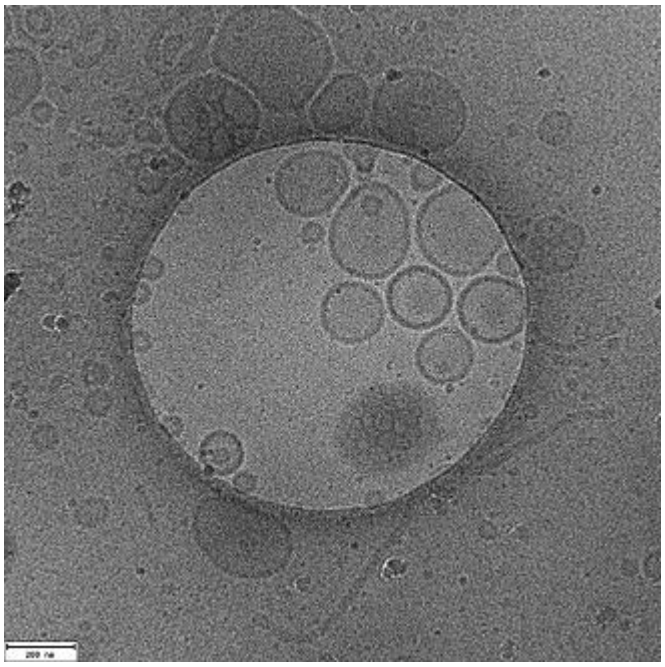

200 nm

PS-Fa: 5 mg /mL PBd(1800)-PEO(600), pH 7.4, 200 nm filter

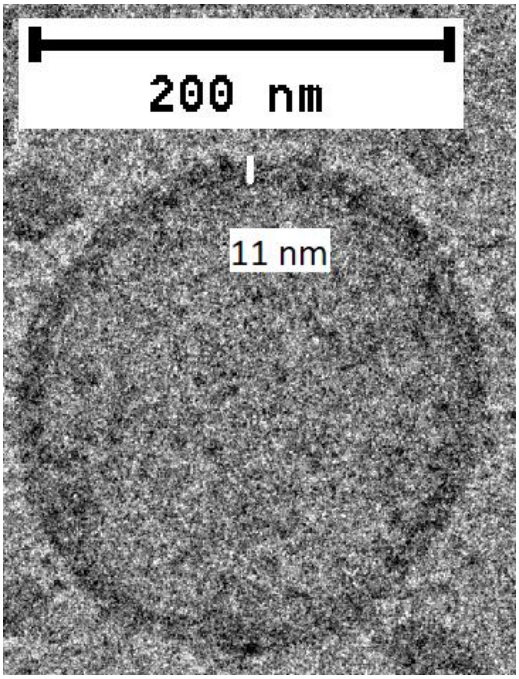

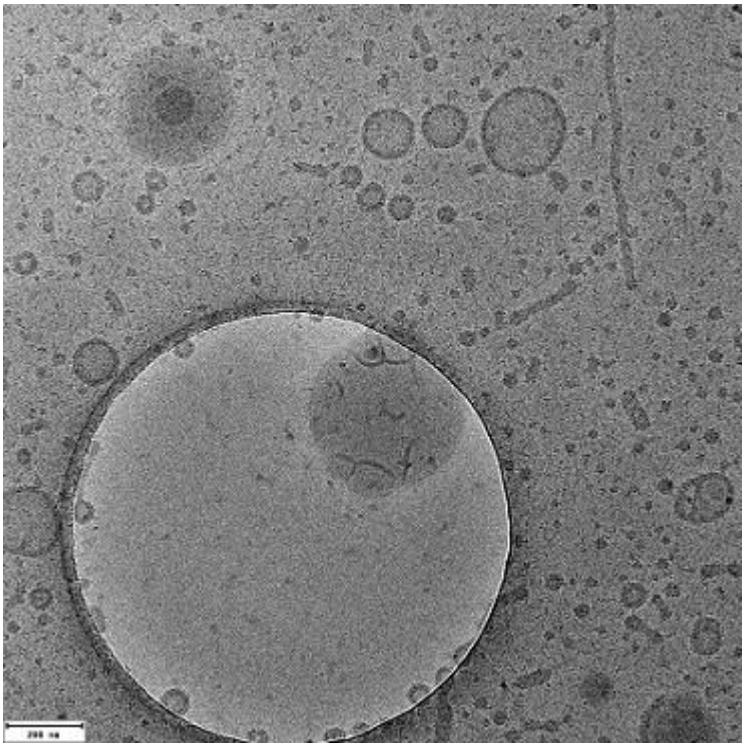

200 nm

Appendix C

Derivation of the activity of an unstable daughter isotope

In this Appendix, a derivation (inspired by [48] and [49]) is given for the activity of the unstable daughter isotope "B" of the following decay chain:

$$A \xrightarrow{\lambda_1} B \xrightarrow{\lambda_2} C$$

where λ_1 and λ_2 represent the decay constant of isotope A and isotope B, respectively. The result of this derivation was used as a basis for the derivation of the secular equilibrium, as discussed in §2.5.

A differential equation for isotope B can be set up:

$$\left.\begin{aligned} &\frac{dN_A(t)}{dt} = -\lambda_1 \cdot N_A(t) \\ &\frac{dN_B(t)}{dt} = \lambda_1 N_A(t) - \lambda_2 N_B(t) \\ &N_A(t) = N_{A,0} \cdot e^{-\lambda_1 t} \end{aligned}\right\} \frac{dN_B(t)}{dt} = \lambda_1 N_{A,0} \cdot e^{-\lambda_1 t} - \lambda_2 N_B(t) \qquad \text{(C.1)}$$

Rearrange the equation:

$$\frac{dN_B(t)}{dt} + \lambda_2 N_B(t) = \lambda_1 N_{A,0} \cdot e^{-\lambda_1 t} \qquad \text{(C.2)}$$

Multiply both sides of the equation with $e^{\lambda_2 t}$:

$$\frac{dN_B(t)}{dt} \cdot e^{\lambda_2 t} + \lambda_2 N_B(t) \cdot e^{\lambda_2 t} = \lambda_1 N_{A,0} \cdot e^{(\lambda_2 - \lambda_1)t} \qquad \text{(C.3)}$$

Apply the product rule $\frac{d}{dt}(u \cdot v) = v\frac{du}{dt} + u\frac{dv}{dt}$

to get:

$$\frac{d}{dt}\left(N_B(t) \cdot e^{\lambda_2 t} \right) = \lambda_1 N_{A,0} \cdot e^{(\lambda_2 - \lambda_1)t} \qquad \text{(C.4)}$$

Take the integral of both sides of the equation:

$$\int \frac{d}{dt}\left(N_B(t) \cdot e^{\lambda_2 t} \right) = \int \lambda_1 N_{A,0} \cdot e^{(\lambda_2 - \lambda_1)t} \qquad \text{(C.5)}$$

$$N_B(t) \cdot e^{\lambda_2 t} = \frac{\lambda_1 N_{A,0} \cdot e^{(\lambda_2 - \lambda_1)t}}{\lambda_2 - \lambda_1} + C \qquad \text{(C.6)}$$

where C is the constant of integration. Rearrange the equation to get:

$$N_B(t) = \frac{\lambda_1 N_{A,0} \cdot e^{-\lambda_1 t}}{\lambda_2 - \lambda_1} + C \cdot e^{-\lambda_2 t} \qquad \text{(C.7)}$$

Determine the constant of integration:

$$\left.\begin{array}{l} t = 0 \\ N_B(t) = N_{B,0} \\ N_{B,0} = \dfrac{\lambda_1 N_{A,0}}{\lambda_2 - \lambda_1} + C \end{array}\right\} C = N_{B,0} - \frac{\lambda_1 N_{A,0}}{\lambda_2 - \lambda_1} \qquad \text{(C.8)}$$

Insert the value of the constant of integration of (C.8) into equation (C.7) to get:

$$N_B(t) = \frac{\lambda_1 N_{A,0} \cdot e^{-\lambda_1 t}}{\lambda_2 - \lambda_1} + (N_{B,0} - \frac{\lambda_1 N_{A,0}}{\lambda_2 - \lambda_1}) \cdot e^{-\lambda_2 t} \qquad \text{(C.9)}$$

Rearranging the equation results to:

$$N_B(t) = \frac{\lambda_1 N_{A,0}}{\lambda_2 - \lambda_1}(e^{-\lambda_1 t} - e^{-\lambda_2 t}) + N_{B,0} \cdot e^{-\lambda_2 t} \qquad \text{(C.10)}$$

Simplification: assume that daughter isotope B is not present initially: $N_{B,0} = 0$. The equation now simplifies into:

$$N_B(t) = \frac{\lambda_1 N_{A,0}}{\lambda_2 - \lambda_1}(e^{-\lambda_1 t} - e^{-\lambda_2 t}) \qquad \text{(C.11)}$$

Multiply both sides of the equation with λ_2:

$$\lambda_2 N_B(t) = \lambda_1 N_{A,0} \frac{\lambda_2}{\lambda_2 - \lambda_1}(e^{-\lambda_1 t} - e^{-\lambda_2 t}) \qquad \text{(C.12)}$$

And note that activity (A) is equal to $A = \lambda N$, so that:

$$A_B(t) = A_{A,0} \frac{\lambda_2}{\lambda_2 - \lambda_1}(e^{-\lambda_1 t} - e^{-\lambda_2 t}) \qquad \text{(C.13)}$$

Short timescale

If the half-life of daughter isotope B is much smaller than the half-life of parent isotope A, then $\lambda_1 << \lambda_2$, and equation (C.13) becomes:

$$A_B(t) \approx A_{A,0}(e^{-\lambda_1 t} - e^{-\lambda_2 t}) \qquad \text{(C.14)}$$

Given that $A_A(t) = A_{A,0} \cdot e^{-\lambda_1 t}$, equation (C.14) becomes:

$$A_B(t) = A_A(t) - A_{A,0} \cdot e^{-\lambda_2 t} \qquad \text{(C.15)}$$

If the half-life of parent isotope A is very long compared to the half-life of daughter isotope B, then the activity of isotope A stays nearly constant at short timescale:

$$A_A(t) \approx A_{A,0}$$

Therefore, at short timescale, equation (C.15) can be approximated by:

$$A_B(t) \approx A_{A,0} - A_{A,0} \cdot e^{-\lambda_2 t} \qquad \text{(C.16)}$$

$$A_B(t) \approx A_{A,0}(1 - e^{-\lambda_2 t}) \qquad \text{(C.17)}$$

Appendix D

The ratio of conjugate base / acid as function of pH

Consider an acid (HA) with its conjugate base (A^-).

$$HA \rightleftharpoons H^+ + A^- \tag{D.1}$$

The acid-dissociation constant is equal to:

$$K_a = \frac{[H^+][A^-]}{[HA]} \tag{D.2}$$

$$\left.\begin{aligned} pK_a &= -\log K_a = -\log\left(\frac{[H^+][A^-]}{[HA]}\right) \\ pH &= -\log\left([H^+]\right) \end{aligned}\right\} pK_a = pH - \log\left(\frac{[A^-]}{[HA]}\right) \tag{D.3}$$

And the ratio of the conjugate base / acid concentration is given by:

$$\left(\frac{[A^-]}{[HA]}\right) = 10^{pH - pK_a} \tag{D.4}$$

- If pH << pK_a, then $[A^-]$ << [HA]
- If pH = pK_a, then $[A^-]$ = [HA]
- If pH >> pK_a, then $[A^-]$ >> [HA]

Appendix E

The isoelectric point of a diprotic acid

Consider a diprotic acid "$\mathbf{AH_2^+}$". The molecule can be present in solution as positively charged $\mathbf{AH_2^+}$**,** neutral **AH**, or negatively charged $\mathbf{A^-}$. The two corresponding acid dissociation constants are:

$$AH_2^+ \underset{}{\overset{K_{a1}}{\rightleftharpoons}} AH + H^+ \Bigg\} K_{a1} = \frac{[AH][H^+]}{[AH_2^+]} \tag{E.1}$$

$$AH \underset{}{\overset{K_{a2}}{\rightleftharpoons}} A^- + H^+ \Bigg\} K_{a2} = \frac{[A^-][H^+]}{[AH]} \tag{E.2}$$

One could rewrite equation (E.2) to express [AH] as function of K_{a2}:

$$[AH] = \frac{[A^-][H^+]}{K_{a2}} \tag{E.3}$$

and insert this result into equation (E.1):

$$K_{a1} = \frac{[A^-][H^+]^2}{K_{a2} \cdot [AH_2^+]} \tag{E.4}$$

The **<u>isoelectric point</u>** is the pH at which the average charge of the molecule is equal to zero. This is only the case, if the presence of the positively charged specie is nullified by the presence of the negatively charged specie. In other words, their concentrations are equal to each other:

$$[A^-] = [AH_2^+] \tag{E.5}$$

So, to calculate the isoelectric point, equation (E.4) simplifies into:

$$K_{a1} = \frac{\cancel{[A^-]}[H^+]^2}{K_{a2} \cdot \cancel{[AH_2^+]}} \Bigg\} K_{a1} = \frac{[H^+]^2}{K_{a2} \cdot} \tag{E.6}$$

Taking the logarithm of this expression, and rewriting yields:

$$-\log(K_{a1}) = -\log\left(\frac{[H^+]^2}{K_{a2}}\right) \tag{E.7}$$

$$-\log(K_{a1}) = -\log\left([H^+]\right)^2 + \log(K_{a2}) \tag{E.8}$$

$$-2\log\left([H^+]\right) = -\log(K_{a1}) - \log(K_{a2}) \tag{E.9}$$

$$2\,pH = pK_{a1} + pK_{a2} \tag{E.10}$$

And thus, the isoelectric point can be estimated with the following equation:

$$pH = \frac{pK_{a1} + pK_{a2}}{2} \tag{E.11}$$

Appendix F

Equilibrium constant of ligand exchange reaction

Consider the formation of a metal-ligand complex and its corresponding stability constant (K_{ML}):

$$M + L \rightleftharpoons ML \tag{F.1}$$

$$K_{ML} = \frac{[ML]}{[M][L]} \tag{F.2}$$

In similar fashion, the formation of a metal-chelator complex and its corresponding stability constant (K_{MC}) is given by:

$$M + C \rightleftharpoons MC \tag{F.3}$$

$$K_{MC} = \frac{[MC]}{[M][C]} \tag{F.4}$$

Consider the ligand exchange reaction in which the ligand in the metal-ligand complex is substituted with the chelator:

$$ML + C \rightleftharpoons MC + L \tag{F.5}$$

The equilibrium constant (K_{ex}) for the ligand exchange reaction is equal to:

$$K_{ex} = \frac{[MC][L]}{[ML][C]} = \left(\frac{[MC]}{[M][C]}\right) \cdot \left(\frac{[M][L]}{[ML]}\right) = \frac{K_{MC}}{K_{ML}} \tag{F.6}$$

Taking the logarithm of this equation produces the result:

$$\log K_{ex} = \log(K_{MC}) - \log(K_{ML}) \tag{F.7}$$

Appendix G

Calculation of amount of encapsulated DTPA in polymersomes

A calculation is made to determine the amount (mol) of encapsulated DTPA chelator within polymersomes. This is used to estimate the ratio of tropolone:DTPA during the loading process.

The symbols that are used for the calculation are listed below:

a is the thickness of the polymersome hydrophobic bilayer (m)
c_{DTPA} is the concentration of DTPA in the cavity (mol m^{-3})
C_{tot} is the mass concentration of the polymer (kg m^{-3})
d is the diameter of the inner cavity of the polymersome (m)
D is the diameter of the polymersome (m)
$f_{hydrophobic}$ is the mass fraction of the hydrophobic part of the polymer
m_{bi} is mass of polymersome membrane (hydrophobic bilayer) (kg)
$m_{vesicle}$ is the mass of 1 polymersome vesicle (kg)
$MW_{hydrophobic}$ is the molecular weight of the hydrophobic part of the polymer (kg mol^{-1})
MW_{tot} is the molecular weight of the polymer (kg mol^{-1})
n_{DTPA} is the amount of encapsulated DTPA available in the sample (mol)
$N_{vesicle}$ is the number of polymersomes
V_{bi} is volume of polymersome membrane (hydrophobic bilayer) (m^3)
V_{cavity} is the volume of one cavity of the polymersome (m^3)
V_{DTPA} is the available total volume (sum of cavities) for DTPA (m^3)
V_{sample} is the volume of the sample (solution, containing polymersomes) (m^3)
ρ_{bi} is the density of polymersome membrane (hydrophobic bilayer) (kg m^{-3})

Calculation

It is assumed that polymersomes are perfect spheres with a hollow cavity, and that all created polymersomes are of equal size. The volume of 1 polymersome membrane is the volume of the sphere, minus the volume of the cavity:

$$V_{bi} = V_{vesicle} - V_{cavity} = \frac{1}{6}\pi D^3 - \frac{1}{6}\pi d^3 = \frac{1}{6}\pi(D^3 - d^3) \qquad [G.1]$$

The mass of the membrane can be calculated using the volume and density of the membrane. The density of the membrane is unknown. Since a Pbd-PEO polymer was used, the approximation is made to set this density equal to the density of polybutadiene, which is about 0.9 g cm^{-3}.

$$m_{bi} = V_{bi} \cdot \rho_{bi} \qquad [G.2]$$

$$\begin{cases} m_{bi} = \frac{1}{6}\pi \cdot \rho_{bi} \cdot (D^3 - d^3) \end{cases} \qquad [G.3]$$

The mass of 1 polymersome vesicle can be calculated using the weight fraction of the hydrophobic part of the polymer. This weight fraction is a constant, since it should be known what polymer is used to create the polymersomes (Pbd(1800)-PEO(600)).

$$f_{hydrophobic} = \frac{MW_{hydrophobic}}{MW_{tot}} \quad [G.4]$$

The mass of the polymersome vesicle is calculated by dividing the mass of the membrane by its weight fraction:

$$m_{vesicle} = \frac{m_{bi}}{f_{hydrophobic}} \quad [G.5]$$

$$\begin{cases} m_{vesicle} = \frac{1}{6}\pi \cdot \rho_{bi} \cdot (D^3 - d^3) \cdot \frac{MW_{tot}}{MW_{hydrophobic}} \end{cases} \quad [G.6]$$

The polymersomes were created using a known mass concentration of polymer. If it is assumed that the entire mass of the polymer is converted into polymersomes, then the number of polymersome vesicles in solution is equal to:

$$N_{vesicle} = \frac{C_{tot}}{m_{vesicle}} \cdot V_{sample} \quad [G.7]$$

$$\begin{cases} N_{vesicle} = \frac{C_{tot}}{\frac{1}{6}\pi \cdot \rho_{bi} \cdot (D^3 - d^3)} \cdot V_{sample} \cdot \frac{MW_{hydrophobic}}{MW_{tot}} \end{cases} \quad [G.8]$$

The volume that is available for the encapsulated DTPA is equal to the sum of the volume of all cavities of the polymersome in solution:

$$V_{DTPA} = N_{vesicles} \cdot V_{cavity} \quad [G.9]$$

The amount of available DTPA (mol) is equal to this volume multiplied by the concentration of DTPA within the cavity:

$$n_{DTPA} = V_{DTPA} \cdot c_{DTPA} = N_{vesicles} \cdot V_{cavity} \cdot c_{DTPA} \quad [G.10]$$

$$\begin{cases} n_{DTPA} = \frac{C_{tot} \cdot V_{sample} \cdot V_{cavity} \cdot c_{DTPA}}{\frac{1}{6}\pi \cdot \rho_{bi} \cdot (D^3 - d^3)} \cdot \frac{MW_{hydrophobic}}{MW_{tot}} \end{cases} \quad [G.11]$$

$$= \frac{C_{tot} \cdot V_{sample} \cdot (\frac{1}{6}\pi d^3) \cdot c_{DTPA}}{\frac{1}{6}\pi \cdot \rho_{bi} \cdot (D^3 - d^3)} \cdot \frac{MW_{hydrophobic}}{MW_{tot}} \quad [G.12]$$

Furthermore, note that the diameter of the inner cavity (d) is a function of the membrane thickness (a), $d = D - 2a$, such that the equation for the amount of DTPA becomes:

$$n_{DTPA} = \frac{C_{tot} \cdot V_{sample} \cdot (D - 2a)^3 \cdot c_{DTPA}}{\rho_{bi} \cdot (D^3 - (D - 2a)^3)} \cdot \frac{MW_{hydrophobic}}{MW_{tot}} \quad [G.13]$$

The diameter D is modified by extrusion and confirmed by DLS measurement, while the thickness of the membrane is visually confirmed using CryoTEM imaging.